Investigation of Hsp90 Regulation by the Aha-type Co-chaperones: Mechanistic Insight into Two Conserved Motifs

by

Rebecca Jean Mercier

A thesis submitted in partial fulfillment of the requirements for the degree of

Doctor of Philosophy

Department of Cell Biology
University of Alberta

Abstract

Hsp90 is a highly conserved and essential molecular chaperone. It regulates the folding, maturation, and activation of client proteins involved in a wide range of cellular processes and pathways, many of which are key players in disease. Hsp90 functions in the context of an ATPase driven conformational cycle that is regulated by co-chaperone proteins. Aha-type co-chaperones are the most potent stimulators of the ATPase activity of Hsp90. Here we describe key structural elements required for the function of Aha-type co-chaperones and investigate the diverse roles of Aha-type co-chaperones in Hsp90 regulation. We show that the conserved *N*-terminal NxNNWHW motif is essential for the biological activity of Aha1p and Hch1p. This work points to a role for the NxNNWHW motif in regulating the apparent affinity of Hsp90 for nucleotide substrates and highlights the importance of nucleotide exchange in the Hsp90 functional cycle. In addition, we show that Lys 60 of the conserved RKxK motif is required for the *in vivo* and *in vitro* functions of Aha1p. While the *in vivo* requirements of Hch1p are consistent with Aha1p, all residues of the RKxK motif appear to be necessary for Hch1p-mediated stimulation of Hsp90. Our work in defining the conserved structural motifs in Aha-type co-chaperones, has provided insight into the ways in which the Aha-types co-chaperones regulate the conformational dynamics of Hsp90. We also investigated different models and approaches to understanding the regulation of Aha-type co-chaperones, which provides a valuable framework for future work to expand upon. Our broadened understanding of Aha-type co-chaperones, offers key insights into the mechanism of Hsp90 function and regulation.

Preface

Work presented in Chapter 3 of this thesis has published as “The conserved NxNNWHW motif in Aha-type co-chaperones modulates the kinetics of Hsp90 ATPase stimulation” (Mercier et al., 2019). Aspects of the research conducted for the completion of this thesis were done in collaboration. Preliminary work for Figure 3.3 was conducted by previous graduate students Natalie Horvat and Dr. Annemarie Wolmarans. The temperature sensitive mutant Hsc82p^{S25P} was identified and provided by Dr. Jill Johnson from the University of Idaho. The experimental design and completion of the PET florescence quenching experiments in Figure 3.17 were completed by Jonathan Schubert under the supervision of Dr. Hannes Neuweiler from the University of Würzburg, Germany. Viral experiments conducted in Figure 5.7 were competed in collaboration with Dr. Anil Kumar and Eileen Reklow under the supervision of Dr. Tom Hobman from the University of Alberta.

All other components of this thesis are my original work conducted under the guidance and supervision of Dr. Paul LaPointe at the University of Alberta.

Acknowledgments

I would like to thank my supervisor, Dr. Paul LaPointe, for his encouragement and support throughout the completion of my graduate degree. His enthusiasm for science and passion for research provided me with motivation and a variety of opportunities to grow as a scientist. I am grateful for his mentorship and all of the stimulating conversations that we shared. His perseverance through challenges has been an inspiration and I am so thankful for the chance to have learned under his guidance and from his knowledge.

Thank you to all the members of the LaPointe Lab, undergraduate students, technicians, and previous graduate students, for their contributions and for their inputs and guidance. I especially want to thank Dr. Annemarie (Annerieke) Wolmarans who made going to lab everyday such a fun experience and whose friendship and support has meant so much.

Thank you to the members of my supervisory committee, Dr. Richard Lehner and Dr. Lynne Postovit, for their intellectual input and support. I would like to thank Dr. Qiumin Tan for serving on my examining committee and Dr. Walid Houry for serving as my external examiner. I am grateful for all of their discussion and valuable feedback on this thesis. Thank you to Dr. Andrew Simmonds for serving as the examination chair and being such a strong advocate and support. Additionally, I want to thank Dr. Ben Montpetit who help shaped the direction of my research as part of my initial supervisory committee.

Thank you to the Department of Cell Biology, Dr. Richard Rachubinski and members of the faculty, for providing their expertise and knowledge as well as encouragement and support. A special thank you to the Simmonds Lab and the Hobman Lab for their collaborations. Thank you to the support staff for all of their help and my fellow graduate students for their support and friendship.

Thank you to Alberta Innovates, NSERC, the Alberta Cancer Foundation, the Department of Cell Biology along with the Faculty of Medicine and Dentistry, the Faculty of Graduate Studies and Research, and the Graduate Students' Association for their financial support.

Thank you to my family, whose encouragement and support has been unwavering. I am truly grateful to have such an incredible family.

Table of Contents

List of tables

List of Figures

List of Abbreviations

2DGE	2-dimensional gel electrophoresis
ADP	Adenosine diphosphate
AAA+	ATPase associated with various cellular activities
ATP	Adenosine triphosphate
AMP-PNP	Adenylyl-imidodiphosphate
BSA	Bovine serum albumin
CK2	Casein kinase 2
CFTR	Cystic fibrosis transmembrane conductance regulator
DNA	Deoxyribonucleic acid
dNTP	Deoxyribonucleotide triphosphate
DMSO	Dimethyl sulfoxide
DTT	Dithiothreitol
ECL	Enhanced chemiluminescence
E. coli	*Escherichia coli*
EDTA	Ethylenediaminetetraacetic acid
FPLC	Fast protein liquid chromatography
FBS	Fetal bovine serum
GA	Geldanamycin
G418	Geneticin
GR	Glucocorticoid receptor
GHKL	Gyrase, Hsp90, Histidine Kinase, and MutL
Hsps	Heat shock proteins
HRP	Horse radish peroxidase
IMAC	Immobilized metal affinity chromatography
IPG	Immobilized pH gradient
IP	Immunoprecipitation
IPGT	Isopropyl-β-D-thiogalactopyranoside
kDa	Kilodaltons
LRRK2	Leucine-rich repeat kinase 2
LB	Luria broth
MAF	Mouse adult fibroblast

MTT	3-(4,5-dimethylthiazol-2-yl)-2,5-diphenyltetrazolium bromide
NADH	Nicotinamide adenine dinucleotide
NEB	New England BioLabs
NB	Novobiocin
NBD	Nucleotide binding domain
NEF	Nucleotide exchange factor
OD	Optical density
PMSF	Phenylmethylsulfonyl fluoride
PBS	Phosphate buffered saline
PEP	Phosphoenolpyruvate
PET	Photoinduced electron transfer
Poly(I:C)	Polyinosinic:polycytidylic acid
PR	Progesterone receptor
PK/LDH	Pyruvate kinase/lactate dehydrogenase
S. cerevisiae	*Saccharomyces cerevisiae*
SDS-PAGE	Sodium dodecyl sulfate polyacrylamide gel electrophoresis
sHsps	Small heat shock proteins
SHR	Steroid hormone receptor
SBD	Substrate-binding domain
SC	Synthetic complete
TBS	Tris-buffered saline solution
TPR	Tetratricopeptide repeat
VSVG	Vesicular stomatitis virus glycoprotein
WNV	West Nile virus
YPD	Yeast peptone dextrose

Chapter 1 Introduction

1.1 Protein folding and function

Proteins are a versatile class of macromolecules that are involved in virtually every cellular process. From signal transduction to gene expression, cell structure, and control of metabolic processes, proteins are vital for cell survival. Proteins are synthesized as linear sequences of amino acids, polypeptide chains, derived from the translation of genetic information. In order to be biologically active, proteins must adopt specific three-dimensional conformations. All of the necessary information for proteins to fold into their biologically active form is contained within their amino acid sequences (Anfinsen et al., 1961; Anfinsen, 1973). There are a vast number of conformational degrees of freedom and possible structures that a polypeptide chain can sample. If an unfolded protein was to randomly sample all of the possible conformations, protein folding should take much longer than it does (the so-called Levinthal paradox) (Levinthal, 1968). The number of conformations that a protein can adopt is refined by structural organization and thermodynamic principles (Linderstrøm-Lang and Schellmand, 1959; Goldberger et al., 1963).

Protein folding is currently best modeled as a funnel-shaped energy landscape (Figure 1.1) (Dill, 1985; Bryngelson et al., 1995; Onuchic et al., 1997). The depth of the funnel represents free energy of a polypeptide chain and conformational entropy is represented across the width. The top of the funnel is wide, representative of the many possible states and conformational degrees of freedom. Protein folding is primarily driven by hydrophobic interactions, isolation of hydrophobic moieties from the aqueous environment, isolation of charged and polar amino acids, and neutralization of ion pairing within the interior of the protein (Dyson et al., 2006). As folding takes place, the ensemble of possible conformations that a protein can adopt decrease along with free energy, resulting in narrowing of the energy landscape. The lowest point of the funnel is the native state of a protein that represents the fully-folded and functional ensemble of conformations that have a global free energy minimum.

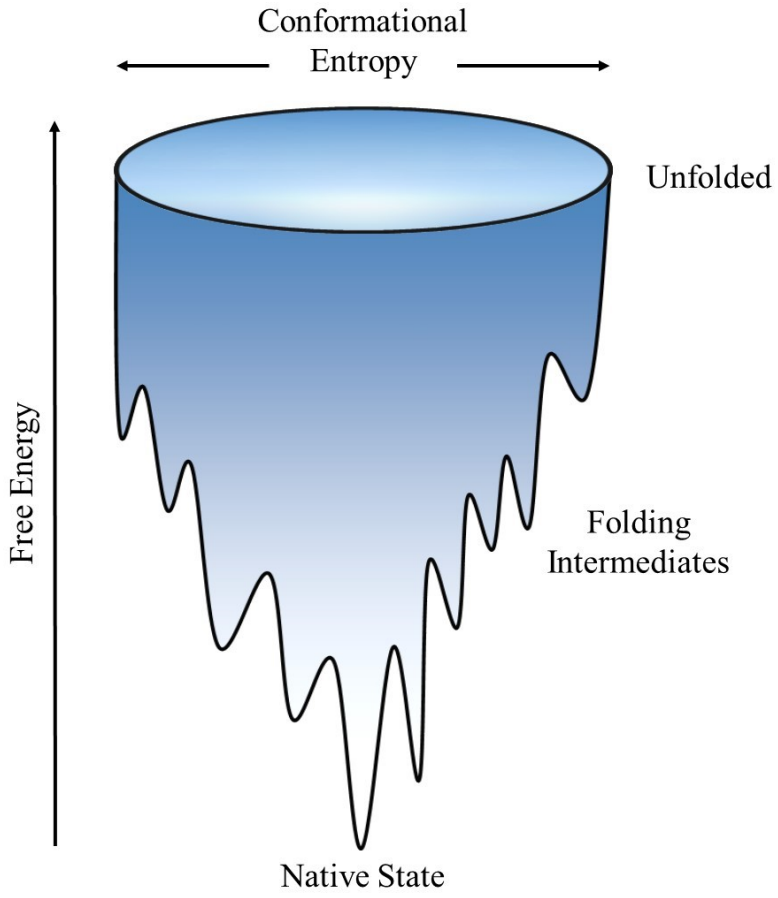

Figure 1.1 Energy landscape schematic of protein folding.

The width of the funnel represents conformational entropy and the depth represents free-energy. Unfolded proteins have both a high free energy and entropy. As a protein begins to the fold and acquire structure closer to its native conformation, free energy and the number of possible conformational states decreases. Local free-energy minima and maxima represent valleys and peaks that are metastable intermediates and barriers to protein folding. The native state of a protein is represented at the bottom of the funnel and is the global free-energy minimum.

Energy landscapes are dynamic and controlled by the protein folding environment. Factors including temperature, pressure, ionic strength, and pH affect the ability of a protein to fold (Lapidus, 2017). Non-native conditions are represented by a shallow energy landscape, a higher proportion of unfolded polypeptide chains, and increased conformational entropy. Unfolded proteins are at a high risk for forming inappropriate interactions, misfolding, being targeted for degradation, and forming aggregates (Dobson, 2003). Protein folding in the cell is further challenged by macromolecular crowding which increases the risk of undesirable interactions. Cells employ extensive quality control networks to maintain the integrity of the proteome and cellular homeostasis (Chen, B. et al., 2011). At the centre of these networks are specialized proteins termed 'molecular chaperones'.

1.2 Heat shock proteins and molecular chaperones

The ability of cells to detect and respond to environmental, chemical, and physiological stress is critical for their survival. Depending on the type of stresses encountered, numerous biological pathways and integrated mechanisms are activated for maintenance of cellular homeostasis. The heat shock response is a universal pro-survival pathway that cells employ to deal with stresses that result in the accumulation of damaged or denatured proteins (Lindquist, 1986; Richter et al., 2010). This response was first detected in the chromosomes of *Drosophila* when puffs, representing sites of newly synthesized RNA, were observed upon exposure to high temperature or chemical treatments (Ritossa, 1962). These sites of increased transcription were linked to the synthesis of a specific group of proteins aptly termed heat shock proteins (Hsps) (Tissières et al., 1974; Lindquist and Craig, 1988; Lindquist, 1986).

Hsps constitute a large group of proteins that are defined based on molecular weight: Hsp100, Hsp90, Hsp70, Hsp60, Hsp40, and small heat shock proteins (Jolly and Morimoto, 2000). The expression of Hsps is well conserved in response to a wide variety of stresses that result in the accumulation of denatured and damaged proteins (Kelley and Schlesinger, 1978; Lemaux et al., 1978; Yamamori et al., 1978; Hightower, 1980; Finley et al., 1984; Ananthan et al., 1986). Initial experiments examining the function of Hsps focused around Hsp70. Hsp70 was found to bind exposed hydrophobic surfaces of proteins during times of stress and prevent aggregation by recurrent cycles of ATP-driven binding and release (Lewis and Pelham, 1985; Pelham, 1986). Furthermore, Hsp70 and homologues transiently associate with newly

synthesized polypeptides to assist in their folding and assembly to prevent aggregation (Haas and Wabl, 1983; Deshaies et al., 1988; Chirico et al., 1988; Zimmermann et al., 1988; Beckmann et al., 1990; Flynn et al., 1991). Homologues of Hsp60 were also shown to play a role in mediating the folding of proteins (Ellis, 1996).

The term 'molecular chaperone' was first used to describe nucleoplasmin, a protein that assists in the assembly of nucleosomes (Laskey et al., 1978). Understanding the function of Hsps led to generalization of the term to include proteins that interact, stabilize, or help ensure the folding and assembly of other macromolecular structures (Ellis, 1987; Hartl and Hayer-Hartl, 2009). In the crowded cellular environment, where concentrations of proteins and other macromolecules are estimated to be 200-400 mg/mL, there is increased risk for protein misfolding and aggregation (Zimmerman and Trach, 1991; van den Berg et al., 1999; Kuznetsova et al., 2014). Chaperones assist in *de novo* protein folding, protection of folding intermediates, refolding of misfolded proteins, assembly of oligomeric complexes, and proteolytic degradation. Chaperones reduce inappropriate intermolecular and intramolecular interactions from taking place and therefore reduce protein aggregation and misfolding in the cell. By binding to folding intermediates chaperones reduce inappropriate interactions and lower kinetic energy barriers required for intermediates to fold into the native state (Kovacs et al., 2005; Kim, Y. E. et al., 2013). Chaperones also assist in the refolding of misfolded proteins into their native state (Parsell et al., 1994; Doyle et al., 2013). Through their role, molecular chaperones support protein flexibility, complexity, and evolution (Rutherford and Lindquist, 1998; Venton, 2016). Molecular chaperones are part of complex networks that are important for protein quality control and cellular homeostasis.

1.3 Molecular chaperone families

Molecular chaperones are a diverse family of multi-domain proteins that assist in protein folding and assembly of polypeptides into higher order structures. Chaperones help prevent protein misfolding and aggregation, play a role in the reversal of protein aggregation, facilitate the degradation of misfolded proteins by the ubiquitin-proteasome system, and also play a role in protein activation (Saibil, 2013; Kampinga and Craig, 2010; Kriegenburg et al., 2012; Bukau et al., 2006). In order to fulfill these roles, chaperones are structurally diverse and function through various mechanisms. Individual classes of chaperones often do not act in isolation, but as

complex chaperone networks. The Hsp chaperone families are discussed in greater detail in the following sections.

1.3.1 Small Hsps

Small heat shock proteins (sHsps) are a family of ubiquitously expressed chaperones that range from ~10-40 kDa (Jakob et al., 1993; Basha et al., 2013). They are ATP-independent and share a conserved α-crystallin domain that is essential for dimerization and function (Figure 1.2 A) (Poulain et al., 2010; Kriehuber et al., 2010). sHsps form dynamic homo-oligomers whose size is dependent upon cell conditions and substrate requirements (Jaya et al., 2009; Stengel et al., 2010). sHsps bind to exposed hydrophobic surfaces of damaged or denaturing proteins to limit aggregation. The mechanism by which ATP-independent chaperones are able to regulate substrate binding and release remains relatively unclear. sHsps are able to prevent protein aggregation, allowing subsequent refolding by ATP-dependent chaperones (van Montfort et al., 2001).

1.3.2 Hsp60 and Hsp10

Members of the Hsp60 family, also called chaperonins, are large cylindrical protein complexes that support protein folding by fully enclosing proteins within a central cavity (Mayhew et al., 1996). Chaperonins are found across all domains of life and exist as homo- or hetero-oligomeric ring complexes. Hsp60 exists as either a single or double heptameric ring structure and functions in concert with Hsp10 to promote substrate folding (Rospert et al., 1993; Höhfeld and Hartl, 1994). The Hsp60 ring structure provides the central cavity for substrate folding and Hsp10 forms a heptameric ring that functions as a lid (Figure 1.2 B). The activity of Hsp60 is driven by ATP-dependent conformational changes. The double ring structure is a back-to-back ring structure where ATP binding and closing of the folding chamber in one ring is accompanied by ADP dissociation and substrate release from the trans-ring (Todd et al., 1994; Rye et al., 1997; Ranson et al., 1997). The two rings act anti-cooperatively as substrate enclosure and ATP binding in one ring leads to substrate and ADP release in the other (Yifrach and Horovitz, 1995; Xu, Z. et al., 1997). Substrate release does not necessarily mean that a protein has reached its native state and further rounds of binding may be necessary to achieve proper protein folding (Weissman et al., 1994).

1.3.3 Hsp70 and Hsp40

The Hsp70 chaperone family is highly conserved across prokaryotes and found throughout the cellular compartments of eukaryotic organisms (Mayer and Bukau, 2005). Hsp70 is a two-domain protein composed of a nucleotide binding domain (NBD) and a substrate binding domain (SBD) (Figure 1.2 C). The *C*-terminal SBD of Hsp70 binds to short segments of substrate polypeptides enriched in hydrophobic residues (Blond-Elguindi et al., 1993; Zhu et al., 1996; Rüdiger et al., 1997). Interactions between Hsp70 and substrate is regulated by the nucleotide status of the NBD (Szabo et al., 1994; Liu, Q. and Hendrickson, 2007). In the ATP-bound state, the affinity of Hsp70 for substrate is low with a high association and dissociation rate. In opposition to the ATP-bound state, the ADP-bound and nucleotide-free states of Hsp70 have a high affinity for substrate and a low exchange rate. In this way, the binding of ATP to the NBD stimulates the opening of the SBD and closing occurs after ATP hydrolysis.

Hsp70 acts in cooperation with co-chaperones. The Hsp40 or J-domain protein family is responsible for substrate recruitment and stimulating the ATPase rate of Hsp70 (Misselwitz et al., 1998; Laufen et al., 1999). These two functions are attributed to the *C*-terminus and *N*-terminus of Hsp40, respectively (Qian et al., 1996; Jiang et al., 2007). Hsp40 is a chaperone itself which binds substrate in the *C*-terminal domain before transferring it to Hsp70 (Rüdiger et al., 1997; Greene et al., 1998). Hsp40 chaperones stimulate the transition of Hsp70 from the low-affinity to high-affinity substrate bound state and ADP dissociation from Hsp70 becomes the rate limiting step of substrate release. Nucleotide exchange factors (NEFs) are co-chaperones that interact with Hsp70 to accelerate ADP release. Hsp70 may undergo several rounds of binding and release before a polypeptide chain reaches its native state (Sharma et al., 2010). In many instances Hsp70 acts in cooperation with additional chaperone complexes to assist in protein folding (Teter et al., 1999; Mayer and Bukau, 2005).

1.3.4 Hsp100

The Hsp100 family of chaperones are unfoldases and disaggregases found in bacteria, yeast, and plants, but not in animals or humans. Hsp100 chaperones are part of the AAA+ (ATPase associated with various cellular activities) family that typically form ring structures with a central channel available to thread polypeptides through (Figure 1.2 D) (Ogura and Wilkinson,

2001). Most Hsp100 proteins contain one or two AAA+ domains that are arranged in a hexameric ring (Martin et al., 2008). Once targeted to Hsp100, an aggregate engages with the central channel loops and ATP hydrolysis is coupled to subdomain rotations and substrate translocation (Glynn et al., 2009). After interaction with Hsp100 unfolded substrates are available for refolding and often interact with other chaperones to achieve their native state.

1.3.5 Hsp90

The Hsp90 chaperone family is found across eukaryotes and is essential for viability. Hsp90 has three conserved domains (*N*-terminal, middle and *C*-terminal domains) and functions as a dimer connected through the *C*-terminus (Figure 1.2 E) (Pearl and Prodromou, 2006). The movements of Hsp90 are extremely dynamic and large conformational rearrangements take place during substrate binding and ATP hydrolysis (Li, J. and Buchner, 2013). Hsp90 is available to bind substrate when in an open V-shaped conformation. When ATP and substrate are bound, the protomers come together, dimerize in the *N*-terminus, and additional contacts between the *N*-terminal and middle domains occur, which are necessary interactions for ATP hydrolysis. After hydrolysis, the reopening of Hsp90 through the dissociation of the *N*-terminal domains, along with release of substrate and ADP, resets the Hsp90 system for a new cycle of substrate binding. Cytosolic Hsp90 functions within a complex system of co-chaperone proteins and post-translational modifications that regulate the ATPase cycle and conformational dynamics (Taipale et al., 2010).

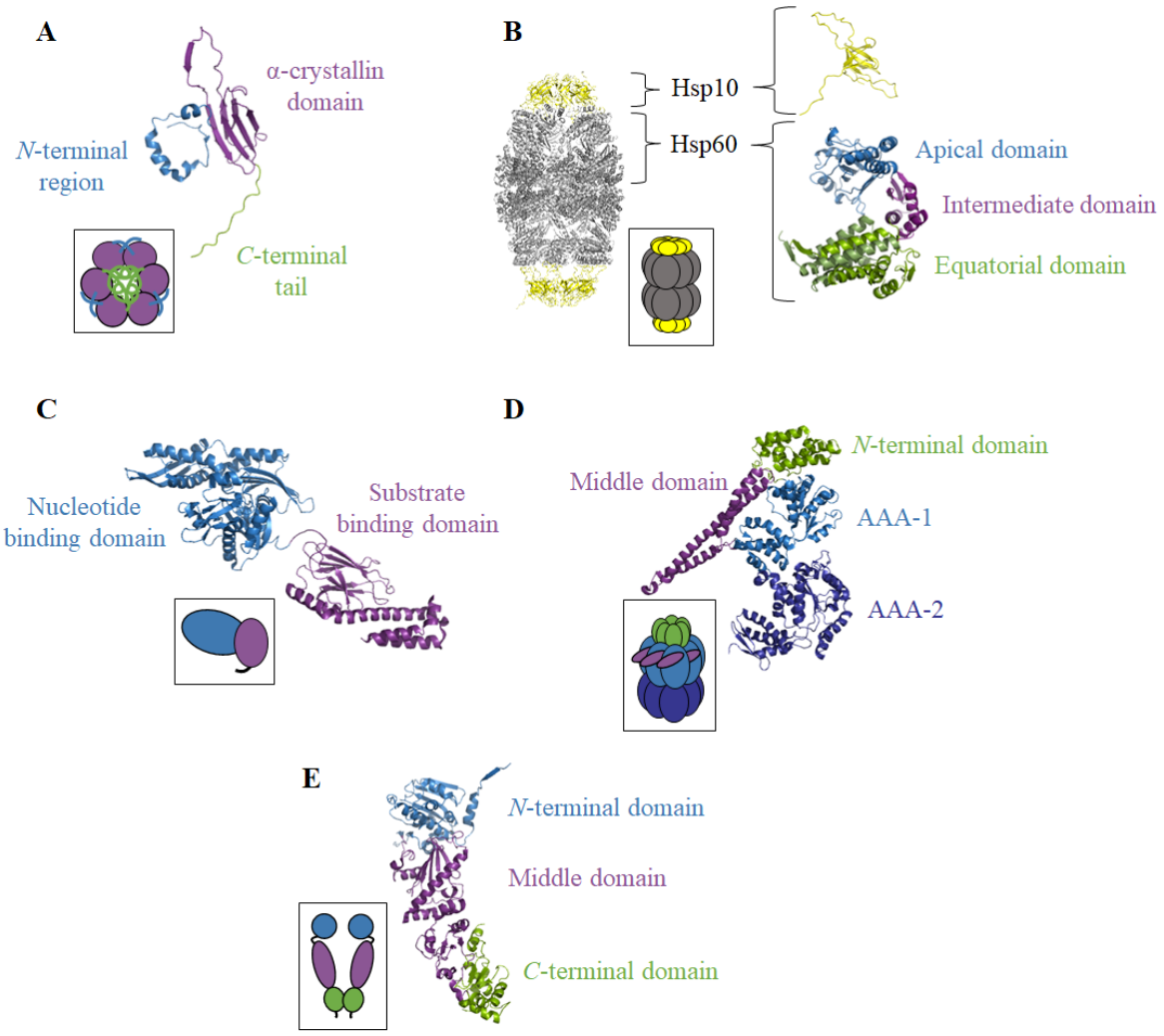

Figure 1.2 Crystal structure and cartoon representation of molecular chaperone families. **A.** sHsps (1GME (van Montfort et al., 2001)). **B.** Hsp10 and Hsp60 (4PJ1, (Nisemblat et al., 2015)). **C**. Hsp70 (2KHO, (Bertelsen et al., 2009)). **D.** Hsp100 (1QVR, (Lee, S. et al., 2003)). **E**. Hsp90 (2CG9, (Ali et al., 2006)). For all of the above, the specific domains of the crystal structures are labelled with corresponding colours and the boxed cartoon represents a proposed functional complex.

1.4 Molecular chaperones in disease

Protein folding is constantly challenged by the cellular environment. Over time, metabolic and chronic stress can lead to the expression of mutant and damaged proteins. Expression of these proteins is associated with many diseases including neurodegenerative diseases, metabolic diseases, and cancer (Morimoto, 2011). Molecular chaperones play a critical role in protecting the stability and function of proteins and therefore represent a therapeutic avenue for treating protein conformational diseases (Rutherford and Lindquist, 1998; Calamini and Morimoto, 2012; Jeng et al., 2015). The development of neurodegenerative diseases including Alzheimer's, Parkinson's, Huntington, and Prion disease correspond with the progressive accumulation of denatured and misfolded proteins (Taylor et al., 2002; Cardinale et al., 2014). An increase in molecular chaperone levels would seemingly be a beneficial therapeutic strategy to alleviate the proteotoxic stress of disease-associated aggregation prone proteins (Klettner, 2004; Maiti et al., 2014). Alternatively, the cytoprotective properties of molecular chaperones can be co-opted during malignance in order to promote the initiation and progression of tumour growth and survival (Calderwood et al., 2006). Inhibition of molecular chaperones would be a mechanism through which tumour growth and cancer progression can be halted. The multi-functional nature of molecular chaperones presents challenges to determining therapeutic interventions.

A majority of chaperones interact promiscuously with a wide range of unfolded and non-native client proteins to assist in proper folding and to prevent aggregation (He and Hiller, 2018). The molecular chaperone Hsp90 is distinct in that it acts on a select group of substrates, termed 'clients' (Nathan et al., 1997; Panaretou et al., 2002). Hsp90 acts during the late-stages of protein folding on partially or full-folded proteins to assist protein maturation and activation (Jakob et al., 1995; Pearl and Prodromou, 2000; Street et al., 2011). Hsp90 clients are highly enriched in signalling proteins which regulate normal cell growth, as well as evolutionary processes and disease progression (Young et al., 2001). In this way, Hsp90 has become a major molecular chaperone target for the treatment of human diseases, with Hsp90 inhibitors being extensively tested as therapeutics (Sidera and Patsavoudi, 2014; Neckers and Workman, 2012; Kim, Y. S. et al., 2009; Zuehlke et al., 2018; Mellatyar et al., 2018; Barrott and Haystead, 2013). Improving the current understanding of the molecular and cellular functions of Hsp90 will allow advancement in therapeutic interventions in the treatment of disease.

1.5 The 90 kDa Heat shock protein (Hsp90)

Hsp90 is a molecular chaperone that is a key regulator of protein homeostasis during normal and stress conditions. Hsp90 is highly conserved, with one or more Hsp90 genes found in all bacteria and eukaryotes. There are two major isoforms of Hsp90 found in the eukaryotic cytosol: Hsp90α, an inducible isoform and Hsp90β, a constitutively expressed isoform (Hsp82p and Hsc82p respectively in yeast) (Csermely et al., 1998; Borkovich et al., 1989). Compartment specific homologues of Hsp90 have also been found in mitochondria (tumor necrosis factor receptor-associated protein 1 (TRAP1)), chloroplasts (Hsp90C), and endoplasmic reticulum (94 kDa glucose-related protein (Grp94)) of various eukaryotes (Csermely et al., 1998; Johnson, J. L., 2012). Hsp90 homologues are thought to have evolved from the bacterial Hsp90, high temperature protein G (HtpG), through multiple duplication events and losses (Stechmann and Cavalier-Smith, 2004; Gupta, 1995; Chen, B. et al., 2006).

Hsp90 is the most abundant stress protein making up 1-2% of the total cytosolic protein pool under normal conditions and is upregulated during times of cell stress (Borkovich et al., 1989). Hsp90 is essential in eukaryotes and reduction in Hsp90 levels results in temperature sensitivity in yeast (Borkovich et al., 1989; Bardwell and Craig, 1988; Picard et al., 1990). Hsp90 exhibits chaperone activity, recognizing non-native proteins and preventing aggregation (Wiech et al., 1992). Initial experiments identified a specific group of substrate proteins termed ‘clients’ for Hsp90 compared to that of Hsp70 or Hsp60, which appear to promiscuously interact with all unfolded proteins. The most well-studied Hsp90 clients are steroid-hormone receptors (SHRs) and cell-cycle kinases (Pratt and Toft, 1997; Picard et al., 1990; Picard, 2002). Hsp90 facilitates the active conformation of proteins, the assembly of multiprotein complexes, and promotes the binding competent state of proteins through ATPase centered conformational rearrangements with the support of co-chaperones.

1.6 Hsp90 Structure

Hsp90 functions as a homodimer (Figure 1.3). Each 90 kDa monomer of Hsp90 consists of 3 conserved domains: an *N*-terminal nucleotide binding domain, a middle domain important for client binding, and a *C*-terminal dimerization domain. The *N*-terminal domain of Hsp90 (residues 1-210, *Saccharomyces cerevisiae*) is composed of nine α-helices and an antiparallel β-sheet (8 strands) that together form an α/β sandwich structure with a hydrophobic pocket at the core. The

pocket represents an unconventional nucleotide binding pocket that is the unifying feature of the gyrase, Hsp90, His kinase, and MutL (GHKL) ATPase/kinase superfamily (Dutta and Inouye, 2000). The conformational changes accompanying ATP binding and hydrolysis are essential for Hsp90 client activation. Within the *N*-terminal domain there are two important features for ATP hydrolysis: the ATP lid (residues 98-121, *S. cerevisiae*) and *N*-terminal 'strap' (residues 1-24, *S. cerevisiae*). The ATP lid plays a role in the stabilization of bound nucleotide. The strap, which is comprised of a β-strand (residues 1-8, *S. cerevisiae*), an α-helix (residues 9-16, *S. cerevisiae*), and a flexible loop (residues 17-24, *S. cerevisiae*), is involved in stabilization of the *N*-terminally dimerized state (McLaughlin et al., 2004; Richter et al., 2002). The *N*-terminal domain is able to bind ATP however, when removed from the other domains, has only negligible ATPase activity (Prodromou et al., 2000).

The middle and *N*-terminal domains of Hsp90 are connected by a charged linker (residues 211-272, *S. cerevisiae*). The linker plays an important role in providing conformational flexibility to Hsp90 and may play additional roles in client activation (Hainzl et al., 2009; Tsutsumi et al., 2012). The middle domain is the largest domain (residues 273-526, *S. cerevisiae*) and is composed of two αβα sandwiches that are connected by an α-coil. The first and larger αβα sandwich contains an amphipathic loop suggested to be important for binding of client proteins (Ali et al., 2006). An essential and highly conserved region of the middle domain is the catalytic loop (residues 370-390, *S. cerevisiae*) (Meyer et al., 2003). Residue Arg 380 within the catalytic loop is critical for ATP hydrolysis (Meyer et al., 2004). The middle and *C*-terminal domains are linked by an extended 25-residue loop. The *C*-terminal domain (residues 527-709, *S. cerevisiae*) is the main dimerization interface for each Hsp90 homodimer (Harris et al., 2004). A pair of helices from the *C*-terminal domain of each monomer pack together forming a four-helix bundle that represents the dimer interface. At the *C*-terminus of each monomer is a conserved MEEVD pentapeptide sequence. This motif serves as a binding site for proteins that contain tetratricopeptide repeat (TPR) domains (D'Andrea and Regan, 2003). Hsp90 activity is dependent upon the cooperative action of all three domains.

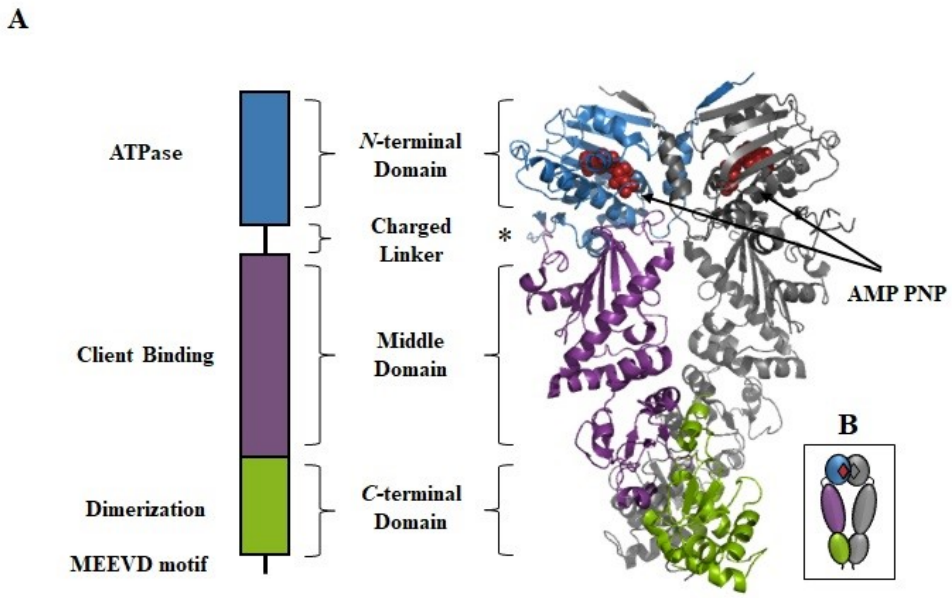

Figure 1.3 Crystal and structural representation of the Hsp90 in the closed conformation. **A.** Each monomer of Hsp90 is composed of an ATPase *N*-terminal domain (blue), client binding middle domain (purple), and dimerization *C*-terminal domain (green). The crystal structure (right) represents *S. cerevisiae* Hsp82p in an *N*-terminal dimerized AMP-PNP (non-hydrolysable ATP analogue) (red) bound state (2CG9 (Ali et al., 2006)). One monomer is coloured to highlight the different domains. Sba1p, which was co-crystalized with Hsp82p, is not shown. *The charger linker region was removed for crystallization. **B.** Cartoon representation of an Hsp90 dimer.

1.7 Hsp90 ATP driven conformational dynamics

Hsp90 proceeds through a conformationally complex cycle in order to chaperone client proteins. A distinct set of conformational states and structural organizations have been linked to the enzymatic properties of Hsp90 (Jackson, 2013). At the most basic level, Hsp90 can be defined as open or closed. In the open conformation Hsp90 can bind and release both client and nucleotide. In the closed state, both nucleotide and client are bound and this represents the catalytically active form of Hsp90. The idea that Hsp90 is an ATP-driven 'molecular clamp' remains a defining feature of the current knowledge about the biochemical mechanism (Prodromou et al., 1997; Prodromou et al., 2000). Further understanding of the conformational intermediates and structural movements have helped to define the details of this process.

In the open state, the *C*-terminal domains of Hsp90 are dimerized while the middle and *N*-terminal domains remain apart and available to bind to client proteins (Ali et al., 2006; Vaughan et al., 2010). In the apo state the ATP lid is open leaving the pocket available to bind nucleotide. ATP binding is a fast reaction and ATP binding and release may happen multiple times before lid closure and commitment to ATP hydrolysis occurs (Hessling et al., 2009). Closure of the ATP lid over bound nucleotide results in restructuring within the *N*-terminal domain that releases the strap (Ali et al., 2006). The strap of each protomer is free to remodel and bond with the opposite protomer. The strap is required for N-terminal dimerization and movement of the strap reveals hydrophobic patches within each *N*-terminal domain that dimerize within the equivalent patch on the opposite monomer (McLaughlin et al., 2004; Richter et al., 2002). Another major structural change that takes place with ATP binding is repositioning between the *N*-terminal and middle domain interface. *N*-terminal dimerization allows Arg 380 of the catalytic loop, found in the middle domain, to interact with the ATP γ-phosphate (Cunningham et al., 2012). Additional contacts between the *N*-terminal and middle domain help to stabilize the closed conformation. Upon hydrolysis of ATP, Hsp90 returns to an open conformation where ADP, inorganic phosphate and mature client are released.

1.8 Hsp90 client interactions

Hsp90 is required for the maturation and activation of a large and diverse group of substrate proteins referred to as 'clients'. Hsp90 clients are define based upon their ability to physically interact with Hsp90 and a decrease in function upon Hsp90 inhibition. A growing list of Hsp90

clients is maintained online: http://www.picard.ch/downloads/Hsp90interactors.pdf (Picard, 2002; Echeverria et al., 2011). A majority of Hsp90 clients are involved in signal transduction while others are involved in innate immunity, RNA modification, viral infection, and more (Zhao et al., 2008; Wang, Y. et al., 2013; Wayne et al., 2011). The diversity and importance of the Hsp90 client base place Hsp90 at the hub of vital regulatory pathways. Hsp90 client interactions differ from other chaperones in that Hsp90 binds to partially or fully folded conformations, rather than unfolded polypeptide chains, to promote maturation and activation of clients. The mechanism behind Hsp90-client protein recognition is still poorly understood.

Early work on Hsp90 clients focused on steroid hormone receptors (SHRs) and kinases (Pratt and Toft, 1997). A 90 kDa protein was found to co-precipitate with v-Src, the first molecularly characterized oncogene, and other virally encoded Src-like kinases (Lipsich et al., 1982; Brugge et al., 1981). Around the same time a 90 kDa protein was also found to be associated with SHRs and the common interactor to both protein groups was identified as Hsp90 (Joab et al., 1984; Schuh et al., 1985). The SHRs progesterone receptor (PR) and glucocorticoid receptor (GR) were found to tightly associate with Hsp90 only when not bound to steroid (Joab et al., 1984; Sanchez et al., 1985). As SHRs are activated when bound to steroid agonists, it was hypothesized that Hsp90 acts as a repressor of SHR activity, keeping them in an apo-receptor state (Dalman et al., 1991). However, structural data revealed that Hsp90 is responsible for remodeling the internal cavity of Hsp90 dependent SHRs making the cavity accessible for hormone binding (Williams and Sigler, 1998; Stancato et al., 1996). Upon ligand binding the receptor dissociates from Hsp90 and is able to translocate to the nucleus to regulate gene expression (Picard, 2006; Grad and Picard, 2007). This context-dependent relationship is also true for client kinases and a large portion of Hsp90 clientele (Caplan, 2003; McClellan et al., 2007).

While common recognition or binding sites for Hsp90 client binding remain elusive, a prevailing determinant of Hsp90 client interaction seems to be conformational instability (Boczek et al., 2015; Taipale et al., 2010; Taipale et al., 2012). This is highlighted by the robust association of Hsp90 with unstable v-Src and only transient association with the more stable normal cellular counterpart c-Src (Falsone et al., 2004; Xu, Y. and Lindquist, 1993; Xu, Y. et al., 1999). This is further supported by examples of oncogenic mutations in EGFR and BRAF that

results in destabilized proteins with increased dependence on Hsp90 interaction (Shimamura et al., 2005; da Rocha Dias et al., 2005; Grbovic et al., 2006; Wan et al., 2004). In this way, Hsp90 is responsible for binding to the open and conformationally labile states of a protein for stabilization and subsequent activation (Vaughan et al., 2006; Kaul et al., 2002). The large binding surface of Hsp90, compared to the defined pocket of other chaperones, may allow Hsp90 to form many low-affinity contacts with client proteins, stabilizing the scattered hydrophobic residues that are characteristic of partially folded intermediates (Karagöz et al., 2014). Once a client protein has bound to Hsp90, the timing of conformational transitions is important for maturation of client proteins (Zierer et al., 2016). Hsp90 does not function in isolation but rather in association with a group of intimately involved co-factors termed 'co-chaperones'. Co-chaperone proteins can provide specificity to Hsp90-client interactions and act as adaptors and regulators of Hsp90 function (Caplan et al., 2007; Polier et al., 2013; Taipale et al., 2012; Zuehlke and Johnson, 2010).

1.9 Hsp90 co-chaperones

In the eukaryotic cytosol, co-chaperones proteins help to regulate and support the function of Hsp90 (Figure 1.4) (Siligardi et al., 2004; Caplan, 2003). They affect the ATPase rate and conformational flexibility of Hsp90, recruit client proteins, and connect Hsp90 with additional factors involved in protein folding and degradation (Li, J. et al., 2012; Cox and Johnson, 2018; Zuehlke and Johnson, 2010). There are more than 20 co-chaperones that have been identified for Hsp90 and many are conserved and functionally equivalent between yeast and humans (Chang and Lindquist, 1994; Johnson, J. L., 2012; Sahasrabudhe et al., 2017). Although a majority of co-chaperones are dispensable for Hsp90 function, alterations in co-chaperone levels can influence Hsp90 client activation and stability (Tranguch et al., 2005; Wang, X. et al., 2006; Marozkina et al., 2010; Cox and Johnson, 2018).

The early stages of the Hsp90 cycle involve client recruitment. Sti1 (stress-induced phosphoprotein 1) is a tetratricopeptide repeat (TPR) domain containing protein and therefore can bind to the *C*-terminal EEVD motifs found in both Hsp70 and Hsp90 (Schmid, A. B. et al., 2012). Simultaneous binding to both chaperones is thought to facilitate the delivery of client from Hsp70 to Hsp90 (Prodromou et al., 1999; Smith, D. F. and Toft, 1993) Sti1 stabilizes Hsp90 in the open conformations and inhibits Hsp90 ATPase activity. Cdc37 (cell division cycle

37 homolog) also facilitates client recruitment, stabilization of Hsp90 in an open conformation and inhibition of ATPase activity however, Cdc37 client recruitment seems to be limited to kinases (Roe et al., 2004; Siligardi et al., 2002). Additional client-specific co-chaperones of Hsp90 include Tah1 (TPR-containing protein associated with Hsp90) and Pih1 (protein interacting with Hsp90) that are involved specifically with chromatin remodeling complexes and small ribonucleoprotein (RNP) maturation (Eckert et al., 2010; Jiménez et al., 2012). The early acting co-chaperones stabilize Hsp90 in an open conformation, preventing ATPase activity, and allowing client binding.

Hsp90 needs to transition from an open to closed state before ATP hydrolysis can occur. Sti1 can be displaced by the co-operative action of Cpr6 (cyclosporine-sensitive proline rotamase 6) with either Aha1 (activator of Hsp90 ATPase) or Sba1 (sensitivity to benzoquinone ansamycins) (Harst et al., 2005; Richter and Buchner, 2011; Li, J. et al., 2012). Together these co-chaperones support *N*-terminal dimerization and the displacement of Sti1. Cpr6, is a TPR-containing peptidyl-prolyl cis-trans isomerare (PPIase). The role of PPIases in Hsp90 regulation is still poorly understood (Freeman et al., 1996; Cox et al., 2007; Pirkl and Buchner, 2001). Aha1 promotes the formation of the *N*-terminally dimerized state and simulates the ATPase activity of Hsp90 (Meyer et al., 2004). Sba1 promotes and stabilizes the closed conformation of Hsp90, slowing the dissociation of the *N*-terminal domains and ADP release to facilitate the maturation of client (Richter et al., 2004; McLaughlin et al., 2006; Ali et al., 2006; Graf et al., 2014). Returning to an open conformation allows for release of mature client and 'resets' Hsp90 for further rounds of client binding and release. In higher eukaryotes, the co-chaperone CHIP (carboxyl terminus of Hsp70-interacting protein) is present and contains both a TPR and ubiquitin ligase domain (Ballinger et al., 1999; Zhang, M. et al., 2005; Xu, Zhen et al., 2006). CHIP interacts with Hsp70 or Hsp90 via the TPR domain and ubiquitinates Hsp70/Hsp90 client proteins to target them to the proteasome for degradation (Connell et al., 2001; Kundrat and Regan, 2010). The functional cycle and the effect that the Hsp90 cycle has on client proteins is poorly understood. Developing an understanding of how co-chaperones regulate the Hsp90 cycle and the interplay between co-chaperones will further elucidate the mechanism of Hsp90 action. The co-chaperones highlighted in this thesis are discussed in greater detail below.

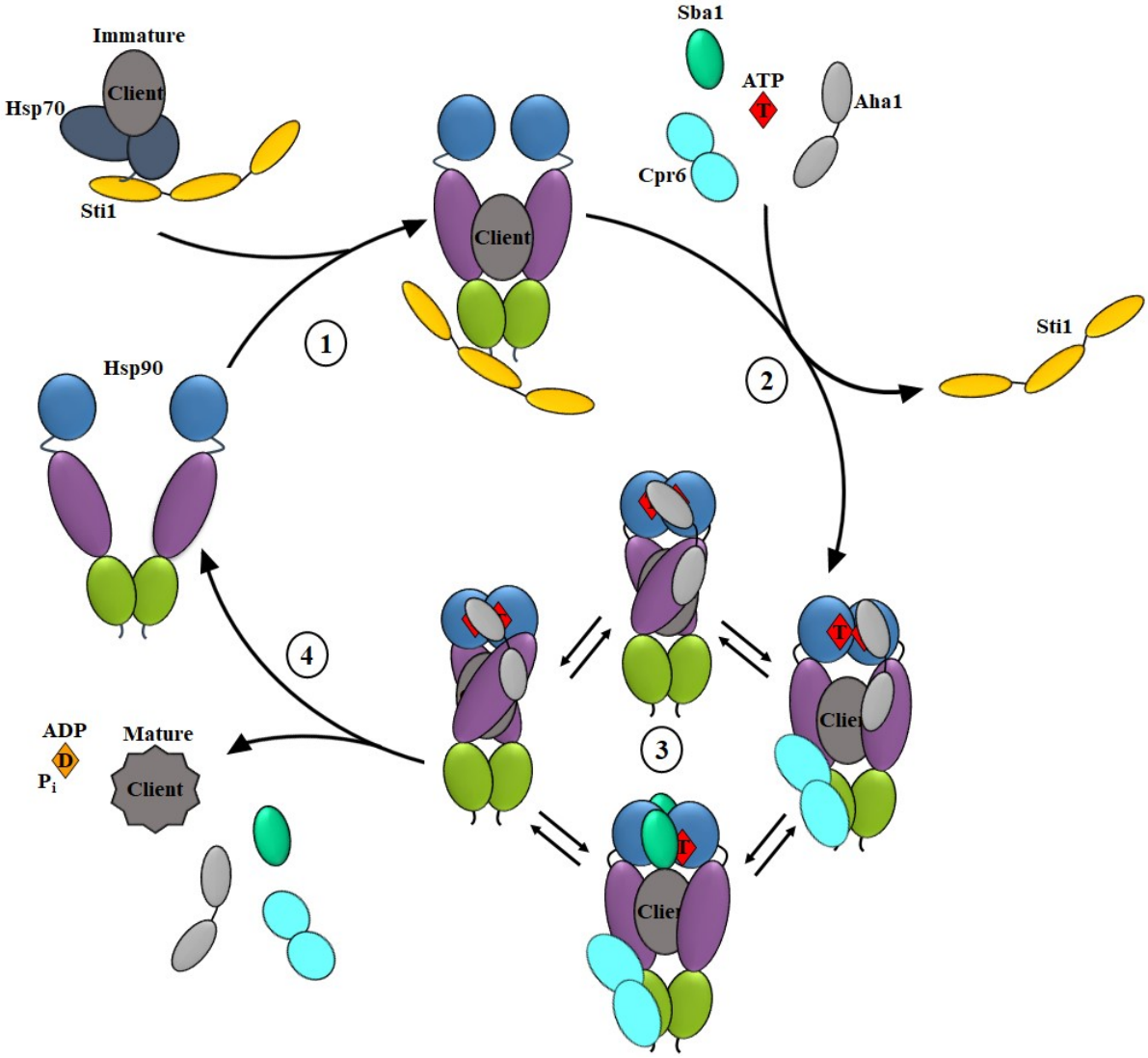

Figure 1.4 Simplified model of the Hsp90 client activation cycle with co-chaperones.
1. Immature client proteins associated with the Hsp70 chaperone system are recruited to Hsp90 by Sti1. **2.** Binding of Cpr6, ATP, Aha1 and/or Sba1 results in the displacement of Sti1 and Hsp90 *N*-terminal dimerization. **3.** Hsp90 occupies a variety of closed conformations where the middle and *N*-domains reposition and a more compact state is achieved. **4.** Upon ATP hydrolysis, mature client is released along with ADP, inorganic phosphate (P_i), and bound co-chaperones, restoring Hsp90 to an open conformation.

1.9.1 Sti1

Sti1 (Sti1 or Hsp70-Hsp90 organising protein (HOP) in mammals) is a ubiquitously expressed Hsp90 co-chaperone (Johnson, J. L. and Brown, 2009; Nicolet and Craig, 1989; Honoré et al., 1992). Sti1 contains three TPR domains (TPR1, TPR2A and TPR2B) each comprised of three TPR motifs, as well as two domains rich in aspartate and proline (DP domains) (DP1 and DP2) (Nelson et al., 2003; Odunuga et al., 2004). Each TPR domain contains an amphipathic channel that directs protein-protein interactions (Blatch and Lässle, 1999). The TPR1 and TPR2B domains both have affinity for the *C*-terminal IEEVD motif of Hsp70 and TPR2A binds the *C*-terminal MEEVD motif of Hsp90 (Schmid, A. B. et al., 2012; Prodromou et al., 1999; Scheufler et al., 2000).

Sti1 is involved in Hsp90 client recruitment and inhibits the ATPase activity of Hsp90 by preventing *N*-terminal dimerization. The simultaneous binding of Sti1 to Hsp70 and Hsp90 forms a macromolecular complex for the transfer of client from Hsp70 to Hsp90 (Wegele et al., 2006; Chen, S. and Smith, 1998). Sti1 is not essential in yeast and mammals however, mutations in Sti1 impair client folding and also result in deficiencies under stress conditions (Chang et al., 1997; Walsh et al., 2011). Sti1 is part of the minimal complement of proteins (Hsp90, Hsp70, Hsp40, Sti1, and Sba1) required for the *in vitro* reconstitution of hormone receptors (Rajapandi et al., 2000; Morishima et al., 2000; Johnson, B. D. et al., 1998). Sti1 is a non-competitive inhibitor of Hsp90 ATPase activity (Richter et al., 2003; Prodromou et al., 1999). Binding of a single Sti1 monomer to the Hsp90 dimer is sufficient for inhibition of the ATPase activity of Hsp90 (Li, J. et al., 2011). Sti1 induces a conformational change in Hsp90 that prevents the association of the *N*-terminal domains (Siligardi et al., 2002; Hessling et al., 2009).

1.9.2 Sba1

Sba1 (p23 in mammals) is the smallest known Hsp90 co-chaperone and is broadly expressed throughout eukaryotes (Garcia-Ranea et al., 2002; Johnson, J. L. and Brown, 2009). Sba1 consists of two domains: a stably folded *N*-terminal domain and an unstructured acidic *C*-terminal tail (Felts and Toft, 2003; Weaver et al., 2000). The *N*-terminal domain is sufficient for Sba1 interaction with Hsp90 (Weikl et al., 1999; Weaver et al., 2000; Ali et al., 2006). Specifically the first 15 residues of the *N*-terminal domain and a conserved motif (104-

WPRLTKEK-110) have been shown to be important for the Hsp90 dependent activity of Sba1 (Forafonov et al., 2008). The *C*-terminal tail is important for the independent chaperoning activity of Sba1 and may be important for cooperative conformation stabilization of Hsp90 clients (Freeman et al., 1996; Weikl et al., 1999; Weaver et al., 2000).

Sba1 was first identified in complex with Hsp90 in the presence of a SHR (Johnson, J. L. et al., 1994; Johnson, J. L. and Toft, 1994). The presence of Sba1 in complex with Hsp90 is dependent on nucleotide binding as inhibition of Hsp90 and mutations that prevent Hsp90 binding to ATP eliminate interaction of Sba1 (Sullivan et al., 1997; Obermann et al., 1998; Johnson, J. L. and Toft, 1994). The conformational changes that accompany Hsp90 ATP binding are also important (Siligardi et al., 2004; Chadli et al., 2000; Prodromou et al., 1997). Sba1 cannot bind to the *N*-terminus of Hsp90 in isolation; ATP-dependent *N*-terminal dimerization is required for Sba1 binding (Prodromou et al., 2000; Siligardi et al., 2004). This is highlighted by the crystal structure of Hsp82 in complex with Sba1 and adenyly-imidodiphosphate (AMP-PNP), a non-hydrolysable ATP analogue, that demonstrates Sba1 interacts at the interface of the Hsp90 *N*-terminal domains (Ali et al., 2006). Binding of Sba1 results in inhibition of the ATPase activity of Hsp90 (Richter et al., 2004; Siligardi et al., 2004; McLaughlin et al., 2006). The inhibition of the ATPase activity of Hsp90 was initially attributed to Sba1 blocking rearrangement of the catalytic loop (Panaretou et al., 2002; Martinez-Yamout et al., 2006). It has now been shown that Sba1 binding results in slowing the release of ADP from Hsp90 (Graf et al., 2014). Sba1 stabilizes the Hsp90-client complex, which facilitates client maturation (Johnson, J. L. and Toft, 1994; Johnson, J. L. et al., 1994; Siligardi et al., 2004).

1.9.3 Aha-type co-chaperones

The co-chaperone Aha1 is a robust stimulator of the low intrinsic ATPase activity of Hsp90 and homologues of Aha1 are conserved across eukaryotes (Lotz et al., 2003; Panaretou et al., 2002; Retzlaff et al., 2010). Aha1 consists of two similarly-sized domains connected by a linker region (Figure 1.5) (Koulov et al., 2010). Mammals possess two Aha1 homologues, Ahsa1 and Ahsa2. *S. cerevisiae*, expresses a canonical Aha1 protein, Aha1p, as well as Hch1p (high copy suppressor of Hsp82p) which corresponds only to the *N*-terminal domain of Aha1 (Figure 1.6) (Nathan et al., 1999; Lotz et al., 2003; Horvat et al., 2014). Aha1 interacts with Hsp90 in an anti-parallel fashion: the *N*-terminal domain of Aha1 binds to the middle domain of Hsp90 and the *C*-

terminal domain of Aha1 binds to the *N*-terminal domain of Hsp90 (Figure 1.5) (Lotz et al., 2003; Retzlaff et al., 2010; Meyer et al., 2004). The extensive networks of complementary charged residues between the *N*-terminal domain of Aha1 and the middle domain of Hsp90 results in these domains being the primary interaction sites for the two proteins (Figure 1.5) (Meyer et al., 2003; Meyer et al., 2004; Panaretou et al., 2002; Retzlaff et al., 2010). This co-crystal structure shows binding of the Aha1 *N*-terminal domain is accompanied by conformational changes in the Hsp90 catalytic loop (residues 370-390) (Meyer et al., 2004). Aha1 contains a conserved RKxK motif (residues 59-62) that is required for remodeling of the catalytic loop (Horvat et al., 2014; Meyer et al., 2004). Mutations of residues within the hydrophobic interface result in reduced Aha1 affinity and reduced activation of Hsp90 ATPase activation by Aha1 (Meyer et al., 2004).

The conformational rearrangements that accompany the binding of the *N*-terminal domain of Aha1 to the middle domain of Hsp90 reveal only a part of the mechanism of Hsp90 ATPase stimulation by Aha1p. Robust stimulation of Hsp90 ATPase activity requires both domains of Aha1 (Meyer et al., 2004; Lotz et al., 2003; Panaretou et al., 1998). The *N*-terminal domain of Aha1p alone and its homolog Hch1p can only weakly stimulate the ATPase activity of Hsp90 (Panaretou et al., 2002; Lotz et al., 2003; Armstrong et al., 2012; Horvat et al., 2014; Meyer et al., 2004). Fusion of the *C*-terminal domain of Aha1p to Hch1p enhances the ability of Hch1p to stimulate the ATPase of Hsp90, but still to a much lower level than the full length Aha1p (Horvat et al., 2014). This supports the findings that Hch1p and Aha1p are not functional homologues. Hch1p and Aha1p differ in their ability to rescue the expression of temperature sensitive Hsp90 mutants and their ability to alter cell sensitivity to Hsp90 inhibitors (Armstrong et al., 2012; Horvat et al., 2014). Interestingly, Hch1p and Aha1p share the conserved RKxK motif that is important for remodeling the catalytic loop as well as the *N*-terminal NxNNWHW motif (Figure 1.6) (Meyer et al., 2004; Horvat et al., 2014). As the most potent stimulator of the low intrinsic ATPase rate of Hsp90, further examination of both the conserved and distinct motifs among Aha1 homologues will provide insight into the role this co-chaperone family plays in Hsp90 regulation and the mechanism of Hsp90 ATPase activity.

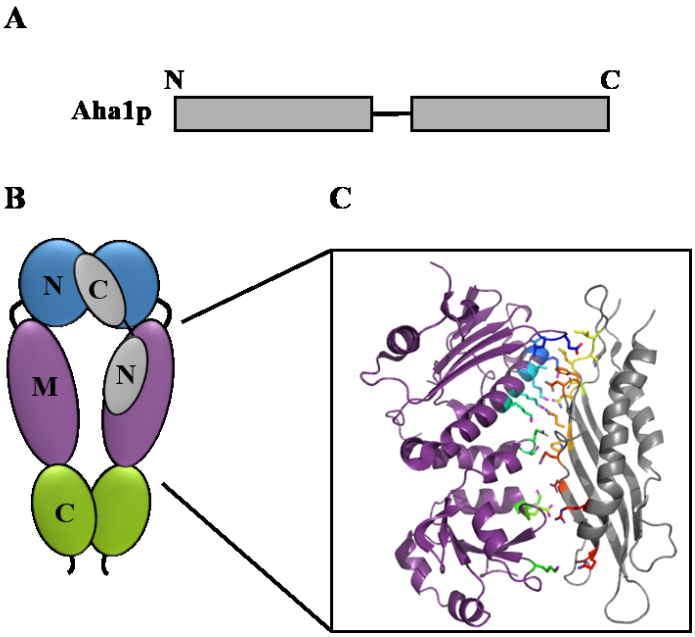

Figure 1.5 Structure of Aha1 and interaction with Hsp90.

A. Aha1 is a two domain protein joined by a flexible linker region. **B.** The *N*-terminal domain of Aha1p binds to the middle domain of Hsp90 and the *C*-terminal domain of Aha1 binds to the *N*-terminal domain of Hsp90 in the closed conformation. **C.** Crystal structure of between the middle domain of Hsp90 (purple) and the *N*-terminal domain of Aha1 (grey) with the core interaction sites shown in rainbow (1USV (Meyer et al., 2004)).

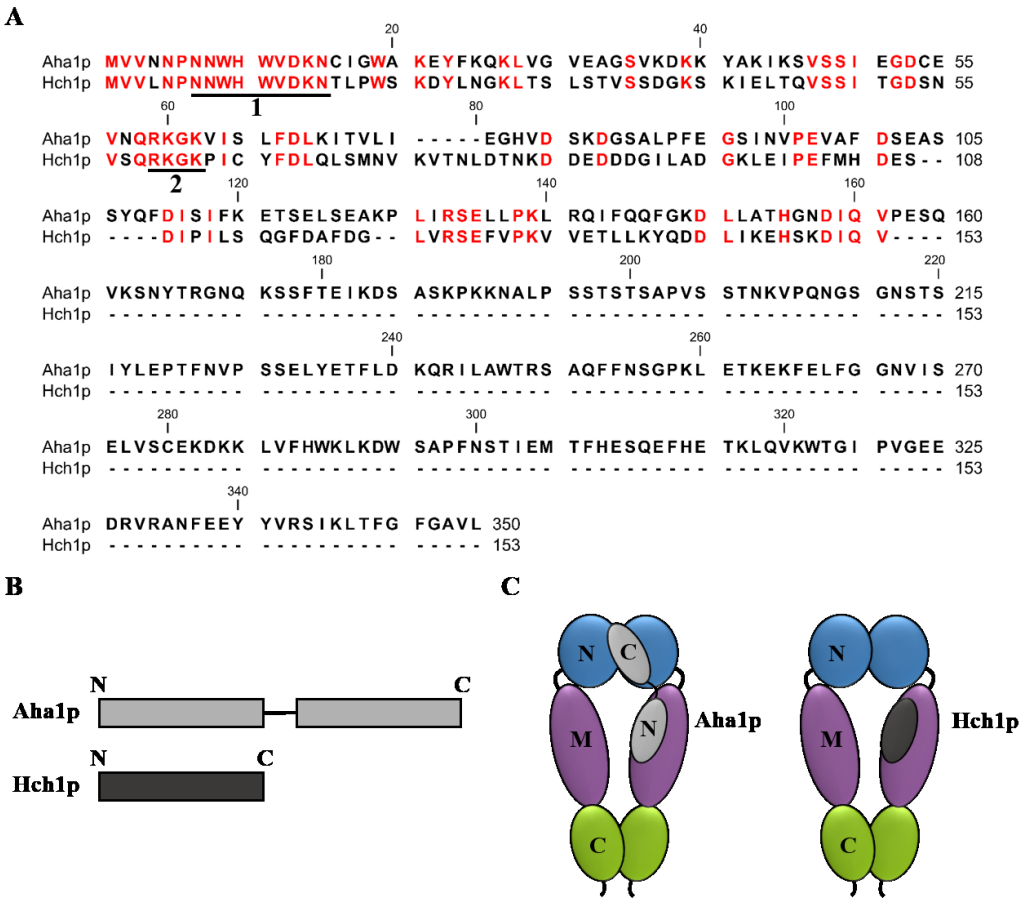

Figure 1.6 Aha-type co-chaperones in *S. cerevisiae*.

A. Sequence alignment of Aha1p and Hch1p from *S.* cerevisiae with conserved motifs highlighted in red. The conserved NxNNWHW and RKxK motifs are underlined number 1 and 2 respectively **B.** Domain structures illustrating that Hch1p corresponds the *N*-terminal domain of Aha1p. **C.** Hch1p binds to the middle of Hsp90 as the *N*-terminal domain of Aha1p.

1.10 Post-translational modifications of the Hsp90 system

Hsp90 function and regulation can be influenced by post-translational modifications (Scroggins and Neckers, 2007; Prodromou and Morgan, 2016). More than 150 post-translational modifications have been identified throughout all domains of Hsp90. They include phosphorylation, SUMOylation, acetylation, methylation, ubiquitylation and S-nitrosylation (Mollapour and Neckers, 2012). The role that phosphorylation and other post-translational modifications play in Hsp90 regulation is only beginning to be understood (Walton-Diaz et al., 2013). Post-translational modifications are able to affect Hsp90 dimerization, ATPase activity, co-chaperone binding, and ultimately regulate client maturation (Soroka et al., 2012; Mollapour and Neckers, 2012; Li, J. and Buchner, 2013). Casein kinase 2 (CK2)-mediated phosphorylation of a conserved threonine reside (Thr 22) of Hsp90, provides a good example of the complexities that post-translational modifications play in Hsp90 regulation. CK2 mediates phosphorylation of Hsp90 and is an Hsp90 client, highlighting that clients can also be regulators of the post-translational modification status of Hsp90 (Mollapour, Tsutsumi, Kim et al., 2011; Mollapour, Tsutsumi, Truman et al., 2011). There is a feedback mechanism that exists for both the activity and activation of Hsp90 and clients. Additionally, while Thr 22 is in the *N*-terminal domain of Hsp90, it is important for interaction with the catalytic loop in the middle domain to stabilize the ATP bound, ATPase-competent state of Hsp90 (Mollapour, Tsutsumi, Truman et al., 2011). Post-translational modifications throughout Hsp90 are able to regulate conformational changes and their effects are not restricted to the domains of Hsp90 that they modify (Soroka et al., 2012; Martínez-Ruiz et al., 2005; Retzlaff et al., 2009). Non-phosphorylatable and phospho-mimetic Thr 22 mutants have defects in Hsp90-dependent chaperoning of some clients (*e.g.* v-Src and Ste11) but not others (*e.g.* GR) (Mollapour, Tsutsumi, Truman et al., 2011). This highlights that post-translational modifications may play a role in differentially regulating Hsp90 in order to accommodate its diverse client base and can both positively and negatively regulate Hsp90 activity. Phosphorylation of Thr 22 also results in increased sensitivity to Hsp90 inhibitors highlighting that post-translational modifications can also change cell sensitivity to Hsp90 inhibitors (Mollapour, Tsutsumi, Truman et al., 2011).

The relationship between post-translational modifications and co-chaperones is complex with each co-chaperone and post-translational modification differentially affecting each other and Hsp90. Mutants of Hsp90 at Thr 22 have reduced interaction with the co-chaperone Aha1,

while the overexpression of Aha1 is able to overcome the chaperoning defects of these mutants (Mollapour, Tsutsumi, Truman et al., 2011). Interestingly, it is suggested that post-translational modifications in higher eukaryotes may represent evolutionary substitutions for co-chaperones found in lower eukaryotes (Zuehlke et al., 2017). Post-translational modification of co-chaperones have also been identified that affect their regulation of Hsp90 (Dunn et al., 2015; Vaughan et al., 2008). Post-translational modifications add an additional layer of regulation to the Hsp90 system and may offer novel strategies for improved drug sensitivity to Hsp90 inhibitors.

1.11 The Hsp90 chaperone network in disease

Hsp90 is involved in regulating a vast number of cellular functions, including signal transduction, cellular trafficking, chromatin remodeling, cell survival, differentiation, and autophagy (Zuehlke and Johnson, 2010). The diverse and essential role of Hsp90 in cells initially led to skepticism about the potential for targeting Hsp90 in disease. However, the ability to simultaneously disrupt multiple signalling pathways and mutant proteins chaperoned by Hsp90, provides a unique combinatorial approach to addressing the complexities of disease.

1.11.1 Hsp90 in cancer

The role of Hsp90 in disease has been best characterized in terms of cancer (Whitesell and Lindquist, 2005; Barrott and Haystead, 2013). As cancer cells are challenged with surviving under stress conditions and have increased mutated and damaged proteins, it is not surprising that they commonly display increased expression of Hsp90 and other Hsps (Chant et al., 1995; Chatterjee et al., 2017). Recognition that Hsp90 was the target of an anti-tumour drug led to a burst in identification of Hsp90 clients and implicated Hsp90 as a novel target for cancer therapy (Whitesell et al., 1994). Cancer-relevant Hsp90 clients include EGFR, BCR-ABL, BRAF, p53, and many others (Miyata et al., 2013). Hsp90 plays an important role in stabilizing the active conformations of mutant proteins that occur through transformation. The diverse client base means that Hsp90 is involved in all hallmarks of cancer development including metastasis, angiogenesis, regulation of tumour growth and invasion (Hanahan and Weinberg, 2011). An increased demand and central role for Hsp90 in cancer cells has been suggested to be the reason for the cancer cells displaying greater sensitivity to Hsp90 inhibitors compared to normal cells (Chiosis et al., 2003; Kamal et al., 2003). Additional explanations for this phenomenon currently

under examination include altered states of Hsp90 post-translational modification, elevated affinity for the Hsp90 complexes that form in cancer cells, and variability in Hsp90-complexes. In the model systems *Drosophila* and *Arabidopsis*, Hsp90 allows the accumulation of inherent genetic mutations at the protein level (Rutherford and Lindquist, 1998; Queitsch et al., 2002). In this same way, Hsp90 may function as a buffer in cancer cells, supporting inherently unstable proteins that result from genetic alterations characteristic of cancer cells. Not only does Hsp90 inhibition have the potential to simultaneously disrupt multiple signalling pathways but it may also restrict the acquisition of mutations responsible for drug resistance experienced with other anti-tumour agents. Our understanding of the highly connected relationship between Hsp90 and cancer is constantly evolving.

1.11.2 Hsp90 in other diseases

The extensive role of Hsp90 in cells implicates Hsp90 in the maintenance and pathogenesis of a broad array of diseases. As in cancer, Hsp90 often supports propagation of disease through stabilizing mutant protein conformations that should otherwise be degraded. For example Hsp90 stabilizes mutant Leucine-rich repeat kinase 2 (LRRK2), a kinase that has been implicated in both familial and sporadic cases of Parkinson's disease (Wang, L. et al., 2008). Inhibition of Hsp90 leads to proteasomal degradation of mutant LRRK2, limiting neuronal toxicity. In tauopathies, Hsp90 has been shown to interact only with mutant tau proteins and inhibition of Hsp90 leads to the elimination of aggregated tau (Luo et al., 2007; Shelton et al., 2017). In neurodegenerative diseases, Hsp90 inhibition is shown to reduce aberrant neuronal protein activity and subsequent formation of toxic aggregates (Luo et al., 2010). Success in preclinical studies has also led to the investigation of Hsp90 inhibitors in the treatment of autoimmune and inflammatory diseases (Liu, Y. et al., 2015; Tukaj and Węgrzyn, 2016). As autoimmune diseases represent a broad group of diseases that are generally poorly understood, the direct role of Hsp90 remains elusive. New evidence has shown that necroptosis, a form of programmed cell death, can contribute to the pathogenesis of human diseases, including neurodegenerative, inflammatory, and autoimmune diseases (Galluzzi et al., 2017; Zhou and Yuan, 2014). Hsp90 is now known to chaperone the core components of the necroptosis pathway and provides a novel strategy for treatment necroptosis-related diseases (Yang, C. K. and He, 2016).

1.11.3 Hsp90 inhibitors

The first Hsp90 inhibitor identified was the natural product geldanamycin (GA) (Whitesell et al., 1994; DeBoer et al., 1970). GA was initially suggested to be a tyrosine kinase inhibitor due to its potent anti-tumour activities and its ability to inhibit the oncogenic kinase activity of v-Src (DeBoer et al., 1970; Whitesell et al., 1992). However, GA was unable to inhibit the activity of purified v-Src and upon further investigation the anti-proliferative activity of GA was revealed to be a result of interaction with Hsp90 (Stebbins et al., 1997; Whitesell et al., 1992; Whitesell et al., 1994). Structural and biochemical studies show that GA binds to the nucleotide binding pocket in the *N*-terminal domain of Hsp90, restricting Hsp90 to an open conformation, blocking chaperone function and resulting in the loss of Hsp90 client activation (Roe et al., 2004; Neckers, 2006; Khandelwal et al., 2016). GA, along with other natural product inhibitors including radicicol and herbimycin, have shown poor clinical potential due to limited *in vivo* stability, poor solubility, and high toxicity (Supko et al., 1995; Neckers and Workman, 2012). Structure-activity analysis of these natural product inhibitors has aided in the development of new derivatives (17-allylamino-17-demethoxygeldanamycin (17-AAG) and 17-dimethylaminoethylamino-17-demethoxygeldanamycin (17- DMAG)) with increased potency and affinity for Hsp90 in cancer cells (Sausville et al., 2003; Solit and Chiosis, 2008). Continued structure-based design strategies led to the development of NVP-AUY922 and STA-9090 (Ganetespib) that progressed through to clinical trials (Menezes et al., 2012; Gaspar et al., 2010; Eccles et al., 2008; Lin, T. et al., 2008; Neckers and Workman, 2012).

Competitive inhibitors of the Hsp90 ATP binding pocket are considered ‘classical’ Hsp90 inhibitors (Khandelwal et al., 2016; Wang, Y. and McAlpine, 2015). These inhibitors have been shown to have greater accumulation and increased toxicity in malignant cells compared to normal tissue, supporting their potential for selective cytotoxicity (Chiosis et al., 2003; Chiosis and Neckers, 2006; Kamal et al., 2003). While the mechanisms responsible for the preferential accumulation of Hsp90 inhibitors in tumour cells is not fully understood, the increased expression of Hsp90 in tumours, altered modifications and protein interactions, as well as changes in localization are all suggested to play a part (Barrott and Haystead, 2013). In addition, oncogenic mutations, that facilitate the transformation of normal cells into malignant cells, often results in unstable oncoproteins that rely heavily on Hsp90 chaperone function

(Whitesell and Lindquist, 2005; Neckers, 2002). Hsp90 is known to buffer the proteome, promoting the evolution of heritable traits (Rutherford and Lindquist, 1998; Queitsch et al., 2002). This means that targeting Hsp90 may limit the acquisition of genetic variation and the accumulation of mutations that are the foremost reason for drug resistance in other cancer therapies (Garraway and Jänne, 2012; Whitesell et al., 2014). Combination therapies with Hsp90 offer a way to enhance anti-tumour activity and limit drug resistance of current target-based therapies.

Hsp90 inhibition shows positive impacts on reducing specific oncogenic client levels, but the complexities of Hsp90 are often not taken into account. The reach of Hsp90 clients extends beyond oncoproteins and also includes tumor suppressors whose degradation upon Hsp90 inhibition would support metastatic growth (Vartholomaiou et al., 2016). In addition, inhibition of the ATPase activity of Hsp90 results in the upregulation of prosurvival mechanisms, including the heat shock response (Whitesell and Lindquist, 2005; Morimoto, 1998; Wang, Y. and McAlpine, 2015). The upregulation in chaperones upon Hsp90 inhibition is part of the rationale for using Hsp90 inhibitors in the treatment of neurodegenerative diseases where protein disaggregation and increased protein folding are advantageous (Klettner, 2004; Luo et al., 2010). However, this is an undesired side effect for the use of Hsp90 inhibitors in cancer treatment. Non-classical inhibitors that bind Hsp90 outside of the nucleotide binding pocket may provide a promising alternative for advancing Hsp90 therapeutics in cancer as they have been shown to inhibit Hsp90 without upregulating the heat shock response (Garg et al., 2016).

There is a distinct nucleotide binding site found in the *C*-terminus of Hsp90 (Soti et al., 2003). The role of this nucleotide binding site is still unclear in terms of the Hsp90 cycle, however, it has been shown to provide an alternative binding site for inhibitors (Marcu et al., 2000; Wang, Y. and McAlpine, 2015). The natural product novobiocin (NB), binds to the *C*-terminal nucleotide binding pocket of Hsp90 and results in destabilization of Hsp90 clients (Marcu et al., 2000). NB disrupts the interaction of Sti1 and Hsp70 with Hsp90 and can allosterically modulate the N-terminal nucleotide binding pocket, but does not induce the prosurvival heat-shock response (Marcu et al., 2000). Subsequent structural-activity relationship studies on NB have led to improvements in specificity and potency (Burlison et al., 2006; Donnelly and Blagg, 2008). Additional *C*-terminal inhibitors have been reported and do not

induce the heat shock response (Eskew et al., 2011; Donnelly and Blagg, 2008; Yin et al., 2009). In order to advance *C*-terminal inhibitors into the clinic, an exact understanding of the structural interactions is necessary.

1.11.4 Hsp90 co-chaperone inhibitors

The interaction of co-chaperone proteins with Hsp90 provides an alternative mechanism through which Hsp90 can be targeted for inhibition. Co-chaperones have distinct Hsp90 functions and are uniquely regulated in different diseases. Targeting protein-protein interactions of co-chaperones with Hsp90 would be a more specific approach for targeting Hsp90 in disease. A majority of work on the inhibition of co-chaperones has focused on disrupting the interaction of Cdc37 and Hsp90. Cdc37 plays a specialized role in the maturation and stabilization of kinases, which are key regulators of protein activation and are therefore critically involved in cancer progression (Gross et al., 2015; Giamas et al., 2007). Hsp90-Cdc37 regulated kinases include EGFR, v-Src, Raf-1, HER-2/ErbB2 and other kinases intimately involved in cell proliferation and tumour progression (Smith, J. R. and Workman, 2009; Polier et al., 2013). Inhibitors thought to disrupt the interaction of Cdc37 with Hsp90 show degradation of Hsp90-dependent client kinases and anti-metastatic activities in multiple cancer cell types (Zhang, T. et al., 2008; Smith, J. R. et al., 2009; Garg et al., 2016; Gray et al., 2007). Alternatively, inhibition of the interaction of Sba1 with Hsp90 shows no impact on the stability of kinases but results in the destabilization of client SHRs and cancer cell death via apoptosis (Hieronymus et al., 2006; Patwardhan et al., 2013). Inhibition of TPR domain containing proteins has also been investigated with preliminary work showing selective cytotoxic activity in cancer cells (Horibe et al., 2011). Targeting the interaction of co-chaperone proteins with Hsp90 provides a more directed approach to Hsp90 inhibition. As the understanding of co-chaperone regulation of Hsp90 continues to progress, there is promise for the development of improved means of Hsp90 inhibition.

1.12 Rationale

Hsp90 is an abundant and essential molecular chaperone involved in the activation and maturation of a diverse group of client proteins. Hsp90 client proteins include key regulatory kinases, hormone receptors, and transcription factors and therefore Hsp90 is known to play a role in the proliferation of cancer, neurodegenerative, and viral diseases (Schopf et al., 2017). For the maturation and activation of client proteins, Hsp90 proceeds through an ATP coupled

conformational cycle in concert with co-chaperone proteins (Cox and Johnson, 2018; Taipale et al., 2014). Co-chaperones provide directionality to the Hsp90 cycle, supporting Hsp90 dynamics and the activation of a varied client base (Li, J. and Buchner, 2013; Hessling et al., 2009). The co-chaperone Aha1 is the most potent stimulator of the Hsp90 ATPase activity identified to date (Lotz et al., 2003; Panaretou et al., 2002; Retzlaff et al., 2010; Li, J. et al., 2013). The role of Aha1 is complex, with Aha1 activity known to limit the activation of some Hsp90 clients while supporting others (Wang, X. et al., 2006; Koulov et al., 2010; Sun et al., 2012). There remains a significant gap in understanding the kinetics of Hsp90 conformational changes and the mechanism of Aha1 regulation. In this thesis, I focus on furthering our understanding of the Aha-type co-chaperones and their impact on Hsp90 activity. Chapter 3 and 4 detail structural and functional analysis of conserved motifs of the Aha-type co-chaperone family. Chapter 3 focuses on the *N*-terminal NxNNWHW motif showing that, in contrast to previous reports, it is important for the function of Aha-type co-chaperones. Chapter 4 looks at the role of the RKxK motif in Aha-type co-chaperones, showing that mutations differentially impair Hsp90 ATPase stimulation and *in vivo* function. Chapter 5 outlines expanded models and phenotypes available to further the investigation of Aha-type co-chaperone function.

Chapter 2 Materials and Methods

2.1 Materials

2.1.1 Reagents

The following chemicals, reagents, enzymes, and commercial kits were used according to the manufacturer's instructions and in adherence with the recommendations and procedures outlined by the University of Alberta Environmental Health and Safety office and Workplace Hazardous Materials Information Systems (WHIMIS).

Table 2.1 List of chemicals and reagents

Chemical/Reagent	**Supplier**
5-fluoroorotic acid	Toronto Research Chemicals
ß-Mercaptoethanol	BioShop Canada Inc.
Acetic acid; glacial	Thermo Fisher Scientific
Acetone	Thermo Fisher Scientific
Acrylamide (30%; 29:1)	BioRad Laboratories
Adenosine diphosphate (ADP)	MP Biomedicals, LLC
Adenosine triphosphate (ATP)	Fisher BioReagents
Adenylyl-imidodiphosphate (AMP-PNP)	Sigma-Aldrich Life Sciences
Agar	Thermo Fisher Scientific
Agarose (UltraPure™)	Thermo Fisher Scientific
Amino Acids	MP BioChemicals, LLC
Ammonium Persulphate (APS)	Life Technologies Inc.
Ammonium Sulphate	Thermo Fisher Scientific
Ampicillin	Sigma-Aldrich Life Sciences
Bovine serum albumin (BSA)	Hoffmann-La Roche Ltd.
Brilliant Blue R-250	Fisher BioReagents
Bromophenol Blue	BDH Laboratory Sciences
Butanol	Thermo Fisher Scientific
CHAPS	Thermo Fisher Scientific
Complete, EDTA-free protease inhibitor cocktail tablets	Hoffmann-La Roche Ltd.
Coomassie Blue Stain	BioRad Laboratories
Delbecco's phosphate buffered saline	Mediatech Inc.
Deoxyribonucleotide triphosphate (dNTP)	Roche Diagnostics
Dextrose (D-Glucose)	Fisher BioReagents
Dimethyl pimelimidate (DMP)	Thermo Fisher Scientific
Dimethyl sulfoxide (DMSO)	Thermo Fisher Scientific
Disodium phosphate (Na_2HPO_4)	Thermo Fisher Scientific
Dithiothreitol (DTT)	Roche Diagnostics
Dulbecco Modified Eagle Medium (DMEM) (high glucose) with L-glut and Na Pyruvate	Gibco, Thermo Fisher Scientific
Ethanol	Thermo Fisher Scientific

Ethanolamine	Thermo Fisher Scientific
Ethylenediaminetetraacetic acid (EDTA)	Thermo Fisher Scientific
Fetal Bovine Serum (FBS)	Gibco, Thermo Fisher Scientific
Filter Paper	Munktel
Galactose	Fisher BioReagents
GeneRuler 1 kb DNA Ladder	Fermentas-Thermo Fisher Scientific
Geneticin (G418)	HyClone
Glutamic acid monosodium salt monohydrate	ACROS organics
Glycerol	Thermo Fisher Scientific
Glycine	MP Biomedicals, LLC
HALT Protease Inhibitor Cocktail, EDTA-free	Thermo Fisher Scientific
Hepes	Brand BioReagents
Hydrochloric acid (HCl)	Thermo Fisher Scientific
Hydrogen Peroxide (H_2O_2)	Thermo Fisher Scientific
Hygromycin	Goldbio
Imidazole	Thermo Fisher Scientific
Iodoacetamide	Sigma-Aldrich Life Sciences
Isopropanol	Thermo Fisher Scientific
Isopropyl-β-D-thiogalactopyranoside (IPTG)	OmniPur
L-glutamine (GlutaMAX supplement)	Thermo Fisher Scientific
Lithium Acetate (LiAc)	Acros Organics
Luminal (3-Aminophthalhydrazide)	Sigma-Aldrich Life Sciences
Luria Broth (LB), Miller	Thermo Fisher Scientific
Magnesium acetate (Mg(OAc))	Sigma-Aldrich Life Sciences
Magnesium chloride ($MgCl_2$)	Thermo Fisher Scientific
Magnesium sulfate ($MgSO_4$)	Thermo Fisher Scientific
Methanol	Thermo Fisher Scientific
Milk protein	Carnation
MTT (3-(4,5-dimethylthiazol-2-yl)-2,5-diphenyltetrazolium bromide)	Sigma-Aldrich Life Sciences
Nickel Sulphate	Thermo Fisher Scientific
Nicotinamide Adenine Dinucleotide (NADH)	Sigma-Aldrich Life Sciences
Nitrocellulose membranes	BioRad Laboratories
NVP-AUY922	Chemie Tek
Opti-MEM I Serum Reduced Media	Gibco, Thermo Fisher Scientific
p-Coumaric Acid	Sigma-Aldrich Life Sciences
PageRuler^{TM} Protein Ladder Plus	Fermentas-Thermo Fisher Scientific
PCR Primers	Integrated Device Technology
PEG3550	Thermo Fisher Scientific
Peptone	Becton, Dickinson and Company (BD)
Phenylmethylsulfonylfluoride (PMSF)	Thermo Fisher Scientific
Phosphoenol Pyruvate (PEP)	Sigma-Aldrich Life Sciences
Polyinosinic:polycytidylic acid (poly(I:C))	Sigma-Aldrich
Ponceau S	MP Biomedicals, LLC
Potassium Acetate	Thermo Fisher Scientific

Potassium Chloride (KCl)	Thermo Fisher Scientific
Pyruvate Kinase/Lactate Dehydrogenase enzyme from Rabbit muscle (PK/LDH)	Sigma-Aldrich Life Sciences
Raffinose	MP Biomedicals, LLC
RPMI Medium 1640	Gibco, Thermo Fisher Scientific
Salmon Sperm DNA	Thermo Fisher Scientific
Sodium Acetate	EMD Millipore
Sodium Borate	Thermo Fisher Scientific
Sodium Chloride (NaCl)	Thermo Fisher Scientific
Sodium Citrate dihydrate	Thermo Fisher Scientific
Sodium Dodecyl Sulphate (SDS)	Thermo Fisher Scientific
Sodium Hydroxide (NaOH)	Thermo Fisher Scientific
Sodium Phosphate (NaH_2PO_4)	Thermo Fisher Scientific
Sodium Pyruvate (100x)	Gibco, Thermo Fisher Scientific
Sorbitol	Thermo Fisher Scientific
SYBR Safe DNA Gel Stain	Invitrogen - Life Technologies
Tetramethylethylenediamine (TEMED)	Thermo Fisher Scientific
Thiourea	Sigma-Aldrich Life Sciences
Trichloroacetic acid (TCA)	Thermo Fisher Scientific
Tris (tris-(hydrocymethyl)aminomethane) (Tris-Base)	Thermo Fisher Scientific
Tris hydrochloride (Tris-HCl)	Thermo Fisher Scientific
Triton X-100	Thermo Fisher Scientific
Tween 20	Thermo Fisher Scientific
Urea	Thermo Fisher Scientific
Yeast Extract	Becton, Dickinson and Company (BD)
Yeast Nitrogen Base w/o ammonium sulphate	Becton, Dickinson and Company (BD)

Table 2.2 DNA modifying enzymes and buffers

Enzyme or Buffer	**Supplier**
PfuTurbo DNA polymerase	Agilent Technologies
Restriction Digest Enzymes	New England BioLabs (NEB)
Restriction Digest Enzymes Buffer	New England BioLabs (NEB)
T4 DNA Ligase	New England BioLabs (NEB)
T4 DNA Ligase Buffer	New England BioLabs (NEB)
TopTaq DNA Polymerase	QIAGEN
TopTaq DNA Polymerase Buffer	QIAGEN

Table 2.3 Commercial kits

Commercial Kit	Supplier
Improm-II Reverse Transcriptase	Promega, Thermofisher
Nucleospin RNA isolation kit	Macherey-Nagel
PerfecCTa SYBR Green SuperMix Low Rox real-time PCR kit	Quanta Biosciences
QIAGEN PCR Purification Kit	QIAGEN
QIAGEN Plasmid Midiprep Kit	QIAGEN
QIAprep Spin Miniprep Kit	QIAGEN
QIAquick Gel Extraction Kit	QIAGEN
QuikChange^{TM} Mutagenesis	Agilent Technologies

Table 2.4 General Laboratory media and buffers

Media/Buffer	Composition
2DGE Lysis Buffer	7 M Urea, 2 M Thiourea, 4% CHAPS, 30 mM Tris-HCl pH 8.7, 1 mM PMSF, 20 mM DTT, 2 mM Mg(OAc)
2DGE Buffer 1	6 M Urea, 30% Glycerol, 2% SDS, 75 mM Tris-HCl pH 8.8, 1% DTT
2DGE Buffer 2	6 M Urea, 30% Glycerol, 2% SDS, 75 mM Tris-HCl pH 8.8 and 2% Iodoacetamide
ATPase Assay Reaction Buffer (4x)	4 mM PEP, 11 mM Hepes, pH 7.2
Alkaline Lysis Buffer	2.2 M NaOH, 10 mM PMSF, 1M β-Mercaptoethanol
Coomassie Stain (50x)	3.33% (w/v) Brilliant Blue R-250, 10% acetic acid (v/v) in Methanol
Destain	10% (v/v) Ethanol, 10% Glacial Acetic acid (v/v)
6X DNA Loading Dye	0.3 % (w/v) Bromophenol Blue, 30 % (v/v) Glycerol, 0.3 % (w/v) Xylene cyanol
ECL Solution #1	0.45 mM p-Coumaric Acid, 2.5 mM Luminol , 1.5% (v/v) DMSO, 0.1 M Tris pH 8.8
ECL Solution #2	0.02 % (v/v) Hydrogen Peroxide, 0.1 M Tris Base, pH 8.8
Electrode (10x)	1.92 M Glycine, 250 mM Tris Base, 1% (w/v) SDS
Gel Filtration Buffer (Co-Chaperone)	25 mM Hepes, pH 7.2, 50 mM NaCl, 5 mM β-Mercaptoethanol
Gel Filtration Buffer (Hsp90)	25 mM Hepes, pH 7.2, 10 mM NaCl, 5 mM β-Mercaptoethanol
Immobilized Metal Ion Affinity Chromatography (IMAC) Buffer A	25 mM NaH_2PO_4, pH 7.2, 500 mM NaCl , 20 mM Imidazole, 1 mM $MgCl_2$, 5 mM β-Mercaptoethanol
Immobilized Metal Ion Affinity Chromatography (IMAC) Buffer B	25 mM NaH_2PO_4, pH 7.2, 500 mM NaCl,1 M Imidazole, 1 mM $MgCl_2$, 5 mM β-Mercaptoethanol

LiAcTE Buffer	10 mM Tris Base, pH 7.2, 100 mM LiAc, 1 mM EDTA
Luria Broth (LB) media	2.5% (w/v) LB powder
Mammalian Lysis Buffer	50 mM Hepes pH 7.4, 100 mM NaCl, 5 mM $MgCl_2$, 20 mM Na_2MoO_4, 20 mM KF, 20% glycerol, 1% TX-100, 2 mM Na_2VO_4, phosphatase inhibitor cocktail, PhosSTOP
Mammalian IP Lysis Buffer	50 mM Tris pH 7.2, 100 mM Potassium Acetate, 1 mM $MgCl_2$, 20 mM Na_2MoO_4, 1% TX-100, 2 mM Na_2VO_4, phosphatase inhibitor cocktail, PhosSTOP
10X PBS	1.36 M NaCl, 27 mM KCl, 17.6 mM KH_2PO_4, 152 mM Na_2HPO_4, pH 7.4
4X Running Gel Buffer	1.5 M Tris Base, pH 8.8, 0.4 % (w/v) SDS
SDS-PAGE Sample Buffer (6X)	120 mM Tris Base, pH 7.0, 30 % (v/v) Glycerol, 6 % (w/v) SDS, 0.6 % (w/v) Bromophenol Blue Drop
Stacking Gel Buffer	140 mM Tris Base, pH 6.8, 0.11% (w/v) SDS
Stripping Buffer	100 mM Tris-HCl pH 6.7, 2% SDS (w/v), 100 mM ß-Mercaptoethanol
Synthetic Complete (SC) Drop-Out Medium	2% (w/v) Carbon source (Glucose or Galactose or Raffinose), 0.175% Yeast Nitrogen Base, 0.5 % Ammonium Sulphate, Appropriate amino acids
Synthetic Complete (SC) Drop-Out Medium- Amino Acid composition	2 mg/mL Adenine Sulphate, 4 mg/mL Arginine, 10 mg/mL Aspartate, 10 mg/mL Glutamic Acid, 6 mg/mL Isoleucine, 10 mg/mL Leucine, 5 mg/mL Lysine, 2 mg/mL Methionine, 5 mg/mL Phenylalanine, 40 mg/mL Serine, 20 mg/mL Threonine, 2 mg/mL Tyrosine, 15 mg/mL Valine, 33 mg/mL Histidine, 10 mg/mL Tryptophan, 2 mg/mL Uracil
Synthetic Complete (SC) Drop-Out Medium- Monosodium Glutamic Acid (for use with drug selection)	2% (w/v) Carbon source (Glucose or Galactose or Raffinose), 0.175% Yeast Nitrogen Base, 0.1% Monosodium glutamic acid, 40 mM Sodium citrate dehydrate pH 6.2
Tris-buffered saline (TBS) (10x)	1.37 M NaCl, 27 mM KCl, 250 mM Tris Base, pH 8.0
Western Transfer Buffer	25 mM Tris Base, 192 mM Glycine, 20% (v/v) methanol
Yeast Lysis Buffer	50 mM Tris, pH 7.5, 100 mM KCl, 5 mM $MgCl_2$, 20 mM Na_2MoO_4, 20% Glycerol, 5 mM β-mercaptoethanol, HALT EDTA-free protease inhibitor
Yeast Peptone Dextrose (YPD)	1% (w/v) Yeast Extract, 1% (w/v) Peptone, 2% (w/v) Glucose, Galactose or Raffinose

2.1.2 Antibodies

Table 2.5 Antibodies

Antibody	Dilution	Host	Supplier
anti-actin	1:2000	Rabbit	Dr. Gary Eitzen (University of Alberta)
anti-AHA (5D11) monoclonal	1:1000	Mouse	Dr. Paul LaPointe (University of Alberta)
anti-Cdc37 (SPC-142) polyclonal	1:1000	Rabbit	StressMarq Biosciences Inc.
anti-His (D3I10) monoclonal	1:1000	Rabbit	Cell Signalling
anti-HOP (SRA-1500)	1:1000	Mouse	Stressgene, Enzo Life Sciences
anti-Hsp82 (K41220A)	1:1000	Mouse	StressMarq Biosciences Inc.
anti-Hsp90 (clone AC88) monoclonal	1:1000	Mouse	Enzo Life Sciences
anti-Hsp90 (SPA-846) polyclonal	1:1000	Rabbit	Enzo Life Sciences
anti-IRF3 (D83B9) monoclonal	1:1000	Rabbit	Cell Signalling
anti-IRF3 (phospho Ser386) (ab76493) monoclonal	1:1000	Rabbit	abcam
anti-IRF3 (phospho Ser396) (4D4G) monoclonal	1:1000	Rabbit	Cell Signalling
anti-myc (4A6) monoclonal	1:1000	Mouse	Millipore
anti-myc (9E10)	1:1000	Mouse	Dr. Paul LaPointe (University of Alberta)
anti-p23 (JJ#) monoclonal	1:1000	Mouse	Thermo Fisher Scientific
anti-phosphotyrosine (SMC-1570)	1:1000	Mouse	StressMarq Biosciences Inc.
anti-Tetra-His (34670)	1:1000	Mouse	QIAGEN
anti-Tubulin (clone B-5-1-2)	1:1000	Mouse	Sigma-Aldrich
anti-v-Src (clone 327)	1:200	Mouse	Sigma-Aldrich

*Secondary antibodies were acquired from Jackson Labs and used at a dilution of 1:4000

2.2 Methods

2.2.1 Extraction, amplification, and modification of DNA

The extraction, amplification, and/or modification of DNA was done using the enzymes included in Table 2.2 and kits outlined in Table 2.3 following manufacturer's protocols.

2.2.2 Yeast plasmid and strain construction

The yeast strains ip82a, iE381K, ip82a *hch1*, ip82a *aha1*, and iTHisHsp82p were derived from ΔPCLDa (Nathan and Lindquist, 1995) and have been previously described (Armstrong et al., 2012; Horvat et al., 2014). All site-directed mutagenesis was carried out using QuikChange™

mutagenesis according to the manufactures protocol (Agilent). Coding sequences for all mutagenized plasmids was verified by sequencing. Yeast galactose-inducible plasmids were constructed by amplifying *HCH1* and *AHA1* (wildtype or variant) coding sequences by PCR to have upstream *Bam*HI and downstream *Sac*I (for *HCH1*) or *Not*I (for *AHA1*) sites for cloning into pRS416GAL (for wildtype Aha1p and Hch1p) or pRS426GAL (for Δ11 variants) (LaPointe et al., 2005). The *HCH1* and *AHA1* coding sequences (wildtype or variant) coding sequences were amplified by PCR with primers designed to have an upstream *Bam*HI site and a downstream *Xho*I site for cloning into similarly cut p41KanTEF (Armstrong et al., 2012; Horvat et al., 2014). We constructed the p42HygGPD vector by digesting the GPD and CYC1 terminator fragment of p414GPD (Mumberg et al., 1995) with *Sac*I and *Kpn*I and ligating into similarly cut pRS42H (Taxis and Knop, 2006). The *HCH1* and *AHA1* (wildtype or variant) coding sequences with the *C*-terminal myc-tag were cut from p41KanTEF plasmids using *BamH*I and *Xho*I and cloned into p42HygGPD cut *BamH*I and *Sal*I to yield p42HygGPD, Hygromycin resistant plasmids. Yeast strains transformed with p41KanTEF and p42HygGPD were selected for with G418 (200 mg/L) or Hygromycin (300 mg/L) respectively.

The mutant Hsc82p^{S25P} was identified in a yeast screen (Kravats et al., 2018). We received the plasmids pRS313-*HSC82* and pRS313-*HSC82-S25P*, along with the yeast strain *hsc82hsp82/*URA3-*HSP82* from Dr. Jill Johnson (University of Idaho, USA). Plasmids were transformed into the yeast strain, selected for using SC-histidine, and URA3-*HSP82* was selected against on 5-fluoroorotic acid. We received the pRS361 v-Src plasmid from Dr. David Morgan (University of California, USA) (Murphy et al., 1993) and transformants were selected on SC-uracil.

2.2.3 Bacterial plasmid construction

pET11dHis expression vectors encoding Hsp82p, Aha1p, Aha1p^{N}, Hch1p, Sti1p, Sba1p, and Cpr6p were constructed as previously described (Armstrong et al., 2012; Horvat et al., 2014; Wolmarans et al., 2016). For the removal of the *N*-terminal 6xHis-tag and insertion of the co-chaperone coding sequence with a *C*-terminal 6xHis-tag Aha1p, Aha1p$^{\Delta 11}$, Aha1p^{N}, Aha1p^{R59A}, Aha1p^{K60A}, and Aha1p^{K62A} were amplified by PCR with primers designed to introduce an *Xba*I site at the 5' end and a 6xHis-tag and *Bam*HI site at the 3' end. Hch1p, Hch1p$^{\Delta 11}$, Hch1p^{R59A}, Hch1p^{K60A} and Hch1p^{K62A} were amplified by PCR with primers designed to introduce an *Nco*I

site at the 5' end and a 6xHis-tag and a *Bam*HI site at the 3' end. PCR products were digested with the appropriate restriction enzymes and ligated into a similarly cut pET11dHis vector. Site-directed mutagenesis for Hsp82p(S25P) was carried out using QuikChange™ mutagenesis according to the manufactures protocol (Agilent).

2.2.4 Mammalian plasmid construction

pcDNA™5/TO (ThermoFisher Scientific) mammalian expression vector was used for the transient expression of protein in cell culture. hAhsa1, mAhsa1, or the *N*-terminal deletion variant (Δ27) were amplified by primers designed to introduce a *Bam*HI site at the 5' end and a myc-tag along with a *Not*I site at the 3' end. PCR products were digested with the appropriate restriction enzymes and ligated into a similarly cut pcDNA™5/TO vectors. All site-directed mutagenesis was carried out using QuikChange™ mutagenesis according to the manufactures protocol (Agilent). Coding sequences for all plasmids was verified by sequencing.

2.2.5 Escherichia coli transformation

DNA was incubated with 50 µL of DH5α or BL21 (DE3) *E. coli* competent cells on ice for 20 minutes. Reactions were heat shocked for 45 seconds at 42°C, then incubated on ice for two minutes. After the addition of 1 mL of LB media, reactions were incubated at 37°C for 30 minutes. Cells were pelleted by centrifugation (1 minute at 13,000 rpm using an Eppendorf 5417C centrifuge with a F45-30-11 rotor) before being plated on LB agar plates containing 100 µg/ml ampicillin. Plates were incubated overnight at 37°C.

2.2.6 Saccharomyces cerevisiae transformation

Yeast strains were transformed using the lithium acetate transformation protocol. Yeast cells were grown overnight at 30°C in 5 mL of appropriate media. After overnight growth they were diluted to OD_{600} of 0.3 and grown for an additional 4 hours. All centrifugation for this protocol took place in an Eppendorf 5417C centrifuge with a F45-30-11 rotor at 3,000 rpm for 2 minutes. Cells were pelleted, washed with 1 mL of ddH_2O, pelleted, resuspended in 1 mL LiAcTE Buffer, and pelleted. Cells were then resuspended in 50 µL of LiAcTE Buffer. Each of the following was added followed by a quick vortex: 10 µL salmon sperm DNA, 1 µg of DNA, 300 µL of PEG solution (40% PEG3550 (w/v) in LiAcTE Buffer), and 6 µL DMSO. Transformations were then

incubated for recovery at 30°C for 1 hour, followed by a 42°C incubation for 15 minutes. Cells were pelleted and resuspended in 1 mL of sorbitol and 1 mL of non-selective media for overnight growth at 30°C. After overnight growth, cells were centrifuged and plated on selective media plates. Plates were grown at 30°C for 2-3 days.

2.2.7 Yeast protein alkaline extraction

Yeast cultures were grown overnight and the following day, 5 OD_{600} units of cells were pelleted by centrifugation (2 minutes at 3,000 rpm in an Eppendorf 5417C centrifuge with a F45-30-11 rotor), washed with 1 mL ddH_2O and pelleted by an additional 2 minute spin. Cell pellets were resuspended in 500 µL ddH_2O and 90 µL Alkaline Lysis Buffer. Samples were vortexed twice for 30 seconds and left to incubate on ice for 10 minutes. 250 µL of 100% TCA was added to each sample followed by a 10 second vortex and 10 minute incubation on ice. Samples were centrifuged for 10 minutes at 13,000 rpm at 4°C (Eppendorf 5417C centrifuge with a F45-30-11 rotor). Supernatants were removed by vacuum and pellets were washed with 80% acetone and left on ice for 10 minutes, before additional centrifugation. Supernatant was removed and pellets were left to dry at room temperature for twenty minutes before SDS-PAGE.

2.2.8 Yeast soluble protein extraction

After overnight growth at 30°C in appropriate media, 35 OD_{600} units of cells were pelleted by centrifugation (2 minutes at 3,000 rpm in an Eppendorf 5417C centrifuge with a F45-30-11 rotor), washed with 1 mL ddH_2O and pelleted by an additional 2 minute spin. Cell pellets were resuspended in 1 mL Yeast Lysis Buffer and transferred to 2 mL screw cap tubes filled half-full with 0.5 mm glass beads (Biospec, Bartlesville, OK, USA). Cells were lysed with a Mini-Beadbeater-16 for a total of 3 minutes, 30 seconds of bead-beating followed by 30 seconds on ice 6 times. The supernatant was clarified by centrifugation at 20,800 rcf for 10 min. 500 µL was taken and 90 µL Alkaline Lysis Buffer was added. Protein was extracted following the remainder of the steps outline in 2.2.7 Yeast protein alkaline extraction.

2.2.9 Yeast growth assays

Yeast cultures were grown overnight at 30°C in 5 mL of appropriate media. After overnight growth yeast strains were diluted to an OD_{600} of 1 followed by 10-fold serial dilutions. Ten µL

drops of the dilutions were plated on appropriate medium followed by growth for 1-3 days at 30°C, 34°C, or 37°C as indicated.

2.2.10 Yeast v-Src activation assay

Yeast cultures were grown overnight at 30°C in 5 mL of appropriate media supplemented with 2% raffinose. After overnight growth, cells were diluted to an OD_{600} of 0.5 and grown for an additional 6 hours at 30°C in 5 mL of appropriate media supplemented with 2% glucose, for inhibition of the plasmid, or 2% galactose, for plasmid induction. After 6 hours the OD_{600} was measured and 5 units of cells were harvested for protein extraction.

2.2.11 Sodium dodecyl sulfate polyacrylamide gel electrophoresis (SDS-PAGE), Coomassie blue staining, and western blot analysis

Proteins were separated by sodium dodecyl sulfate polyacrylamide gel electrophoresis (SDS-PAGE). Proteins samples were diluted 5:1 with 6x Sample Buffer or cell pellets were resuspended in 70 µL of 2x sample buffer (1:3 6x SDS-PAGE Sample Buffer in ddH_2O). Once in sample buffer, samples were boiled for 10 minutes, centrifuged, and 10 µL aliquots were loaded onto gels for separation by SDS-PAGE. Gel percentage was chosen to best resolve the protein/proteins of interest. Following SDS-PAGE, protein was visualized by Coomassie blue staining or western blot.

Total protein levels were visualized by Coomassie blue staining. Gels were immersed in Coomassie Stain (1X (1:50 Coomassie Stain (50X) in Destain)), heated in a microwave for 30 seconds, and rocked until desired band intensity was achieved. Gels were then placed in Destain and rocked until sufficient background dye was removed. Gels were visualized using the Cell BioSciences FluorChemQ system.

Visualization of specific proteins was achieved by western blot. Proteins separated by SDS-PAGE were transferred to nitrocellulose membrane (0.45µm, BioRad) in Western Transfer Buffer. Membranes were blocked with 2% BSA in 0.1% TBS-tween (0.1% (v/v) Tween 20 in Tris-buffered saline (TBS)). After blocking, membranes were incubated with the primary antibody corresponding to the protein of interest, Table 2.5. After incubation with primary antibody membranes were washed 3 times in 0.1% TBS-tween. Membranes were then incubated

with 2° Horseradish peroxidase (HRP)-conjugated antibody. Membranes were washed with 0.1% TBS-tween prior to detection and visualization using enhanced chemiluminescence (ECL) (50:50 ECL Solution #1 and ECL Solution #2) and the Cell BioSciences FluorChemQ system. For the stripping of membranes, membranes were submerged in Stripping Buffer at 55°C for 30 minutes with occasional agitation. Membranes were washed twice, rocking at room temperature for 10 minutes in 0.1% TBS-tween. Membranes were blocked with 2% BSA- 0.1% TBS-tween prior to incubation with antibodies, as above.

2.2.12 Protein expression and purification

Proteins were expressed in the *E. coli* strain BL21 (DE3) from the pET11d vector encoding the 6xHis-tagged protein of interest. Cells were grown in 50 mL LB supplemented with 5 mg ampicillin overnight at 37°C while shaking at 200 rpm. 10-15 mL of starter culture was used to inoculate 750 mL LB media supplemented with 75 mg ampicillin. Cultures were grown at 37°C while shaking at 200 rpm to an OD_{600} of 0.8-1.2 before induction with 1 mM isopropyl-1-thio-D-galactopyranoside (IPTG). Once induced, cultures were grown overnight at 30°C or 6 hours at 37°C and then harvested at 4°C using a Beckman Coulter Avanti J-26XP1 with a JLA-8.1 rotor for 15 minutes at 7,000 rpm. Cell pellets were resuspended in 1x PBS, transferred to 50 mL conical centrifuge tubes, and centrifuged at 4°C for 15 minutes at 4,150 rpm in a Thermo Scientific Sorval Legend T+ (7500 6445 swinging bucket rotor). Pellets were used immediately or stored at -80°C.

Pellets were resuspended in IMAC Buffer A, supplemented with HALT Protease Inhibitor Cocktail and lysed by running through the Avestin Emulsiflex C3 (Avestin, Ottawa, Ontario, Canada) 5-7 times. Lysates were clarified by ultracentrifugation at 36,000 rpm for 30 minutes at 4°C using a Beckman Coulter Optima L-100K centrifuge and Ti60 rotor. Protein purifications were performed using an AKTA Explorer Fast Protein Liquid Chromatography (FPLC) system with a Frac-950 collector (GE Healthcare). The supernatant, cytoplasmic fraction cleared of cell debris, was injected over a 5 mL HisTrap FastFlow (FF) Nickel column (GE Healthcare). Weakly bound proteins were washed from the column with IMAC Buffer A and 5% IMAC Buffer B before a gradient of 5-100% of IMAC Buffer B and 2 column volumes of 100% IMAC Buffer B were used to elute the proteins of interest. Eluted proteins were collected in 1 mL fractions and fractions containing the protein of interest were determined using the FPLC

absorbance chromatography and SDS-PAGE. Nickel columns were stripped, cleaned, and recharged between every purification.

Protein fractions were pooled and concentrated, using the appropriate 15 mL Amicon Ultra Centrifugal Filter Device, by centrifugation in a Thermo Scientific Sorvall Legend T+ (7500 6445 swinging bucket rotor) at 4,150 rpm and 4°C for 5 minute intervals. Hsp82p was pooled and concentrated in the presence of 5 mM EDTA. Before further purification by size exclusion chromatography, the concentrated protein samples were cleared of insoluble particulates by centrifugation at 13,000 rpm (Eppendorf 5424 centrifuge with FA-45-21-11 rotor). For size exclusion chromatography samples were injected in 1-3 mL sample loops via the FPLC loading port and run over a Superdex 200 column (GE Healthcare) using the appropriate Gel Filtration Buffer. Proteins were eluted in 2 mL fractions and fractions containing the protein of interest were determined using the FPLC absorbance chromatography and SDS-PAGE. Protein fractions were pooled and concentrated. Protein concentration was calculated according to the Beer-Lambert law: $A = \varepsilon lc$, where A is absorbance, ε is extinction or molar absorption coefficient and l is the path length. Protein absorbance at 280 nm (A_{280}) was measured using a NanoDrop Spectrophotometer where l was 1 cm and ε was calculated using Vector NTI based on amino acid composition. Multiple readings at different dilutions were averaged to ensure absorbance was accurate. The final protein concentration was determined using the following formula: $\text{Concentration } (\mu\text{M}) = \frac{A_{280}}{\varepsilon} \times 1{,}000{,}000$

Purified proteins were aliquoted and snap frozen in liquid nitrogen and stored at -80°C.

2.2.13 ATPase assays

All ATPase reactions were carried out in triplicate at 30°C in 100 µL volumes, using a 96-well plate. Hsp82p activity was analyzed by using a pyruvate kinase/lactate dehydrogenase (PK/LDH) regenerated system where the regeneration of ATP is coupled to the oxidation of NADH. Absorbance of NADH (340 nm) was measured using a BioTek Synergy 4 plate reader every minute for 90 minutes. The final conditions for reactions was 25 mM Hepes (pH 7.2), 12.5-16 mM NaCl, 5 mM $MgCl_2$, 1 mM DTT, 0.3-0.6 mM NADH, 2 mM ATP (co-chaperone titration and cycling experiments) or 0.00125-1.6 mM ATP (ATP titration experiments), 1 mM phosphoenol pyruvate (PEP), 2.5 µL of PK/LDH, and 5% DMSO. Identical reactions were

quenched with 100 μM NVP-AUY922 and subtracted from unquenched reactions (DMSO) to correct for contaminating ATPase activity. Data was collected by the Gen5 software program with the path-length correction function enabled and absorbance values were exported to Microsoft Excel. The decrease in NADH absorbance was converted to micromoles of ATP using Beer's Law and expressed as a function of time (min^{-1}) (Ali et al 1993). Average values of the experiments are shown with error expressed as standard error of the mean, with the exception of those shown as fold ATPase stimulation or ATPase inhibition which are shown with error expressed as standard deviation. In co-chaperone titration experiments, binding affinities were calculated according to the following equation: $Y=((Bmax*X)/(Kapp+X))+X_0$, where Bmax is the top asymptote, X_0 is the offset and Kapp is the apparent binding affinity (Retzlaff et al., 2010). In ATP titration experiments the ATPase rates and K_m values were analyzed with the Michaelis-Menton non-linear regression function in GraphPad Prism.

2.2.14 Mammalian cell culture

A549, MAF (Didier Picard, University of Geneva), and melanoma (MelanA, B16-F0, B16-F10) cell lines were maintained in DMEM with high glucose, L-glutamate, sodium pyruvate, and 10% FBS. MDA-MB-321-TB cells were maintained in RPMI with L-glutamate and 10% FBS. All cells were maintained in a humidified atmosphere of 5% CO_2 at 37°C.

2.2.15 Mammalian cell culture transfection

Transfection of plasmids for the transient expression of proteins was performed on cells grown to be 70-90% confluent at the time of transfection. Transfections were completed using Lipofectamine® 2000 (Thermo Fisher Scientific) or Lipofectamine® 3000 (Thermo Fisher Scientific) according to the manufacturer's instruction and cultured overnight for protein expression. For small interference RNAs (siRNAs) (Silencer® Select Negative control #1 siRNA or AHSA1 Silencer® Select Pre-designed siRNA ID:s20802 (Ambion)) reverse transfections were performed using RNAiMax (Invitrogen) according to the manufacturer's instructions. Cells were reverse transfected at 70-90% confluency. For the transfection of poly(I:C), confluent cells were transfected with 1 ug of poly(I:C) using Lipofectamine® 2000 (Thermo Fisher Scientific) for the indicated times. For cell lysis, cells were washed with 1xPBS and then rocked in Mammalian Lysis buffer at 4°C for 30 minutes before being scraped and pipetted into 1.5 mL

tubes for clarification by centrifugation (10 minutes at 13,000 rpm at 4°C (Eppendorf 5417C centrifuge with a F45-30-11 rotor) and visualization by SDS-PAGE and western blotting.

2.2.16 Mammalian cell culture viral infection

Experiments with WNV (strain NY99) were performed in CL-3 facilities (University of Alberta). Virus stocks were diluted in serum free growth medium to achieve a multiplicity of infection (MOI) of 0.5. Cells were incubated with the virus for 2-4 hours and then the inoculum was replaced with growth medium for additional growth as indicated. Total RNA was isolated using a Nucleospin RNA isolation kit (Macherey-Nagel) according to manufacturer's instructions. Improm-II Reverse Transcriptase (Promega, Thermofisher) was used to transcribe isolated RNA into cDNAs. qRT-PCR reactions were conducted using the PerfecCTa SYBR Green SuperMix Low Rox real-time PCR kit (Quanta Biosciences) with appropriate primers in a Stratagene MX3005P^{TM} thermocycler. Reactions were performed in duplicate. The comparative CT (ΔΔCT) method (Livak and Schmittgen, 2001) was used to quantify the relative levels of each RNA transcript. Relative levels of the mRNA for the gene of interest were calculated compared to the levels of β-actin or GAPDH as a control.

2.2.17 Mammalian cell viability assay- MTT assay

Cells were plated 5000 cells/well in a 96 well plate and grown for 24 hours before being treated with varying concentration of NVP-AUY922 or DMSO (control) in triplicate and grown for an additional 48 hours. Media was removed and 100 µL Opti-MEM media with 10 µL of 12 mM of MTT (3-(4,5-dimethylthiazol-2-yl)-2,5-diphenyltetrazolium bromide) were added to each well and incubated for 3 hours at 37°C. Media was removed and 50 µL of DMSO was added to each well followed by a 10 minute incubation at 37°C. Reduction of MTT (yellow) to purple formazan by living cells was measured by reading the absorbance at 560 nm using a BioTek Synergy 4 plate reader. Averages for triplicates of each inhibitor concentrations were calculated and expressed as a percentage of the control for each experiment.

2.2.18 Crosslinking antibodies to beads

All spins were completed at 3000 rpm at 4°C (7500 6445 swinging bucket rotor). Antibodies were crosslinked at 5 mg of antibody per 1 ml of Ultralink Protein G beads (Pierce Thermo

Fisher). For crosslinking beads were washed with 10x volume (corresponding to initial bead volume) of 1xPBS, spun down, and PBS was removed before the appropriate amount of anti-body was added. Anti-bodies were allowed to bind for 1 hour rotating at room temperature. Beads were washed twice with 10x the bead volume of 100 mM Sodium Borate. Beads were resuspended in 10x volume of 100 mM Sodium Borate with 20 mM dimethyl pimelimidate (DMP) and cross-linking was allowed to proceed for 30 minutes rotating at room temperature. Beads were spun down and liquid removed before the reaction was stopped by the addition of 10x volume of 200 mM Ethanolamine. Beads were spun down and resuspended in 10x the bead volume of 200 mM Ethanolamine and allowed to rotate at room temperature for 2 hours. Beads were then washed three times with 10x the bead volume of PBS before being stored in 50% (v/v) PBS.

2.2.19 Immunoprecipitation assay

Cells were washed twice with 500 µL of 1xPBS and the lysed in 300 µL of Mammalian IP Lysis Buffer. Lysates were clarified by centrifugation for 10 minutes at 4°C and 13,000 rpm (Eppendorf 5417C centrifuge with a F45-30-11 rotor). 50:50 bead slurry was added (based on the size of cell lysate) to the supernatant and incubated rotating at room temperature for 1 hour. Beads were washed in Mammalian IP Lysis Buffer before 2-DGE or SDS-PAGE.

2.2.20 2-dimensional gel electrophoresis (2DGE)

Plated cells were scraped and resuspended in 500 µL of 2DGE Lysis Buffer and allowed to rotate for 1.5 hours at 4°C. Samples were then centrifuged at 13,000 rpm at 4°C for 10 minutes (Eppendorf 5417C centrifuge with a F45-30-11 rotor). To 125 µL of clarified cell lysate or resuspended IP sample, 2.5 µL 1 M DTT and 1.25 µL of IPG buffer (pH 4-7) (GE Healthcare Life Sciences) was added. Samples were then incubated with Immoniline™ DryStrip (pH 4-7, 7 cm) (GE Healthcare Life Sciences) at room temperature for 20 hours followed by first dimensional electrophoresis (1. Step and hold: 300 V, 2.5 hours; 2. Gradient 1000 V, 30 minutes; 3. Gradient: 5000 V, 1.5 hours; 4. Step and hold: 5000 V, 30 minutes). For equilibration, strips were incubated in 2DGE Buffer 1 for 15 minutes rocking at room temperature, washed with water, and then incubated in 2DGE Buffer 2 for 15 minutes rocking at room temperature. For

second dimension electrophoresis, strips were placed on a 10% SDS-PAGE gel and sealed using Stacking Gel Buffer containing 0.1% SDS.

2.2.21 Genomic analysis

Reciprocal BLAST (Basic Local Alignment Search Tool) searches were performed using Hch1p and Aha1p protein sequences against a large number of published genomes with which predicted protein sequences exist. Proteins were classified as Hch1p-like if they contained one or more of the NxNNWHW, D53, and RKxK motifs but lacked a recognizable *C*-terminal domain similar to Aha1p$^{157\text{-}350}$. Aha1p-like proteins were similarly identified except in possession of a recognizable *C*-terminal domain.

Chapter 3 The conserved NxNNWHW motif in Aha-type co-chaperones modulates the kinetics of Hsp90 ATPase stimulation

A version of this chapter has been published in:
"Mercier, R., Wolmarans, A., Schubert, J., Neuweiler, H., Johnson, J.L., and LaPointe, P. (2019). The conserved NxNNWHW motif in Aha-type co-chaperones modulates the kinetics of Hsp90 ATPase stimulation. Nature Communications *10*(1), 1273. DOI:10.1038/s41467-019-09299-3"

3.1 Introduction/Rationale

Aha1p is the most potent activator of the ATPase activity of Hsp90 identified to date. Although present across eukaryotes, Aha-type co-chaperones are relatively weakly conserved. While yeast and human Hsp90 possess ~60% identity, yeast Aha1p and human Aha1 share only 23% identity. Despite weak conservation, Aha-type co-chaperones are able to stimulate the ATPase activity of Hsp90 (Carrigan et al., 2004; Nelson et al., 2004). Canonical Aha1p is comprised of two domains joined by a flexible linker and yeast also possess a related co-chaperone called Hch1p that lacks the *C*-terminal domain. Hch1p has 36.5% identity and 50% similarity to the *N*-terminus of Aha1p, and both can bind to the middle domain of Hsp90 (Figure 1.6) (Panaretou et al., 2002; Lotz et al., 2003). Homologues of Hch1, which correspond only to the *N*-terminal domain of Aha1, have been found in some members of the subphylum *Saccharomycotina* whereas canonical two-domain Aha1p family members are found across eukaryotes (Figure 3.1). The biological significance of the ATPase stimulation activities of the Aha-type co-chaperones and the manner in which these co-chaperones regulate Hsp90 activity and function remains poorly understood.

The core interaction between Aha1 and Hsp90 is the binding of the *N*-terminal domain of Aha1 with the middle domain of Hsp90 (Figure 1.5) (Meyer et al., 2003; Meyer et al., 2004). Therefore, while both Hch1p and the *N*-terminal domain of Aha1 ($Aha1p^{1-156}$) are able to stimulate the ATPase activity of Hsp90, the *C*-terminal domain of Aha1 alone is not (Panaretou et al., 2002; Horvat et al., 2014). Shared functional and enzymatic activity of proteins are often linked to regions of sequence conservation. Comparative analysis of the Aha-type co-chaperones reveal that the most strongly conserved region is found at the *N*-terminus of the *N*-terminal domain and defined by the NxNNWHW motif (Figure 3.1). The co-crystal structure between the *N*-terminal domain of Aha1 and the middle domain of Hsp90, shows that the *N*-terminal Asn/Trp-rich motif is unstructured but predicted to extend towards the *N*-terminal ATP binding domains of the Hsp90 (Figure 3.2) (Ali et al., 2006; Meyer et al., 2004). The predicated proximity of this region and high level of conservation led us to hypothesize that the NxNNWHW motif plays a role in regulating conformational dynamics associated with the ATPase activity of Hsp90. Investigation of the biological function of this motif and the effect on Hsp90 ATPase stimulation provide insight into the role of the NxNNWHW motif in Hsp90 regulation.

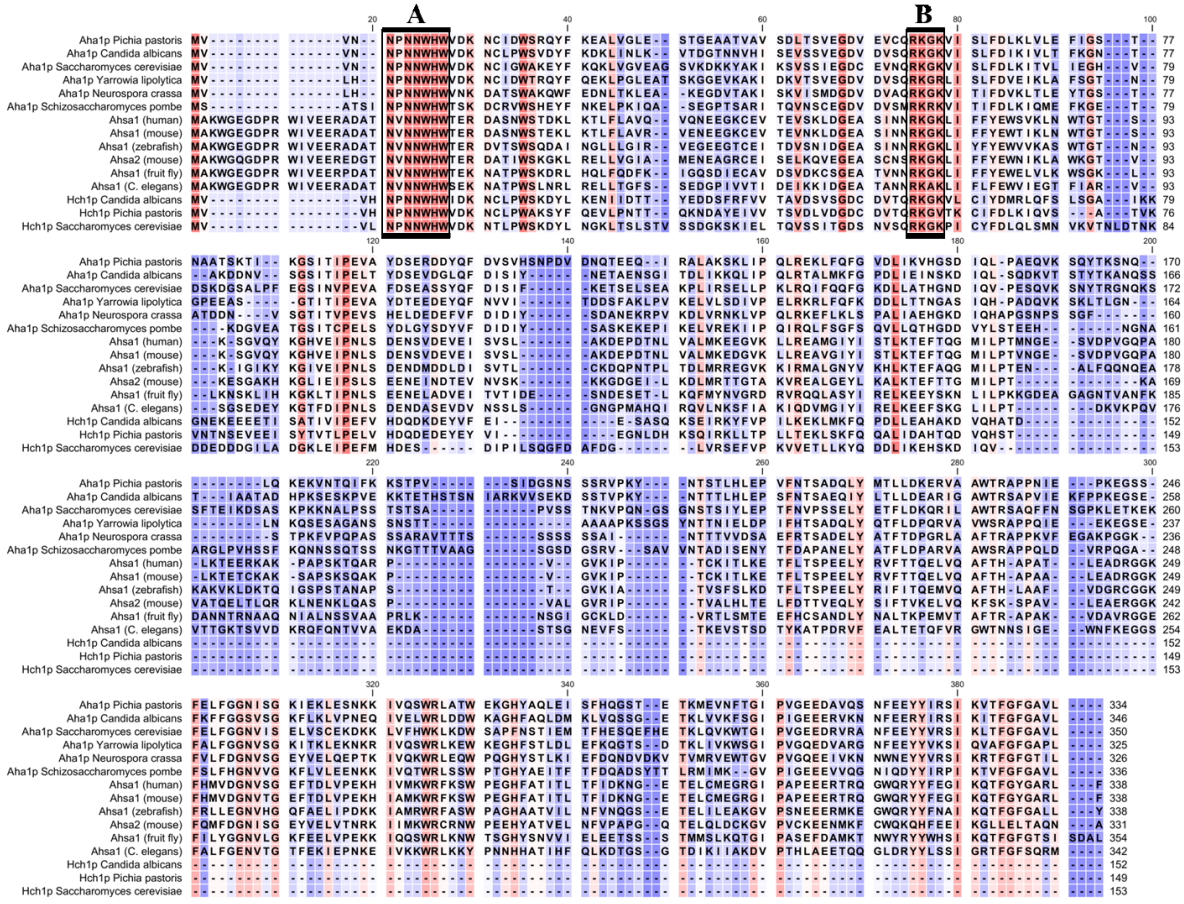

Figure 3.1 Alignment of Aha-type co-chaperones across multiple eukaryotic species. Conserved sequences are highlighted in red and non-conserved sequences are highlighted in blue. The conserved NxNNWHW and RKxK motifs are outlined by boxes A and B respectively.

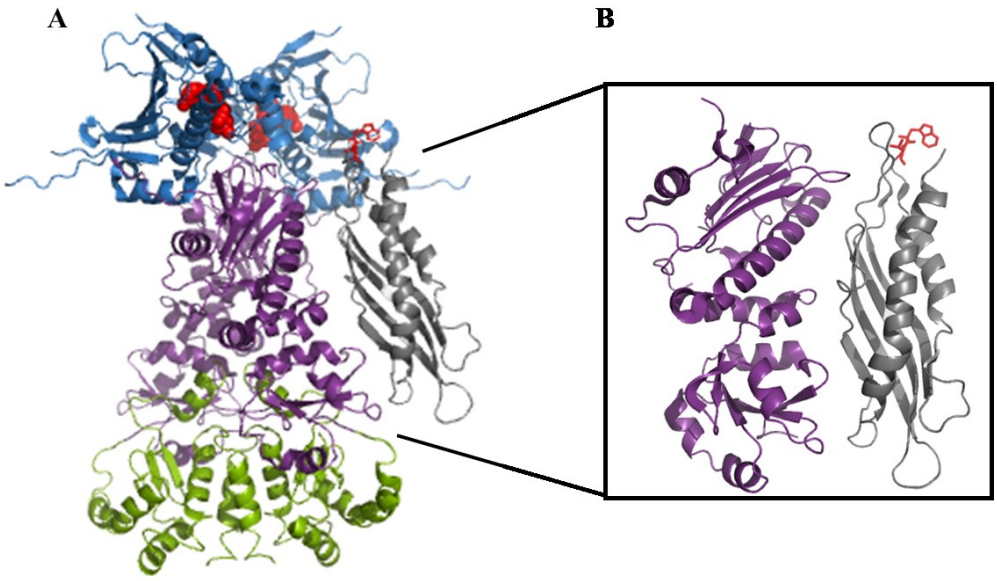

Figure 3.2 Crystal structure of the predicted position of the NxNNWHW motif.
A. Crystal structure of full length, closed Hsp90 dimer (*N*-terminal domains- blue, middle domains- purple, *C*-terminal domains- green, ATP- red) (2CG9 (Ali et al., 2006)) with the *N*-terminal domain of Aha1p (grey) (1USV (Meyer et al., 2004)) superimposed. Trp 11 and Val 12 (red sticks) indicate where the *N*-terminal NxNNWHW motif would be present (it is unstructured in 1USV). **B.** A model of the complex between the middle domain of Hsp90 (purple) and the *N*-terminal domain of Aha1p (grey) shown in (A) (1USV (Meyer et al., 2004)).

3.2 Results

3.2.1 The NxNNWHW motif is required for optimal stimulation of Hsp82p ATPase activity

The main function ascribed to the Aha-type co-chaperones is stimulation of the low intrinsic ATPase activity of Hsp90 (Panaretou et al., 2002; Meyer et al., 2004). We are able to examine this function *in vitro,* through the use of ATPase assays with Hsp82p and an enzymatic ATP regenerating system (Panaretou et al., 1998). For purification purposes, proteins harbour a 6xHis-tag that is conventionally placed at the *N*-terminus. Previous analysis has shown that the *N*-terminal 11 amino acids of Aha1p, which includes the conserved NxNNWHW motif, are not required for Hsp82p ATPase stimulation by Aha1p (Meyer et al., 2004). Our lab has shown that Hch1p and Aha1p differ in their ability to rescue the temperature sensitive phenotype of various Hsp90 mutants and in their ability to alter sensitivity to Hsp90 inhibitors (Horvat et al., 2014; Armstrong et al., 2012). In addition, while a mutation in the catalytic loop of Hsp90, E381K, impairs the ability of Aha1p to stimulate Hsp90, stimulation by Hch1p is not changed (Horvat et al., 2014; Meyer et al., 2003). We wanted to determine if the *N*-terminal motif plays a role in the ability of Hch1p to stimulate the ATPase activity of Hsp90. To do this we constructed mutants of Aha1p and Hch1p lacking the *N*-terminal 11 amino acids which includes the NxNNWHW motif (Aha1p$^{\Delta 11}$ and Hch1p$^{\Delta 11}$ respectively). As we were looking to determine the consequences of the deletion of the NxNNWHW motif found at the very *N*-terminus of these co-chaperones, we performed these experiments with co-chaperones that, as dictated by convention, harboured an *N*-terminal 6xHis-tag (6xHis-Aha1p, 6xHis-Aha1p$^{\Delta 11}$, 6xHis-Hch1p, and 6xHis-Hch1p$^{\Delta 11}$) and we also purified and tested co-chaperones with a *C*-terminal 6xHis-tag (Aha1p-6xHis, Aha1p$^{\Delta 11}$-6xHis, Hch1p-6xHis, and Hch1p$^{\Delta 11}$-6xHis).

Consistent with previous results, deletion of the *N*-terminal motif did not alter the ability of 6xHis-Aha1p to stimulate the ATPase activity of Hsp90 (Figure 3.3 A) (Meyer et al., 2004). Interestingly, the removal of this motif from 6xHis-Hch1p results in increased stimulation of Hsp90 (Figure 3.3 B). In contrast, removal of the NxNNWHW motif from *C*-terminally tagged Aha1p and Hch1p reveals impairments in the ATPase stimulation by both co-chaperones (Figure 3.4). For the *C*-terminally 6xHis-tagged co-chaperones the maximal ATPase activity upon the addition of Aha1p$^{\Delta 11}$ was ~2.8 fold lower than Aha1p and the difference between Hch1p$^{\Delta 11}$ and Hch1p was ~1.7 fold. Surprisingly, deletion of the NxNNWHW motif did not impair ATPase

stimulation by the Aha1p *N*-terminal domain on its own (Figure 3.5). Comparison of the *N*- and *C*-terminally 6xHis-tagged versions of Aha1p show that stimulation is higher for full length Aha1p when the 6xHis-tag was on the *C*-terminus (Figure 3.6). This suggests that the presence of an *N*-terminal 6xHis-tag interferes with ATPase stimulation by the Aha-type co-chaperones. All further *in vitro* assays were preformed using *C*-terminally 6xHis-tagged Aha-type co-chaperones. The deletion of the NxNNWHW motif did not alter the folding of either Aha1p or Hch1p as ThermoFluor thermal shift assays, completed by Dr. Paul LaPointe, showed the melting curves for Aha1p$^{\Delta 11}$ and Hch1p$^{\Delta 11}$ were identical to those obtained for their wildtype counterparts. The melting temperature (Tm) of Aha1p and Aha1p$^{\Delta 11}$ were 63.6 +/- 0.9 and 63.3 +/- 0.9°C, respectively. The Tm of Hch1p and Hch1p$^{\Delta 11}$ were 51.5 +/- 2.0 and 52.6 +/- 1.8°C, respectively (n=9). Together, these data show that the NxNNWHW motif is required for maximal ATPase stimulation by both Hch1p and Aha1p.

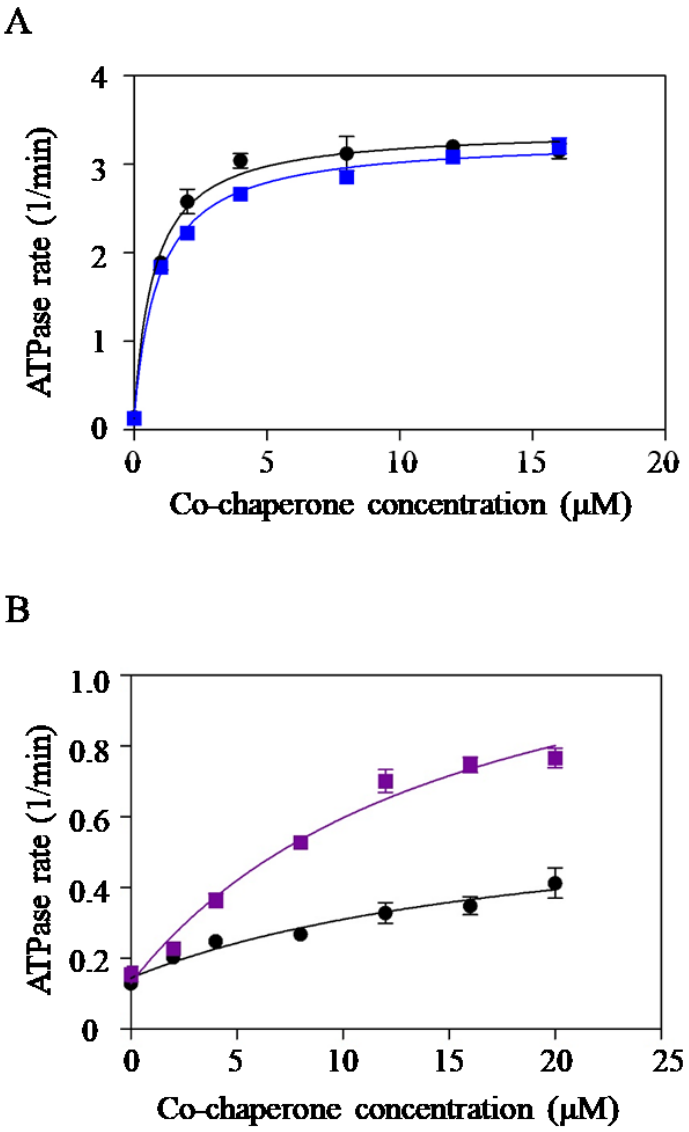

Figure 3.3 Hsp90 ATPase stimulation by *N*-terminally tagged Aha1p and Hch1p.
A. Stimulation of Hsp82p ATPase activity by increasing concentration of Aha1p (black circles) and Aha1p$^{\Delta 11}$ (blue squares). Reactions contained 1 μM Hsp82p and indicated concentrations of co-chaperone (n=3). **B.** Stimulation of the Hsp82p ATPase activity by increasing concentrations of Hch1p (black circles) and Hch1p$^{\Delta 11}$ (purple squares). Reactions contained 1 μM Hsp82p and indicated concentration of co-chaperone (n=3).

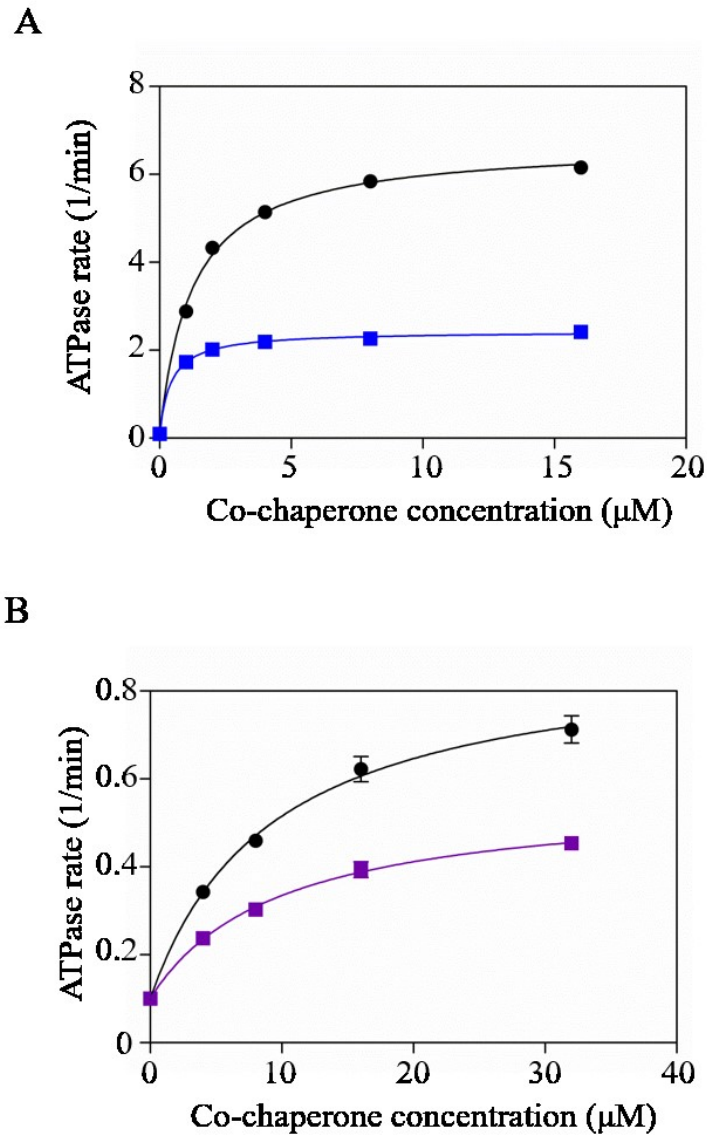

Figure 3.4 Hsp90 ATPase stimulation by *C*-terminally tagged Aha1p and Hch1p.
A. Stimulation of Hsp82p ATPase activity by increasing concentration of Aha1p (black circles) or Aha1p$^{\Delta 11}$ (blue squares). Reactions contained 1 μM Hsp82p and indicated concentrations of co-chaperone (n=3). **B.** Stimulation of the Hsp82p ATPase activity by increasing concentrations of Hch1p (black circles) or Hch1p$^{\Delta 11}$ (purple squares). Reactions contained 4 μM Hsp82p and indicated concentration of co-chaperone (n=3).

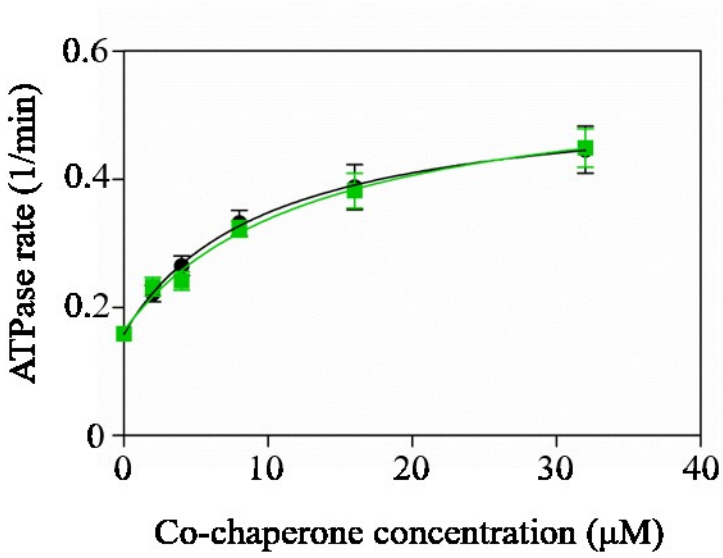

Figure 3.5 Deletion of the NxNNWHW motif does not affect ATPase stimulation by the Aha1 *N*-terminal domain alone.

Stimulation of the Hsp82p ATPase activity by increasing concentrations of Aha1p^{N} (black circles) and Aha1p$^{N\text{-}\Delta 11}$ (green squares). Reactions contained 4 μM Hsp82p and indicated concentration of co-chaperone (n=3).

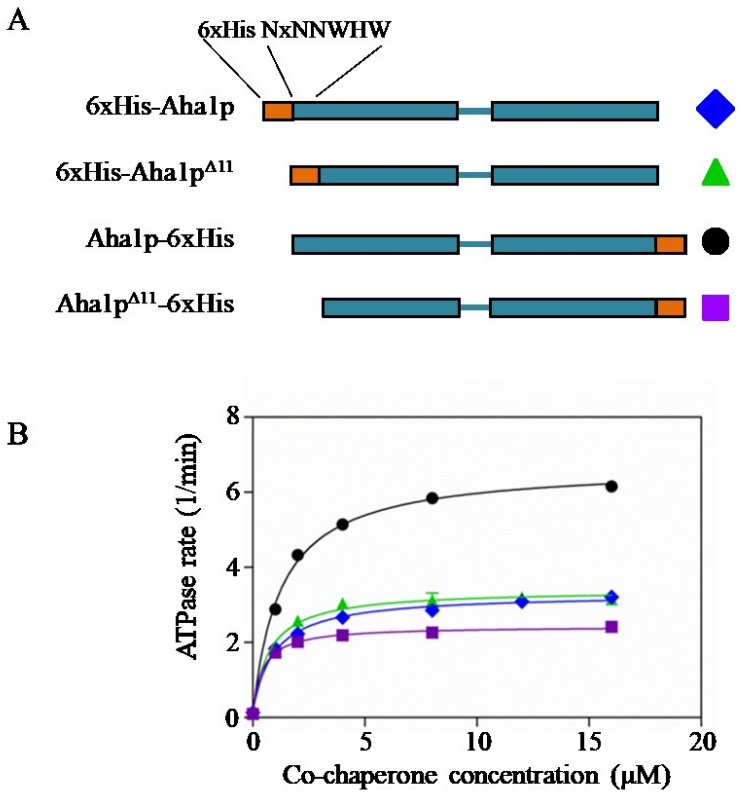

Figure 3.6 Hsp90 ATPase stimulation by *N*- and *C*-terminally 6xHis-tagged Aha1p.
A. Schematic of *N*-and *C*-terminally 6xHis-tagged Aha1p constructs. **B.** Stimulation of Hsp82p ATPase activity by increasing concentrations of 6xHis-Aha1p (blue diamonds), 6xHis-Aha1p$^{\Delta 11}$ (green triangles), Aha1p-6xHis (black circles), and Aha1p$^{\Delta 11}$-6xHis (purple squares). Reactions contained 1 μM Hsp82p and indicated concentration of co-chaperone (n=3).

3.2.2 The NxNNWHW motif is required for Hch1p action in cells

The importance of the *N*-terminal motif for *in vivo* function of Aha-type co-chaperones has not been investigated. Several different yeast assays have been previously employed that demonstrate a role for Hch1p in Hsp90 regulation *in vivo* (Nathan et al., 1999; Armstrong et al., 2012; Horvat et al., 2014). The phenotype that led to the identification of Hch1p, showing the overexpression of Hch1p rescues the temperatures sensitive growth of yeast expressing the temperature sensitive mutant Hsp82p^{E381K}, provides one such assay (Nathan et al., 1999). Importantly, the overexpression of Hch1p^{D53K}, a mutation that disrupts the interaction of Hch1p with the Hsp90 middle domain, does not rescue Hsp82p^{E381K} demonstrating that direct interaction is necessary (Meyer et al., 2004; Horvat et al., 2014). We transformed yeast expressing wildtype Hsp82p or Hsp82p^{E381K} with plasmids that overexpress either Hch1p or Hch1p$^{\Delta 11}$ in a galactose-inducible fashion. Initial experiments using the same promoter for both co-chaperones showed lower expression of Hch1p$^{\Delta 11}$. To establish equal expression of the co-chaperones, we expressed Hch1p$^{\Delta 11}$ under a stronger promoter and show the overexpression of Hch1p is able to rescue the growth of yeast expressing Hsp82p^{E381K} but the overexpression of Hch1p $^{\Delta 11}$ is not (Figure 3.7 A). Comparable levels of both the wildtype and *N*-terminally truncated versions of Hch1p were determined by western blot for soluble and total protein levels (Figure 3.7 B). We have previously shown that the overexpression of Hch1p results in hypersensitivity to the Hsp90 inhibitor NVP-AUY922 (Armstrong et al., 2012; Horvat et al., 2014). We overexpressed either Hch1p or Hch1p$^{\Delta 11}$ and show that the loss of the *N*-terminal motif abolishes the ability of Hch1p to induce hypersensitivity to Hsp90 inhibitors (Figure 3.8 A). Hch1p and Hch1p $^{\Delta 11}$ were expressed to similar levels (Figure 3.8 B). Together, these experiments reveal that the NxNNWHW motif is important for the *in vivo* function of Hch1p. The role of the NxNNWHW motif in the function of Aha1p was not addressed in these assays as changing the expression level of Aha1p does not result in a phenotype (Armstrong et al., 2012; Horvat et al., 2014).

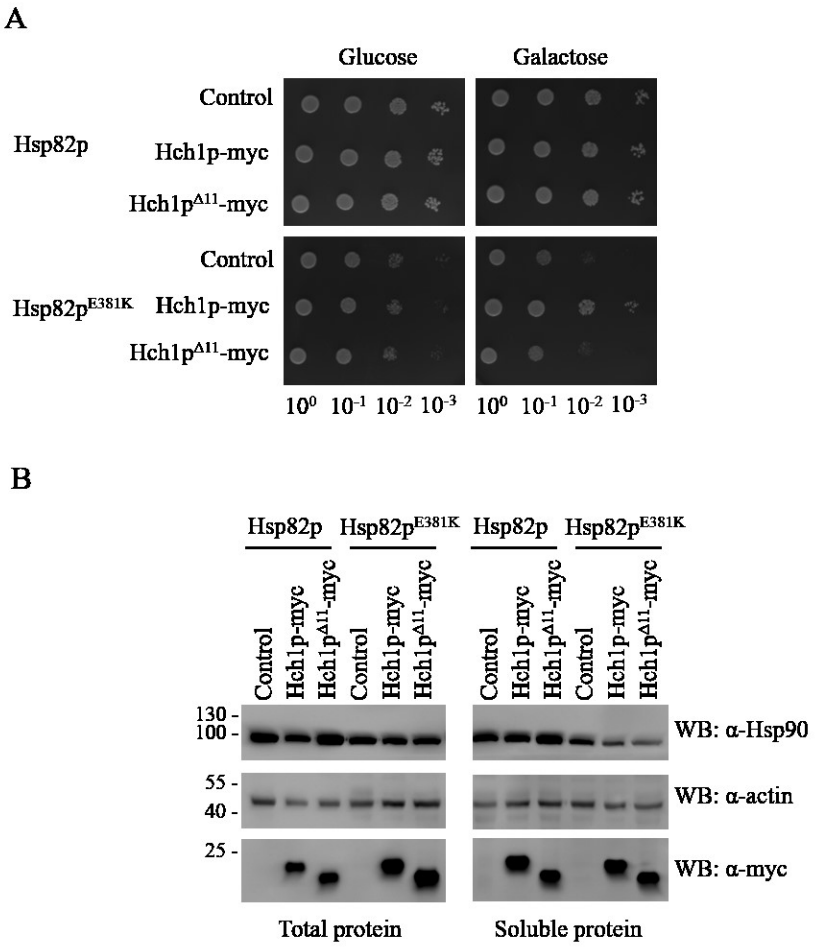

Figure 3.7 The NxNNWHW motif is required for Hch1p-mediated rescue of the Hsp82p^{E381K} mutant *in vivo*.

A. Overexpression of Hch1p, but not Hch1p$^{\Delta 11}$, rescues growth defects of yeast expressing Hsp82p^{E381K}. Yeast expressing wildtype Hsp82p (ip82a) or Hsp82p^{E381K} (iE381Ka) and harbouring expression plasmids encoding the indicated myc-tagged co-chaperones were grown overnight at 30 °C in SC media lacking uracil (SC-Ura) and containing 2% raffinose and then diluted to 1 × 10^8 cells per milliliter. We prepared 10-fold serial dilutions and spotted 10 µL aliquots on SC-Ura agar plates supplemented with either 2% glucose or galactose. Plates were incubated for 2 or 3 days for ip82a and iE381Ka strains, respectively, at 30 °C. **B.** Western blot of total lysates and the soluble protein fraction from the yeast strains shown in (A) were probed with anti-Hsp90, anti-actin, and anti-myc antibodies. Representative results of three independent experiments are shown.

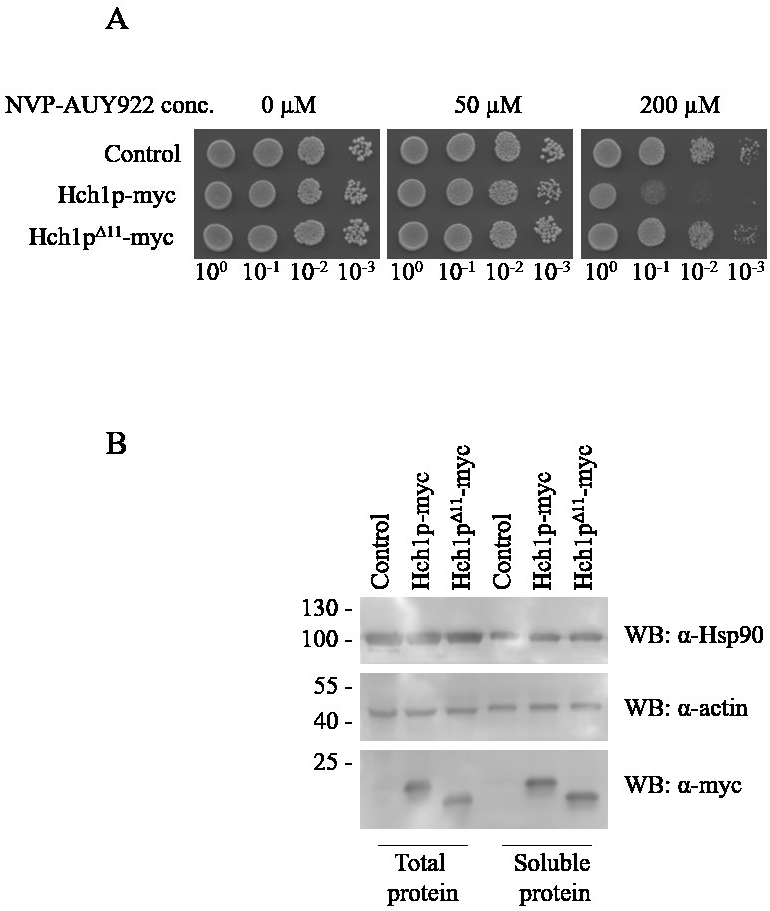

Figure 3.8 The NxNNWHW motif is required for Hch1p to confer sensitivity to Hsp90 inhibitors.

A. Overexpression of Hch1p, but not Hch1p$^{\Delta 11}$, confers hypersensitivity to NVP-AUY922 in yeast. Yeast expressing wildtype Hsp82p (ip82a) and harbouring expression plasmids encoding the indicated myc-tagged co-chaperones were grown overnight at 30 °C in YPD supplemented with G418 (200 mg/L) and then diluted to 1 × 10^8 cells per milliliter. We prepared 10-fold serial dilutions and spotted 10 μL aliquots on YPD agar plates supplemented with G418 (200 mg/mL) and the indicated concentrations of NVP-AUY922. Plates were incubated for 2 days at 30°C. B. Western blot of total lysates and the soluble protein fraction from the yeast strains shown in (A) were probed with anti-Hsp90, anti-actin, and anti-myc antibodies. Representative results of three independent experiments are shown.

3.2.3 The NxNNWHW motif is required for Aha1p action in cells

There have been few assays that clearly demonstrate a role for Aha1 in the *in vivo* regulation of Hsp90. In an attempt to understand the overlapping or competing functions that take place between co-chaperones others have shown that the overexpression of *SBA1*, *PPT1*, *AHA1*, or *HCH1* results in the negative growth of yeast that also express a mutation in the essential co-chaperone *SGT1* (*sgt1-K360E*) (Johnson, J. L. et al., 2014). While Sgt1 is a conserved and essential co-chaperone its role remains poorly characterized. Sgt1 is comprised of 3 domains (a TPR domain, CS (Chord-containing proteins and Sgt1) domain, and VR (Variable Region) domain) and although it contains a TRP domain it is interacts with Hsp90 through the CS domain (Willhoft et al., 2017). Sgt1 has been linked to folding and degradation pathways and is known to be important for immune response (Azevedo et al., 2006; Mayor et al., 2007; Willhoft et al., 2017). The reason for the negative growth defects of the *sgt1-K360E* mutant and the exacerbation effect of the overexpression of other co-chaperones in this mutant background is unknown, however, it can be used to show the consequences of alteration of Aha-type co-chaperone levels *in vivo*. We overexpressed Hch1p, Hch1p$^{\Delta 11}$, Aha1, or Aha1p$^{\Delta 11}$ in yeast expressing the K360E mutant of Sgt1p and analyzed changes in growth. Overexpression of both wildtype Hch1p and Aha1p resulted in growth defects of Sgt1p^{K360E} as previously described (Figure 3.9 A) (Johnson, J. L. et al., 2014). Interestingly, neither Hch1p$^{\Delta 11}$ nor Aha1p$^{\Delta 11}$ affected the growth (Figure 3.9 A). Aha1 and Aha1p$^{\Delta 11}$ were expressed to a similar levels (Figure 3.9 B). Hch1p appears to be expressed to a much lower level compared to Hch1p$^{\Delta 11}$ (Figure 3.9 B). This could be due to the severe growth impairment that results from the overexpression of Hch1p but not Hch1p$^{\Delta 11}$.

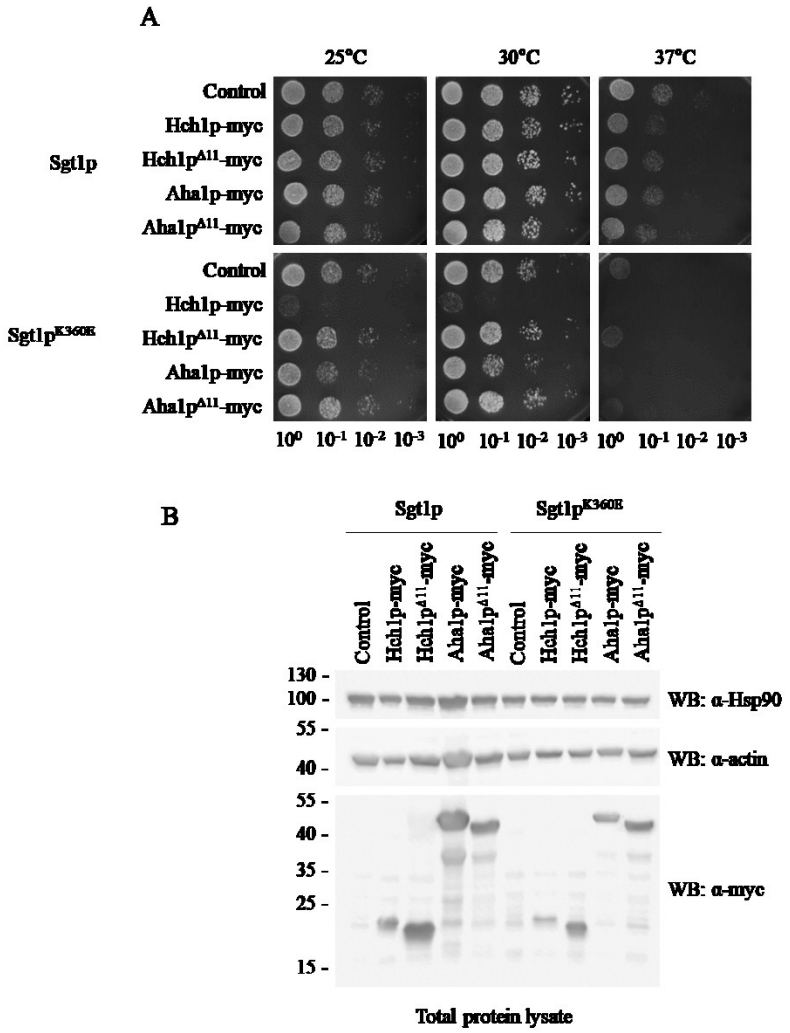

Figure 3.9 The NxNNWHW motif is required for Hch1p and Aha1p-mediated growth impairment of yeast expressing Sgt1p^{K360E}.

A. Overexpression of Hch1p or Aha1p, but not Hch1p$^{\Delta 11}$ or Aha1p $^{\Delta 11}$, confers slow growth to yeast expressing the Sgt1p^{K360E} mutant. Yeast expressing wildtype Sgt1p or Sgt1p^{K360E} and harbouring expression plasmids encoding the indicated myc-tagged co-chaperones were grown overnight at 30°C in YPD supplemented with Hygromycin (300 mg/L) and then diluted to 1 × 10^8 cells per milliliter. We prepared 10-fold serial dilutions and spotted 10 µL aliquots on YPD agar plates supplemented with Hygromycin (300 mg/L). Plates were incubated for 2 days at 30°C. **B.** Western blot of total lysates from the yeast strains shown in (A) probed with anti-Hsp90, anti-actin, and anti-myc antibodies. Representative results of three independent experiments are shown.

A recent screen for temperature sensitive Hsc82p mutants revealed several mutants that are affected by altering the expression level of co-chaperones (Jill Johnson, University of Idaho). Yeast expressing Hsc82p^{S25P} as the sole source of Hsp90 exhibit temperature sensitive growth that is worsened by the deletion of *AHA1* (Figure 3.10 A). This mutant allows for a more direct approach to determining Aha1p function in relation to Hsp90. Overexpression of Aha1p rescued growth in this strain at elevated temperatures, however, the overexpression of Aha1p$^{\Delta 11}$ did not (Figure 3.10 B). We determined that both wildtype and *N*-terminal truncated versions of Aha1p were expressed to comparable levels and were soluble in this strain (Figure 3.10 C). This suggests that the NxNNWHW motif is required for the *in vivo* function of Aha1p.

To determine the role that the NxNNWHW motif plays in the ability of Aha1p to support the interaction and activation of Hsp90 client proteins, we looked at activation of the Hsp90 dependent client v-Src. The activity of v-Src can be measured by assessing phosphotyrosine levels, with impairments in Hsp90 or components of the Hsp90 system reducing tyrosine phosphorylation (Xu, Y. and Lindquist, 1993; Lotz et al., 2003). We expressed galactose-inducible v-Src in a yeast strain expressing Hsc82p^{S25P} as the sole source of Hsp90 with *AHA1* deleted and a control, Aha1p or Aha1p$^{\Delta 11}$ overexpression plasmid. The overexpression of Aha1p, but not Aha1p$^{\Delta 11}$, showed an increase in the level of v-Src activity over the control (Figure 3.11). This suggests that the NxNNWHW motif is important for Aha1p to support Hsp90 activation of client proteins.

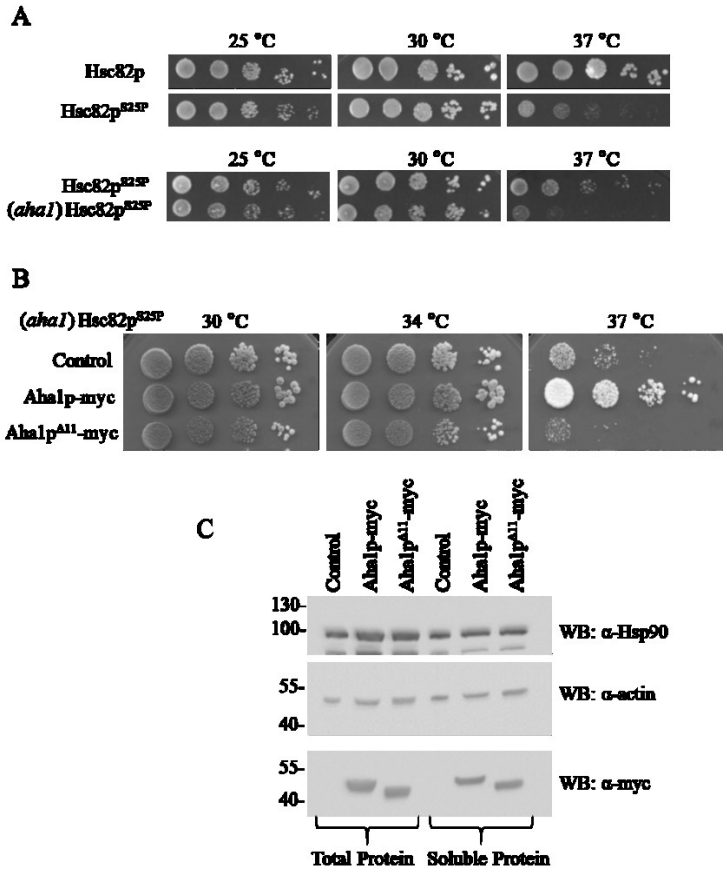

Figure 3.10 The NxNNWHW motif is required for Aha1p-mediated rescue of yeast expressing Hsc82p^{S25P}.

A. Yeast expressing Hsc82p^{S25P} as the sole source of Hsp90 in the cell exhibit temperature sensitive growth. The deletion of *AHA1* in yeast expressing Hsc82p^{S25P} exacerbates the temperature sensitive growth defect. **B.** Overexpression of Aha1p, but not Aha1p$^{\Delta 11}$, rescues the growth of yeast expressing Hsc82p^{S25P}. Yeast expressing Hsc82p^{S25P}, in an *AHA1* deletion background, and harbouring expression plasmids encoding the indicated co-chaperones were grown overnight at 30°C in YPD supplemented with Hygromycin (300 mg/L) and then diluted to 1x10^{8}cells per milliliter. We prepared 10-fold serial dilutions and spotted 10 µL aliquots on YPD plates supplemented with Hygromycin (300 mg/L). Plates were incubated for 2 days at the indicated temperatures. **C.** Western blot of total lysates and soluble protein extracts from yeast strains shown in (B) were probed with anti-Hsp90, anti-actin, and anti-myc antibodies. Representative results of three independent experiments are shown.

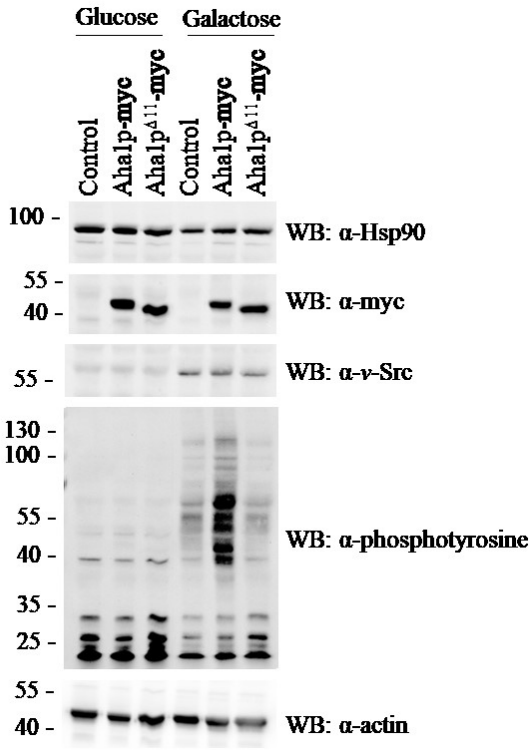

Figure 3.11 Overexpression of Aha1p but not Aha1p$^{\Delta 11}$ enhances v-Src activation in yeast expressing Hsc82p^{S25P}.

Western blot of total protein fraction of yeast expressing Hsc82p^{S25P} in an *AHA1* deletion background, harbouring expression plasmids encoding the indicated myc-tagged co-chaperones, and a galactose inducible v-Src expression plasmid. Cells were grown overnight at 30°C in SC-Ura containing 2% raffinose, supplemented with Hygromycin (300 mg/L). Cells were diluted to an OD_{600} of 0.5 and grown for an additional 6 hours in SC-Ura containing either 2% glucose or galactose, supplemented with Hygromycin (300 mg/L). Yeast strains were probed with anti-Hsp90, anti-myc, anti-v-Src, anti-phosphotyrosine, and anti-actin antibodies. Representative results of three independent experiments are shown.

3.2.4 The S25P mutation impairs ATPase stimulation by Aha1p

The ATPase activity of the S25P mutant has not been tested and we wondered if this mutation conferred an ATPase defect to Hsp82p. We expressed and purified Hsp82p^{S25P} for analysis in our ATPase assays. The intrinsic ATPase activity of Hsp82p^{S25P} was comparable to that of Hsp82p, displaying a small, but statistically significant, increase in intrinsic ATPase activity (Figure 3.12 A). As Aha1p but not Aha1p$^{\Delta 11}$ was able to rescue the S25P mutant we wondered if this was due to an effect on ATPase stimulation. We tested Aha1p and Aha1p$^{\Delta 11}$ in ATPase assays with wildtype Hsp82p and Hsp82p^{S25P}. Both Aha1p and Aha1p$^{\Delta 11}$-mediated ATPase stimulation were impaired with the S25P mutant compared to wildtype Hsp82p (Figure 3.12 B). While stimulation of wildtype Hsp82p was reduced ~2 fold with Aha1p$^{\Delta 11}$ compared to Aha1p, the difference in Hsp82p^{S25P} stimulation between Aha1p and Aha1p$^{\Delta 11}$ was ~6 fold.

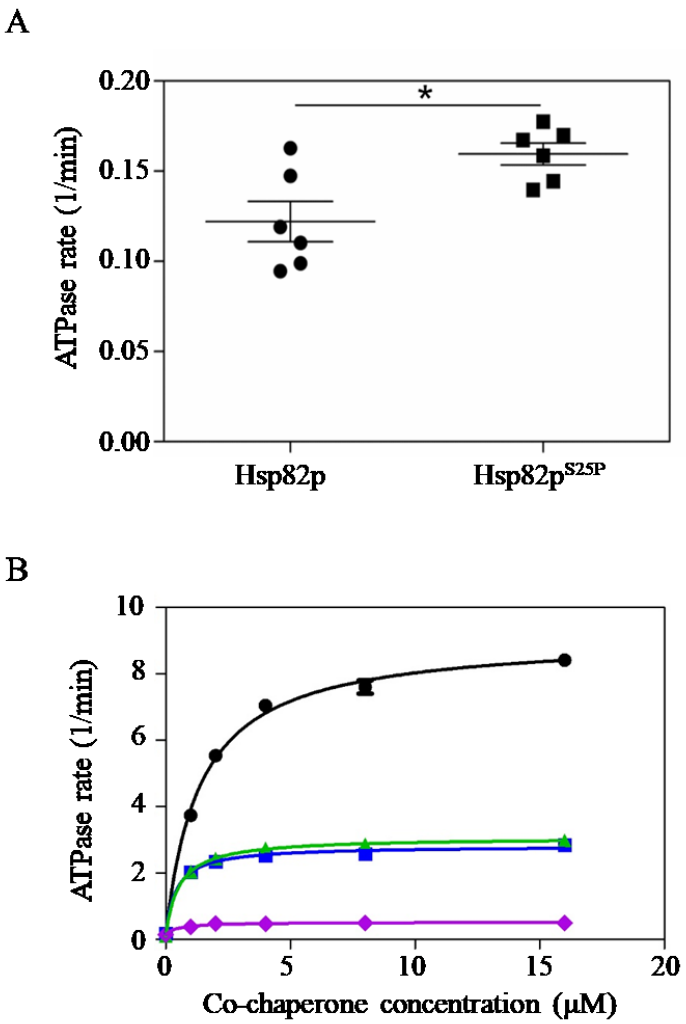

Figure 3.12 Aha1p-mediated ATPase stimulation of Hsp82p^{S25P} is dependent on the NxNNWHW motif.

A. The intrinsic ATPase activity of Hsp82p^{S25P} is comparable to that of wildtype Hsp82p (n=6).

B. Stimulation of Hsp82p by Aha1p (black circles), Hsp82p^{S25P} by Aha1p (blue squares), Hsp82p by Aha1p$^{\Delta 11}$ (green triangles), or Hsp82p^{S25P} by Aha1p$^{\Delta 11}$ (purple diamonds). Reactions contained 1 μM Hsp82p or Hsp82p^{S25P} and indicated concentrations of co-chaperone (n=3).

3.2.5 Deletion of NxNNWHW motif increase the apparent affinity for ATP of Hsp90

To further explore the underlying mechanism of the different stimulated ATPase rates we observed between the wildtype and NxNNWHW mutant co-chaperones, we measured ATP hydrolysis at different concentrations of ATP. We carried out ATPase assays with Hsp82p on its own, or during stimulation by Aha1p or Hch1p, with and without the *N*-terminal motif. We used varying concentrations of ATP (12.5, 25, 50, 100, 200, 400, 800, or 1600 μM) to determine the apparent K_m for ATP of Hsp90. Consistent with previous studies, we observed no change in the apparent K_m for ATP in Aha1p-stimulated reactions when compared to Hsp90 alone (Figure 3.13) (Panaretou et al., 2002). Alternatively, Hch1p-stimulated reactions showed a large increase in K_m for ATP (~3.5 fold) suggesting this co-chaperone reduces the affinity for nucleotide (Figure 3.13). The curve fits had R^2 values of greater than 0.95 (>0.9 for Hsp82p alone) providing confidence in the K_m values that we calculated. Deletion of the NxNNWHW motif in either Aha1p or Hch1p resulted in a significant decrease in K_m relative to their full-length counterparts (Figure 3.13).

A

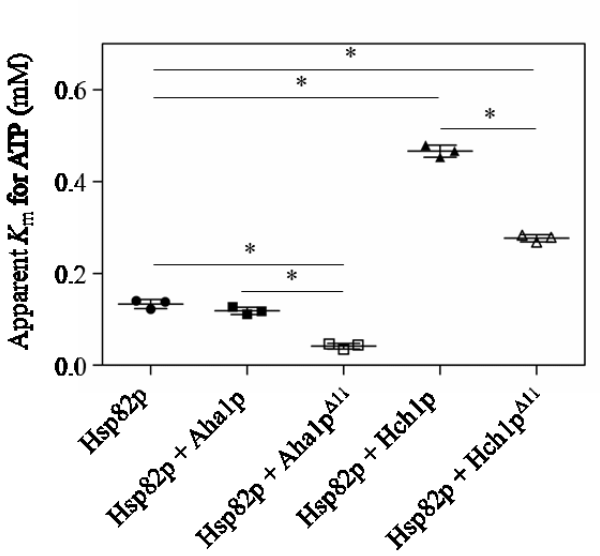

B

Condition	Hsp82p (●)	Hsp82p + Aha1p (■)	Hsp82p + Aha1p$^{\Delta 11}$ (□)	Hsp82p + Hch1p (▲)	Hsp82p + Hch1p$^{\Delta 11}$ (△)
Apparent K_m for ATP	0.133 +/- 0.010	0.118 +/- 0.008	0.042 +/- 0.006	0.466 +/- 0.013	0.277 +/- 0.008

Figure 3.13 The NxNNWHW motif in Aha1p and Hch1p modulates the apparent K_m for ATP of Hsp90.

A. Kinetic analysis was carried out for Hsp82p alone or in the presence of Aha1p, Aha1p$^{\Delta 11}$, Hch1p, or Hch1p$^{\Delta 11}$. ATPase reactions were carried out with increasing concentrations of ATP (12.5, 25, 50, 100, 200, 400, 800, 1600 μM) and ATPase rates were analyzed with the Michaelis-Menten non-linear regression function in GraphPad Prism. The curve fits all had R^2 values greater than 0.95 (>0.9 for Hsp82p alone). The apparent K_m values for three experiments are shown in the scatter plots. Reactions contained 2 μM Hsp82p with 20 μM Aha1p or Aha1p$^{\Delta 11}$ or 4 μM Hsp82p with 40 μM Hch1p or Hch1p$^{\Delta 11}$ **B.** The apparent K_m for ATP of conditions shown in (A). Statistical significance was calculated pair-wise with a t-test (n=3; n=4 for Hsp82 alone). *p-value < 0.05

3.2.6 Role of the NxNNWHW motif in co-chaperone switching

The progression of the Hsp90 cycle involves specific conformational transitions that can be regulated by co-chaperones (Li, J. et al., 2011; Prodromou, 2012). Several distinct Hsp90 client-co-chaperone complexes are sequentially formed during the client activation process (Li, J. et al., 2011; Hessling et al., 2009; Li, J. et al., 2013). One of the first complexes consists of Sti1p and Hsp90 (Richter et al., 2003; Hessling et al., 2009). Sti1p is a potent inhibitor of the ATPase activity of Hsp90 and must be displaced in order for cycle progression to occur (Prodromou et al., 1999; Li, J. et al., 2011). While Sti1p inhibits Aha1p binding to Hsp90, it was recently revealed that Cpr6p in concert with Aha1p or Sba1p can efficiently displace Sti1p from Hsp90 to allow cycle advancement (Lee, C. et al., 2012; Wolmarans et al., 2016; Li, J. and Buchner, 2013). The mechanism behind this 'co-chaperone switching' is not fully understood. While Sti1p and Cpr6p bind to the *C*-terminus of Hsp90, the interaction of Sba1p or Aha1p with the *N*-terminus of Hsp90 is sufficient to displace Sti1p (Wolmarans et al., 2016). As the NxNNWHW motif is predicted to extend towards the *N*-terminus of the Hsp90 we wondered if it is required for 'co-chaperone switching'. To test this, we reconstituted ATPase cycling reactions *in vitro*. Consistent with previous results, Sti1p was unable to inhibit Aha1p stimulation of Hsp90 ATPase activity in the presence of Cpr6p (Figure 3.14) (Wolmarans et al., 2016). Interestingly, Aha1p$^{\Delta 11}$ was also able to stimulate Hsp90 ATPase activity in the presence of Sti1p and Crp6p (Figure 3.14). This suggests that the NxNNWHW motif is not required for co-chaperone switching *in vitro*.

The co-chaperone Sba1p is also known to inhibit the ATPase activity of Hsp90 (Panaretou et al., 2002). In contrast to Sti1p which inhibits the ATPase activity by restricting Hsp90 in an open conformation, Sba1p inhibits the ATPase activity of Hsp90 by binding to the closed conformation (Ali et al., 2006; McLaughlin et al., 2006). As such, Sba1p inhibition can be used as a sensor for the Hsp90 closed conformation (Retzlaff et al., 2010; Richter et al., 2004). To analyze the effect of the NxNNWHW motif of Aha1p on the conformational state of Hsp90, we titrated Sba1p into Aha1p or Aha1p$^{\Delta 11}$ stimulated reactions. Despite Aha1p$^{\Delta 11}$ having a higher apparent affinity for Hsp82p than Aha1p (0.44 +/- 0.03 μM compared to 1.24 +/- 0.06 μM; *p-value 0.0035), Sba1 had a significantly higher apparent affinity for Hsp82p that was stimulated by Aha1p $^{\Delta 11}$ compared to Aha1 (1.15 +/- 0.02 μM compared to 6.21 +/- 1.38 μM; *p-

value 0.0235) (Figure 3.15). This suggests that in the presence of Aha1p$^{\Delta 11}$, Hsp90 is in an *N*-terminally dimerized conformation that is more readily recognized by Sba1p.

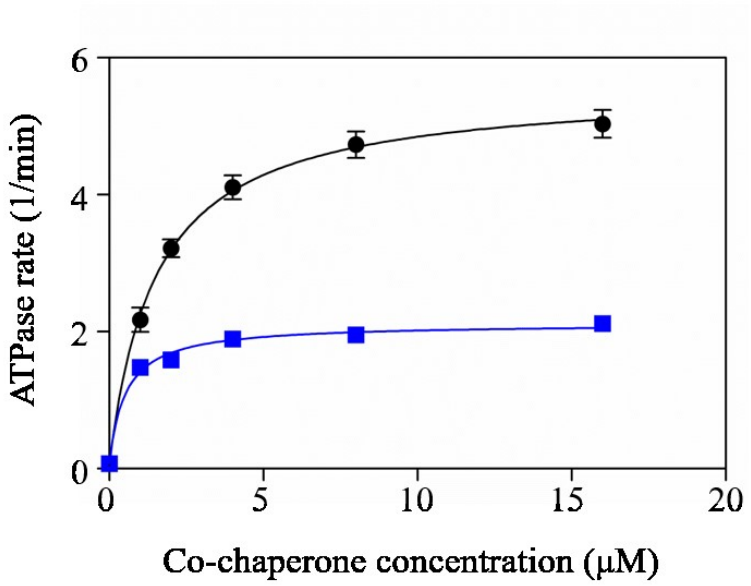

Figure 3.14 The NxNNWHW motif is not required for co-chaperone switching *in vitro*. Stimulation of Hsp82p ATPase activity by increasing concentration of Aha1p (black circles) and Aha1p$^{\Delta 11}$ (blue squares). Reactions contained 1 μM Hsp82p, 4 μM Sti1p, and 4 μM Cpr6p and indicated concentrations of Aha1p or Aha1p$^{\Delta 11}$ (n=3).

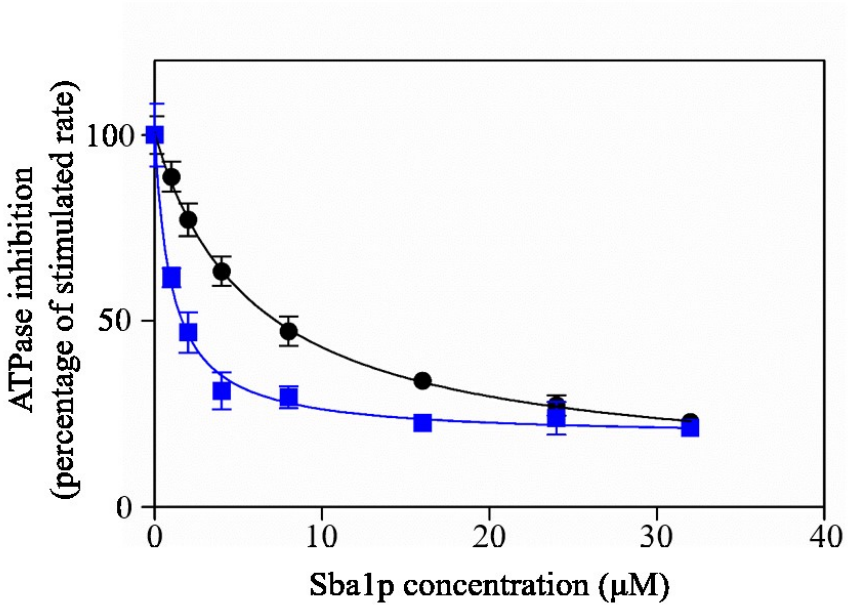

Figure 3.15 Sba1p inhibition of Aha1p- and Aha1p$^{\Delta 11}$-mediated Hsp82p stimulation. Inhibition of stimulated Hsp82p with Aha1p (black circles) or Aha1p$^{\Delta 11}$ (blue squares) by increasing concentrations of Sba1p. Reactions contained 1 μM Hsp82p, 5 μM of Aha1p or Aha1p$^{\Delta 11}$ and indicated concentrations of Sba1p (n=4).

3.2.7 The NxNNWHW motif does not influence lid closure after ATP binding

ATP-hydrolysis by Hsp90 is rate-limited by conformational change (Graf et al., 2009; Hessling et al., 2009). Local conformational changes are kinetically linked and have been shown to be cooperative (Schulze et al., 2016). Briefly, ATP binding drives closure of the ATP lid, *N*-terminal strand exchange between the two protomers of *N*-terminally dimerized Hsp90, and *N*-terminal and middle domain association (Figure 3.16 A). The addition of Aha1p was previously demonstrated to mobilize lid closure and accelerate the other associated conformational events (Schulze et al., 2016). The location of the NxNNWHW motif and our observed alteration of K_m when this motif is deleted support the idea that this conserved motif influences the *N*-terminal ATP-binding domain of Hsp90. To explore the mechanistic basis for reduced ATPase stimulation of Hsp90 by Aha1p$^{\Delta 11}$ and the associated reduction of K_m of ATP we collaborated with the Neuweiler lab (University of Würzburg, Germany) who determined the rate constants of Hsp90 lid closure using photoinduced electron transfer (PET) fluorescence quenching (Figure 3.16 B) (Schulze et al., 2016). In Michaelis-Menton kinetics, a reduction of K_m can originate from a reduction of rate constant of ATP hydrolysis or from modulation of ATP binding (*i.e.* from a reduced rate constant of ATP dissociation or increased rate constant of ATP association), or both (Atkins and Nimmo, 1980; Schnell, 2014). We hypothesized that the deletion of the NxNNWHW motif would likely affect kinetics of conformational change (*i.e.* would slow lid closure and therefore reduce the rate constant of ATP hydrolysis by Hsp90). In agreement with previous findings the time constant of lid closure of yeast Hsp90 was $\tau = 320\pm100$ s (Figure 3.17 A) (Schulze et al., 2016). Surprisingly, we found that lid closure was accelerated to the same degree by Aha1p and Aha1p$^{\Delta 11}$ ($\tau = 14\pm2$ s and $\tau = 15\pm2$ s, respectively) (Figure 3.17 B). This shows that the decrease in ATPase stimulation by Aha1p$^{\Delta 11}$ is not due to a defect in the acquisition of the catalytically-competent state of Hsp90. We also tested Hch1p and Hch1p$^{\Delta 11}$ and found, again, that time constants of lid closure were within error ($\tau = 105\pm13$ s and $\tau = 120\pm16$ s, respectively) (Figure 3.17 C). Interestingly, different fluorescence intensities of the label positioned on the *N*-terminal domain were observed between the Aha-type co-chaperones with and without the NxNNWHW motif, which shows that there is an interaction of the NxNNWHW motif with the *N*-terminal domain (Figure 3.17 B-C).

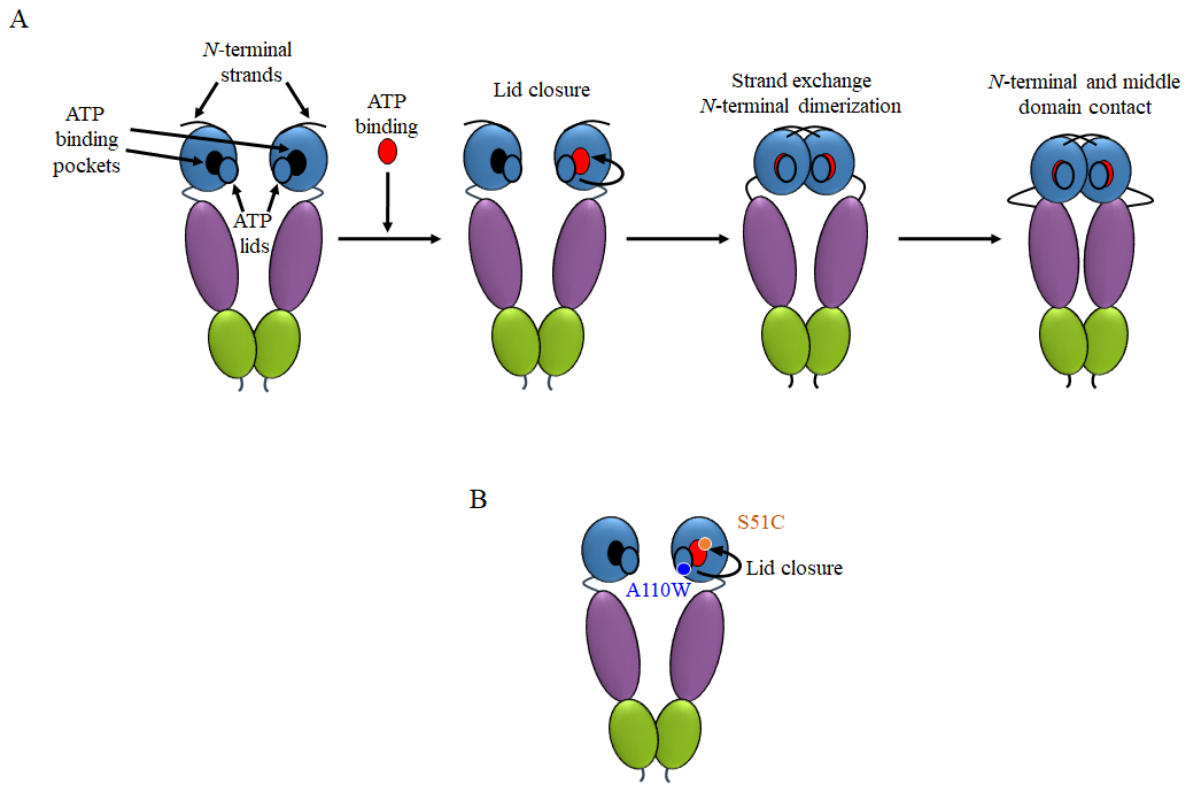

Figure 3.16 Conformational dynamics associated with Hsp90 ATP binding.

A. ATP binding drives ATP lid closure, *N*-terminal strand exchange and *N*-terminal dimerization, and *N*-terminal and middle domain contact. **B.** PET-reporter construct S51C-A110W used to probe kinetics of Hsp90 lid dynamics. Mutations were engineered to introduce a cysteine (C) residue for attachment of a fluorophore (AttoOxa11) and a tryptophan (W) residue to measure fluorescence quenching.

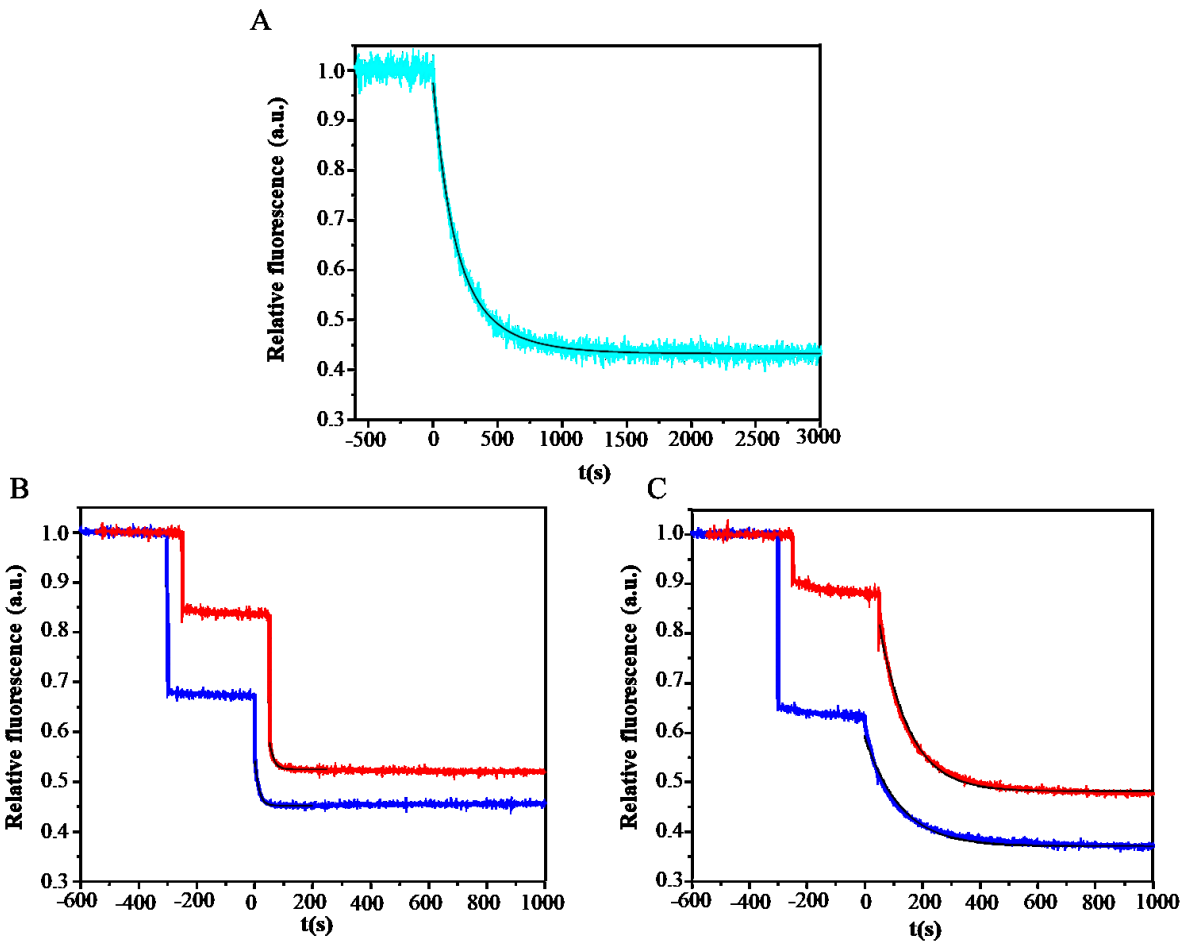

Figure 3.17 Kinetics of lid closure of Hsp90 and its modulation by Aha-type co-chaperones. **A.** Time course of PET fluorescence quenching of fluorescently modified Hsp90 mutant S51C-A110W (cyan). The non-hydrolyzable ATP analogue AMP-PNP, which traps Hsp90 in the closed-clamp conformation, was added at time t=0. The black line is a fit to a bi-exponential decay function. **B.** Same experiment as shown in (A) but Aha1p (blue) or Aha1p$^{\Delta 11}$ (red) was added 300 seconds prior to addition of AMP-PNP. Black lines are fits to exponential decay functions. **C.** Same experiment as shown in (A) but Hch1p (blue) or Hch1p$^{\Delta 11}$ (red) was added 300 seconds prior to addition of AMP-PNP. Black lines are fits to exponential decay functions. Data sets of Aha1p$^{\Delta 11}$and of Hch1p$^{\Delta 11}$ are offset along the x-axis for reasons of clarity. Experiments were conducted by Jonathan Schubert from Dr. Hannes Neuweiler's Lab (University of Würzburg, Germany).

3.3 Summary

Aha1p and Hch1p are important regulators of Hsp90 activity (Armstrong et al., 2012; Horvat et al., 2014; Meyer et al., 2004; Nathan et al., 1999; Panaretou et al., 2002). While the residues involved in the binding of Aha1p and Hch1p to Hsp90 are relatively conserved, the most highly conserved segment is the NxNNWHW motif found within the first 11 amino acids (Figure 3.1) (Meyer et al., 2004). In Chapter 3, we reveal the importance of this motif for both Hsp90 ATPase stimulation and *in vivo* activity of Aha1p and Hch1p. In the co-crystal structure between the Aha1p *N*-terminal domain and the middle domain of Hsp90 the NxNNWHW motif is unresolved (Meyer et al., 2004). However, inferences from the location and orientation of these domains within the resolved structure of full-length Hsp90, suggest that the *N*-terminal segment is likely extended towards the *N*-terminal Hsp90 ATPase domains (Figure 3.2) (Ali et al., 2006; Koulov et al., 2010; Retzlaff et al., 2010).

Employing the temperature sensitive mutants Hsp82p^{E381K} and Hsc82p^{S25P}, we were able to show that the NxNNWHW motif is required for the *in vivo* function of both Hch1p and Aha1p, respectively (Figure 3.7 and Figure 3.10). Importantly, rescue of Hsc82p^{S25P} function by Aha1p, but not Aha1p$^{\Delta 11}$, was reflected in the chaperoning of the Hsp90 client v-Src (Figure 3.11). Our initial investigation into the role of the NxNNWHW in Hsp90 ATPase stimulation confirmed previous reports that it was not necessary for stimulation (Figure 3.3) (Meyer et al., 2004). Upon further investigation, however, we revealed that the presence of *N*-terminal 6xHis-tags for purification of proteins plays a role in masking the function of these proteins (Figure 3.6). By moving the purification tags from the *N*- to the *C*-terminus we show that the NxNNWHW motif is indeed required for both Aha1p and Hch1p stimulation of Hsp90 (Figure 3.4).

The Hsp90 ATP hydrolysis cycle involves several intra- and inter-subunit rearrangements for the activation of client proteins. Restructuring of the ATP lid is thought to initiate this process (Richter et al., 2006). In the absence of nucleotide, the ATP lid is in an open position and the binding of ATP results in rapid remodelling and slow closure (Schulze et al., 2016). Closure of the lid over bound ATP is accompanied by remodeling of the *N*-terminal segments, *N*-terminal dimerization, and stabilization of the catalytic loop in its open and active state (Li, J. et al., 2013; Schulze et al., 2016; Hessling et al., 2009). The conformational changes that occur after ATP

binding comprise the rate limiting step(s) of the ATPase cycle (Weikl et al., 2000; Graf et al., 2009; Hessling et al., 2009). Aha1p is known to activate Hsp90 ATPase activity by accelerating these steps (Hessling et al., 2009; Li, J. et al., 2013; Richter et al., 2006; Richter et al., 2001; Schulze et al., 2016). In turn, after ATP hydrolysis occurs, these events must be reversed to allow the release of ADP and inorganic phosphate so that a new cycle of ATP binding and hydrolysis can be initiated (Figure 3.18).

The order and events associated with each of the steps involved in ATP hydrolysis and release are not well understood, especially in the context of co-chaperone proteins. Deletion of the NxNNWHW motif results in a clear defect in the function of Aha-type co-chaperones. Interestingly, the deletion of the NxNNWHW motif did not impair Hsp90 ATPase stimulation by the Aha1p *N*-terminal domain on its own (Figure 3.5). This suggests that the NxNNWHW motif is not required for remodeling of the catalytic loop and appears to be dependent on the *C*-terminal domain of Aha1p. The *C*-terminal domain of Aha1p is required for full stimulation of Hsp90 ATPase activity as it supports the acquisition of the Hsp90 *N*-terminally dimerized state (Wolmarans et al., 2016). Aha1p has been shown to efficiently displace Sti1p from Hsp90 in concert with Cpr6p, to allow Hsp90 to proceed to a closed conformation (Li, J. et al., 2013). We show that the NxNNWHW motif is not required for this function of Aha1p (Figure 3.14). Sba1p is known to stabilize the *N*-terminally dimerized state of Hsp90, slowing ADP release after hydrolysis has occurred (Graf et al., 2014). We show that Sba1p bound with a higher apparent affinity to Hsp90 in complex with Aha1p$^{\Delta 11}$ compared to Aha1p (Figure 3.15). While we acknowledge that the NxNNWHW could be simply acting as a steric barrier to Sba1p binding, we were unable to identify a defect in the ability of Aha1p $^{\Delta 11}$ mutant to promote the catalytically active *N*-terminally dimerized state. We specifically monitored conformational changes in lid closure, and reveal that Aha1p and Aha1p$^{\Delta 11}$ showed identical rate of lid mobilization (Figure 3.17). We also observed an increase in apparent affinity for nucleotide in ATPase assays with both Aha1p$^{\Delta 11}$ and Hch1p$^{\Delta 11}$, compared to their wildtype counterparts (Figure 3.13). Together, these findings suggest that the NxNNWHW motif is not involved in the acquisition of the closed *N*-terminally dimerized, catalytically active, state of Hsp90 (Figure 3.18- Step 1). We propose that the impairment in ATPase stimulation by the NxNNWHW mutants (Step 2), is due to changes in ADP release after hydrolysis has occurred (Step3) and therefore resetting of the Hsp90 cycle (Figure 3.18).

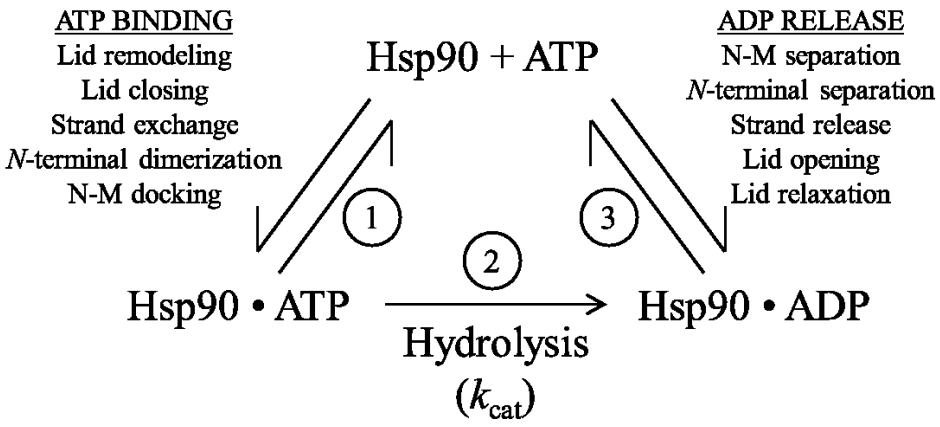

Figure 3.18 Simplified schematic of the Hsp90 ATPase cycle.

1. ATP binding is accompanied by several conformational rearrangements that must occur for Hsp90 to attain its catalytic state. **2.** ATP hydrolysis occurs. **3.** Conformational changes are reversed for the release of ADP and another round of ATP binding and hydrolysis to by initiated.

Deletion of the NxNNWHW motif affects Aha1p and Hch1p in a similar manner despite the different roles these co-chaperones play in regulating Hsp90 biology in yeast (Armstrong et al., 2012; Horvat et al., 2014). While the role of Aha1p in eliciting a partially closed lid conformation should make ATP-trapping more efficient and thus lower the K_m for ATP, we confirm previous reports that the addition of Aha1p does not change apparent K_m (Figure 3.13) (Panaretou et al., 2002). Alternatively, Hch1p has a marked effect on the apparent affinity for ATP (Figure 3.13). It is interesting that despite these difference, the deletion of the *N*-terminal motif resulted in a decrease in the apparent K_m, which means an increase in nucleotide affinity, for Aha1p$^{\Delta 11}$ and Hch1p $^{\Delta 11}$ compared to their wildtype counterparts (Figure 3.13). For Aha1p the NxNNWHW appears to act cooperatively with the *C*-terminal domain, as it is not necessary for stimulation by the Aha1p *N*-terminus alone (Figure 3.5). For Hch1p the pronounced effect on the apparent K_m of Hsp90 for ATP may explain the ability of Hch1p, but not Aha1p, to confer sensitivity to Hsp90 inhibitors (Armstrong et al., 2012). If Hch1p in part promotes ATPase activity through nucleotide exchange, as suggested by the increased K_m, this may allow more access of Hsp90 inhibitors to the ATP-binding pocket and therefore the ablated ability of Hch1p$^{\Delta 11}$ to sensitize yeast to Hsp90 inhibitors (Figure 3.8).

We show that the NxNNWHW motif is essential for the *in vivo* activity of Hch1p and Aha1p, while only affecting nucleotide exchange *in vitro*. The deletion of the NxNNWHW motif does not affect the ability of Aha1p$^{\Delta 11}$ and Hch1p $^{\Delta 11}$ to promote the acquisition of the catalytically active state but eliminates their biological activity. This suggests that nucleotide exchange (or release) is a critical function of these co-chaperones. Future work focusing on the elements of the functional cycle, such as ATP hydrolysis and nucleotide exchange dynamics, may reveal important insights into how Hsp90 client activation is regulated.

Chapter 4 Characterization of the role of the RKxK motif in Aha-type co-chaperone function

4.1 Introduction/Rationale

The conformational dynamics of Hsp90 are currently best described in terms of ATP binding and hydrolysis. In the apo state Hsp90 is found in an open conformation, dimerized only at the *C*-terminus. ATP binding in the *N*-terminal binding pocket leads to ATP lid closure, *N*-terminal dimerization, and further structural rearrangements that result in the association of the *N*-terminal and middle domains. Upon ATP hydrolysis dissociation of the *N*-terminal domains and release of ADP and inorganic phosphate occurs. Along with achieving the closed state, repositioning of the catalytic loop (residues 370-390) in the middle domain has been shown to be critical for ATP hydrolysis (Cunningham et al., 2008; Meyer et al., 2003). Specifically, Arg 380 has been suggested to interact with the γ-phosphate of Hsp90 bound ATP, acting as an ATP sensor and stabilizing the connection between the *N*-terminal and middle domains (Meyer et al., 2003). Interestingly, new data suggests that Arg 380 does not directly participate in ATP hydrolysis and instead indirectly supports ATPase activity of Hsp90 by stabilizing the closed conformation (Cunningham et al., 2012). This fits within the models that suggest that Hsp90 conformational changes are not coupled to ATP hydrolysis, but that conformational dynamics are rate-limiting for Hsp90 activity (Schopf et al., 2017; Zierer et al., 2016; Schmid, S. et al., 2018).

The RKxK motif (residues 59-62), found at the tip of a flexible loop in the Aha1 *N*-terminal domain, is conserved across Aha-type co-chaperones (Figure 3.1). Structural studies reveal that these residues are pointed towards the catalytic loop of Hsp90 (residues 370-390), in close proximity to the conserved NxNNWHW motif discussed in Chapter 3 (Figure 4.1). Mutating any of the RKxK residues in the isolated *N*-terminus of Aha1 (Aha1p^{N}) results in a decrease in stimulation of the ATPase activity of Hsp90 (Meyer et al., 2004). Consistent with this, mutating residues of the RKxK motif in Hch1p results in a decrease in Hsp90 ATPase stimulation (Horvat et al., 2014). Interestingly, only mutation of Lys 60, of the Hch1p RKxK motif, results in impaired *in vivo* function. The different *in vivo* and *in vitro* requirements of Hch1p for this motif, suggests that the biological function of Hch1p is not explicitly linked to stimulation of the ATPase activity of Hsp90 (Horvat et al., 2014). The role of the RKxK motif in full length Aha1p has not been explored. Previously demonstrated differences between Hch1p and Aha1p led us to hypothesize that the RKxK motif is important for both the *in vivo* and *in vitro* function of Aha1p.

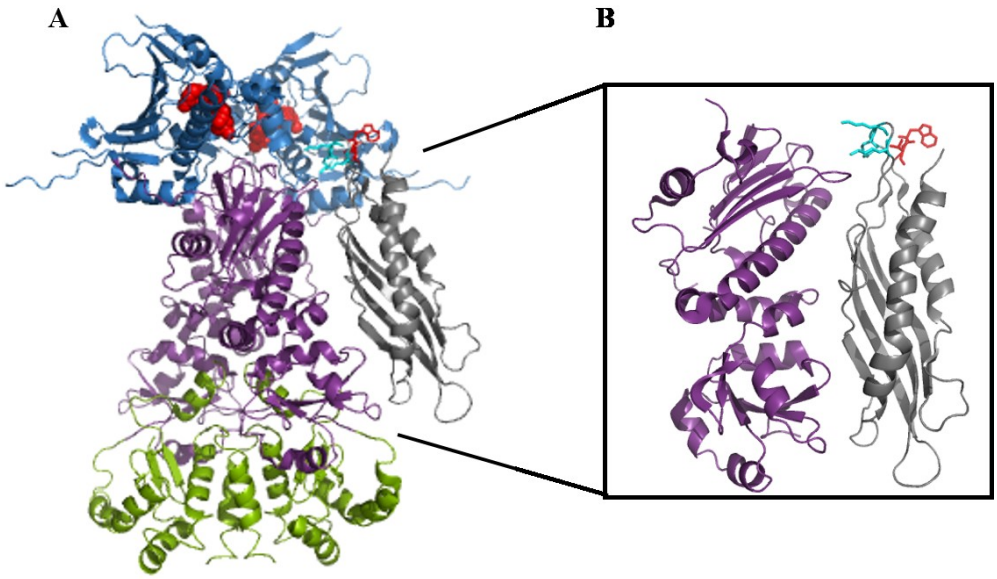

Figure 4.1 Crystal structure of the predicted position of the RKxK motif.

A. Crystal structure of full length, closed Hsp90 dimer (*N*-terminal domains- blue, middle domains- purple, *C*-terminal domains- green, ATP- red) (2CG9 (Ali et al., 2006)) with the *N*-terminal domain of Aha1p (grey) (1USV (Meyer et al., 2004)) superimposed. The RKxK motif is highlighted as cyan sticks. Trp11 and Val12 (red sticks) indicate where the *N*-terminal NxNNWHW motif would be present (it is unstructured in 1USV). **B.** A model of the complex between the middle domain of Hsp90 (purple) and the *N*-terminal domain of Aha1p (grey) shown in (A) (1USV (Meyer et al., 2004)).

4.2 Results

4.2.1 Lys 60 of the RKxK motif is required for optimal Aha1p-mediated ATPase stimulation

Initial work on the RKxK motif has shown that these residues are important for Hsp90 ATPase stimulation by Aha1p^{N} (Meyer et al., 2004). Mutating any of these residues to an alanine (Aha1p$^{N\text{-}R59A}$, Aha1p$^{N\text{-}K60A}$, or Aha1p$^{N\text{-}K62A}$) results in impaired Hsp90 ATPase stimulation (Meyer et al., 2004). Similarly, work from our lab has shown that mutating any of these residues to an alanine in Hch1p (Hch1p^{R59A}, Hch1p^{K60A}, and Hch1p^{K62A}) also results in reduced stimulation of Hsp90 ATPase activity (Horvat et al., 2014). In Chapter 3, we demonstrate that the NxNNWHW motif is important for Hsp90 ATPase stimulation by full-length Aha1p, but not Aha1p^{N}. To test the importance of the RKxK motif in full-length Aha1p-mediated Hsp90 stimulation, we generated mutants encoding alanine mutations for each of the RKxK residues (Aha1p^{R59A}, Aha1p^{K60A}, and Aha1p^{K62A}). Surprisingly, unlike mutations in Hch1p, only Aha1p^{K60A} was impaired in its ability to stimulate Hsp90 ATPase activity (Figure 4.2). We re-examined Hsp90 ATPase stimulation by the Hch1p harbouring mutations in the RKxK motif using *C*-terminally tagged co-chaperones. Consistent with the *N*-terminally tagged co-chaperones (Horvat et al., 2014), all Hch1p RKxK mutants were impaired in their ability to stimulate Hsp90 ATPase activity (Figure 4.3). These results demonstrate that Lys 60 is specifically important for Aha1p-mediated stimulation of Hsp90.

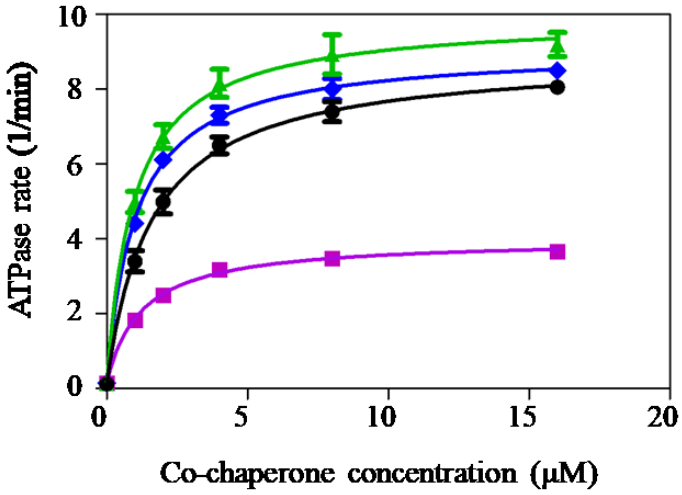

Figure 4.2 Aha1p requires only Lys 60 of the RKxK motif for optimal stimulation of Hsp90 ATPase activity.

Stimulation of Hsp82p by Aha1p (black circles), Aha1p^{R59A} (blue diamonds), Aha1p^{K60A} (purple squares), and Aha1p^{K62A} (green triangles). Reactions contained 1 μM Hsp82p and indicated concentrations of co-chaperone (n=3).

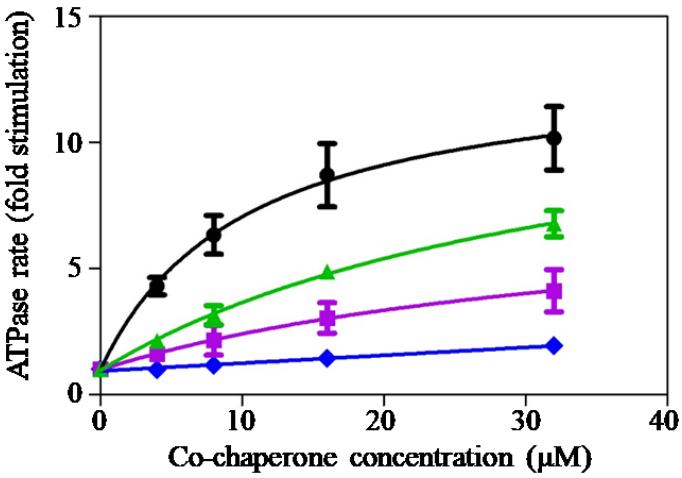

Figure 4.3 Hch1p requires the RKxK motif for optimal stimulation of Hsp90 ATPase activity.

Stimulation of Hsp82p by Hch1p (black circles), Hch1p^{R59A} (blue diamonds), Hch1p^{K60A} (purple squares), and Hch1p^{K62A} (green triangles). Reactions contained 4 μM Hsp82p and indicated concentrations of co-chaperone (n=3). The ATPase rate is shown as fold stimulation of the intrinsic Hsp82p rate.

4.2.2 Aha1p employs Lys 60 of the RKxK motif to rescue the in vivo activity of Hsc82p^{S25P}

As highlighted in Chapter 3, the Hsc82p^{S25P} mutant provides a means of interrogating Aha1p function in cells. Our lab has previously shown that yeast expressing the temperature sensitive mutant Hsp82p^{E381K}, as the sole source of Hsp90, are rescued by the overexpression of Hch1p, Hch1p^{R59A} and Hch1p^{K62A}, but not Hch1p^{K60A} (Horvat et al., 2014). This is striking because mutation of any of these residues results in impaired Hsp90 ATPase stimulation (Figure 4.3) (Horvat et al., 2014). To test the importance of the RKxK motif in full-length Aha1p-mediated Hsp90 stimulation, we employed the temperature sensitive mutant, Hsc82p^{S25P}, for which impairments by the deletion of *AHA1* can be rescued by the overexpression of Aha1p (Figure 3.10). We looked at the ability of Aha1p, Aha1p^{R59A}, Aha1p^{K60A} and Aha1p^{K62A} to rescue yeast that expressed Hsc82p^{S25P} and had *AHA1* deleted. Similar to Hch1p, mutating Lys 60 (Aha1p^{K60A}) resulted in a decreased ability to rescue the temperature sensitive growth phenotype, whereas the overexpression of Aha1p, Aha1p^{R59A}, and Aha1p^{K62A} rescued the growth of Hsc82p^{S25P} (Figure 4.4). Co-chaperones expressed in yeast cells have a *C*-terminal myc-tag and we confirmed expression levels by western blot (Figure 4.4).

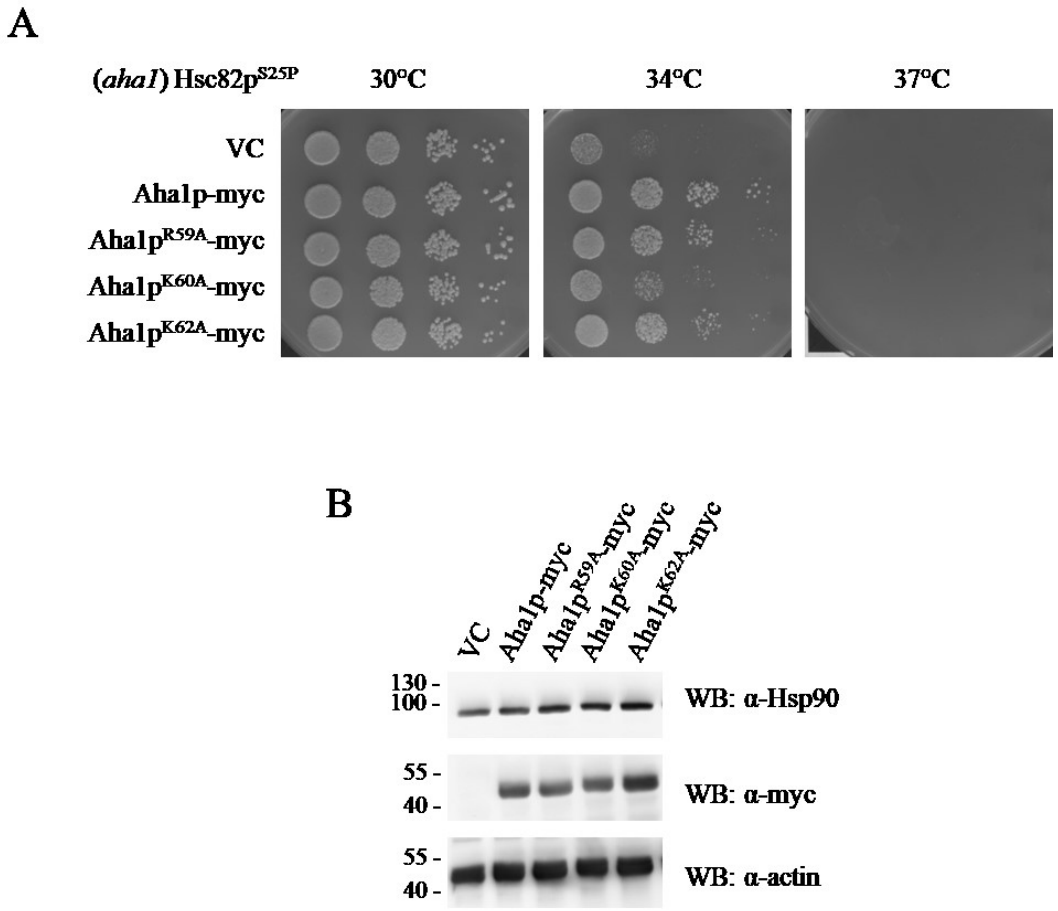

Figure 4.4 Aha1p employs Lys 60 of the RKxK motif to rescue Hsc82p^{S25P} function *in vivo*. **A.** Overexpression of Aha1p, Aha1p^{R59A}, and Aha1p^{K62A}, but not Aha1p^{K60A}, can rescue the growth of yeast expressing Hsc82p^{S25P}. Cells were grown overnight at 30°C in YPD supplemented with Hygromycin (300 mg/L). 10-fold serial dilutions were prepared and 10 µL aliquots were spotted on YPD + Hygromycin (300 mg/L) plates. Plates were grown for 2 days at the indicated temperatures. **B.** Western analysis of yeast shown in (A) with anti-Hsp90, anti-myc, and anti-actin antibodies. Representative results of three independent experiments are shown.

4.2.3 Analysis of Hsp82p^{S25P} co-chaperone-mediated ATPase stimulation

While Hch1p is able to rescue Hsp82p^{E381K}, the overexpression of Aha1p and Aha1p^{N} are not (Horvat et al., 2014). Interestingly, Aha1p and Aha1p^{N}-mediated Hsp90 ATPase stimulation is impaired by the E381K mutation but stimulation by Hch1p is not (Horvat et al., 2014). This supports the hypothesis that, as the overexpression of either Aha1p or Hch1p rescues the poor growth phenotype of Hsc82p^{S25P}, Hsp90 ATPase stimulation by either co-chaperone would be unaffected by the S25P mutation. While we show that Aha1p mediated stimulation of Hsp82p^{S25P} is impaired (Figure 3.12), Hch1p-mediated ATPase stimulation of Hsp82p^{S25P} is unaffected (Figure 4.5).

To determine the role that the RKxK motif plays, we tested the ability of the three Aha1p mutants (Aha1p^{R59A}, Aha1p^{K60A} and Aha1p^{K62A}) to stimulate the ATPase activity of Hsp82p^{S25P}. Wildtype Aha1p, Aha1p^{R59A}, and Aha1p^{K62A} were all able to stimulate Hsp82p^{S25P} to a similar degree (Figure 4.6). However, stimulation of Hsp82p^{S25P} by Aha1p^{K60A} was impaired (Figure 4.6). Even though the magnitude of stimulation of Hsp82p^{S25P} by Aha1p does not reach that observed for wildtype Hsp82p, it seems that stimulation in general is important for the functional rescue *in vivo*.

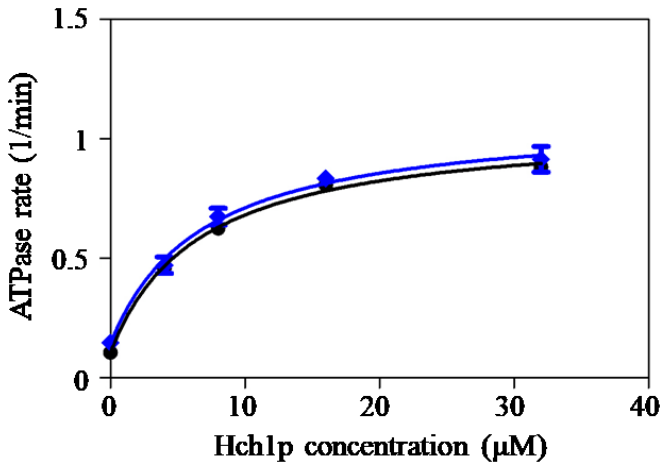

Figure 4.5 Mutation of Ser 25 in Hsp90 does not affect ATPase stimulation by Hch1p. Stimulation of the Hsp82p (black circles) or Hsp82p^{S25P} (blue diamonds) by increasing concentrations of Hch1p. Reactions contained 4 µM Hsp82p or Hsp82p^{S25P} and indicated concentration of co-chaperone (n=3).

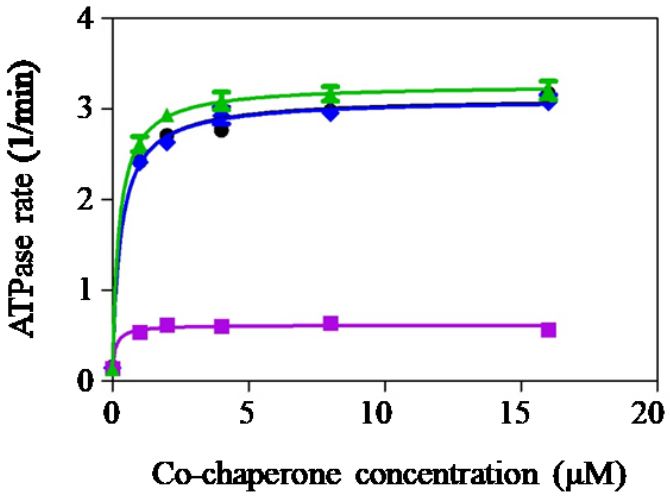

Figure 4.6 Lys 60 of the RKxK motif is required for Aha1p stimulation of Hsp82p^{S25P}. Stimulation of Hsp82p^{S25P} by Aha1p (black circles), Aha1p^{R59A} (blue diamonds), Aha1p^{K60A} (purple squares), and Aha1p^{K62A} (green triangles). Reactions contained 1 μM Hsp82p^{S25P} and indicated concentrations of co-chaperone (n=3).

4.3 Summary

The kinetics and structural basis for Hsp90 ATPase stimulation are still under much debate. Here we build on evidence that suggests a three-step model for ATPase stimulation by Aha1p (Wolmarans et al., 2016). The first and second steps occur when the *N*-terminal domain of Aha1p interacts with the middle domain of Hsp90, potentially driving a small increase in ATPase activity through interaction with the catalytic loop. The third step results in rearrangement of one or both of the Hsp90 *N*-terminal domains allowing for the participation of the *C*-terminal domain of Aha1p and full Hsp90 ATPase stimulation. The findings outlined in Chapter 4 help to define a role for the RKxK motif in Aha1p ATPase stimulation.

We confirmed previous reports that, similar to Aha1p^{N}, the RKxK motif of Hch1p is required for Hsp90 ATPase stimulation (Figure 4.3) (Meyer et al., 2004; Horvat et al., 2014). This suggests that mutation of these residues results in alterations in step 1 and/or 2, changing co-chaperone interaction with the catalytic loop of Hsp90, resulting in a decrease in ATPase activity. Surprisingly, Aha1p^{R59A} and Aha1p^{K62A} were able to stimulate the ATPase activity of Hsp90 to a similar level as Aha1p (Figure 4.2). This suggests that the *C*-terminal domain, present in full length Aha1p but not Aha1p^{N}, is able to overcome the defects of mutations at either Arg 59 or Lys 62, allowing for rearrangement of the Hsp90 *N*-terminal domains, required for full stimulation. This is not the case for mutation of Lys 60, which has decreased ATPase stimulation (Figure 4.2).

We employed the temperature sensitive mutant, Hsc82p^{S25P} to investigate the *in vivo* role of the RKxK motif in Aha1p function. The ATPase stimulation of Hsp90 is directly reflected in the ability of the Aha1p RKxK mutants to rescue growth defects of the temperature sensitive mutant Hsc82p^{S25P}, as Aha1p, Aha1p^{R59A}, and Aha1^{K62A} are able to rescue growth defects but Aha1p^{K60A} is not (Figure 4.4). Our lab previously employed the temperature sensitive mutant, Hsp82p^{E381K} to investigate the role of the RKxK motif in the *in vivo* function of Hch1p (Horvat et al., 2014). While Hch1p, Hch1p^{R59A} and Hch1p^{K62A} rescue the growth of Hsp82p^{E381K}, Hch1p^{K60A}, Aha1p, or Aha1p^{N} do not (Horvat et al., 2014). In addition, Hch1p-mediated stimulation of Hsp82p^{E381K} was unaffected, whereas stimulation by Aha1p and Aha1p^{N} were greatly reduced (Horvat et al., 2014). Our initial investigation into Hsp82p^{S25P} showed that, similar to the Hsp82p^{E318K}, Hch1p-mediated stimulation of Hsp82^{S25P} was unaffected by this

mutation and surprisingly stimulation by Aha1p was greatly reduced (Figure 4.5) (Horvat et al., 2014). Further investigation revealed that although Aha1p, Aha1p^{R59A}, and Aha1p^{K62A} show a reduction in stimulation of Hsp82p^{S25P} ATPase activity, Aha1p^{K60A} is further reduced (Figure 4.6).

Together, these results suggest that impairments in Hsp90 ATPase stimulation by Aha1p may reflect a defect in the biological function of Aha1p. While the defects seen when the RKxK motif is mutated in Hch1p or Aha1p^{N} can be overcome in the case of R59A and K62A when present in full length Aha1p, the mechanism behind this is still unknown (Meyer et al., 2004; Horvat et al., 2014). Lys 60 is thought to reside closest to Glu 372 and Asp 373 of the catalytic loop, where the formation of ion-pair interactions would result in stabilization of the catalytic loop in the active conformation (Meyer et al., 2004). In the apo state, Arg 380 has been shown to interact with the middle domain resulting in stabilization of Hsp90 in an open conformation (Cunningham et al., 2012; Southworth and Agard, 2011). Perhaps, while mutation of any of the RKxK residues results in loss of stabilization of the catalytic loop in the active conformation, mutation of Lys 60 actually supports the interaction of Arg 380 with the middle domain and therefore the apo conformation of Hsp90. The close proximity of Arg 59 and Lys 62 to Lys 60 and the fact that our structural models are based on an ATPase inhibited conformation of Hsp82p, means a deeper analysis is required.

Chapter 5 Analysis of additional models and methods to further elucidate the function of Aha-type co-chaperones

5.1 Introduction/Rational

Aha1p was identified as a co-chaperone of Hsp90 based on a homology search of the previously identified co-chaperone Hch1p (Nathan et al., 1999; Panaretou et al., 2002). Prior to identification as a co-chaperone of Hsp90, Aha1 was identified as a 38-kDa protein (p38) that bound the cytoplasmic tail of vesicular stomatitis virus glycoprotein (VSVG) (Sevier and Machamer, 2001). The name Aha1 was adopted because '**a**ctivation of **H**sp90 **A**TPase' is the prominent role of Aha1. However, while ATPase activity is central to Hsp90 function, Aha1 is not essential and there are only limited reports outlining the effects of Aha1 on well-known Hsp90 clients (Panaretou et al., 2002; Lotz et al., 2003; Sun et al., 2012; Harst et al., 2005). One of the relationships that best outlines the importance of Aha1 in Hsp90 function has been shown using the cystic fibrosis transmembrane conductance regulator (CFTR) and a cystic fibrosis disease causative mutant, $CFTR^{\Delta F508}$ (Wang, X. et al., 2006; Koulov et al., 2010). Upon inhibition of Hsp90, maturation of nascent CFTR and therefore its export to the cell surface is prevented (Loo et al., 1998). Interestingly, over-expression of Aha1 results in the degradation of CFTR and the mutant form $CFTR^{\Delta F508}$. Conversely, downregulation of Aha1 results in maturation and increased stabilization of $CFTR^{\Delta F508}$, allowing for its export and activity at the cell surface (Wang, X. et al., 2006).

The relationship between Aha1 and Hsp90 is complex. We have used the model organism *S. cerevisiae* to examine the role and differences between Aha1p and Hch1p in Hsp90 regulation (Armstrong et al., 2012; Horvat et al., 2014). In addition, *in vitro* assays have allowed our lab to further understand and define the mechanism of Aha1-mediated stimulation of Hsp90 ATPase activity (Horvat et al., 2014; Armstrong et al., 2012; Wolmarans et al., 2016). Imbalances in the Hsp90 machinery have been shown to contribute to the onset and progression of disease such as neurodegenerative diseases and cancer (Shelton et al., 2017; Barrott and Haystead, 2013). Thus while Hsp90 has long been a target of therapeutic intervention in disease treatment, a greater understanding of co-chaperone regulation may provide important therapeutic alternatives. We hypothesize that Aha1 plays additional roles in Hsp90 regulation that have not been revealed. To further our understanding of Aha1 function and regulation, we investigated additional models and phenotypes.

5.2 Results

5.2.1 Expression levels of Hsp90 and co-chaperones are altered in melanoma

Mutations that drive cancer cell proliferation and metastasis often result in proteins becoming heavily reliant and/or obligate clients of Hsp90. It is now appreciated that Hsp90 functions within the context of co-chaperones proteins which may also contribute to the hallmarks of cancer. The constitutive overexpression of Hsps in tumour cells is well reported (Calderwood and Gong, 2016; Wu et al., 2017) The expression of co-chaperone proteins, including Aha1, has been shown to vary across different cancer types (Uhlen et al., 2017; Holmes et al., 2008). In melanoma, a frequently observed point mutation of BRAF ($BRAF^{V600E}$) results in its obligate dependence on Hsp90 (Grbovic et al., 2006; Ascierto et al., 2012). Hsp90 has been identified as a marker of melanoma progression and increased demand for Hsp90 in melanoma cells is well established (McCarthy et al., 2008). We used melanoma as a model to examine changes in other components of the Hsp90 system. Non-transformed immortalized melanocytes (MelanA) were used as a control for the spontaneously occurring melanoma cell line (B16-F0) and its highly metastatic derivative (B16-F10) (Fidler and Nicolson, 1976). We determined changes in protein expression level by western blot (Figure 5.1). Total protein levels were quantified and experiments were performed in replicate. Consistent with previous reports, Hsp90 expression was increased in the transformed cell lines compared to the controls (Uhlen et al., 2017; McCarthy et al., 2008). Aha1expression levels were also increased in the melanoma cells whereas, no change in the expression level of Cdc37 or p23 was observed and HOP exhibited a shift in molecular weight (Figure 5.1). The shift in molecular weight suggests that HOP may be heavily post-translationally modified in the transformed cells or that transformed cells may express a different splice variant. Overall, the diversity in co-chaperone highlights the varied roles that co-chaperones play in Hsp90 function.

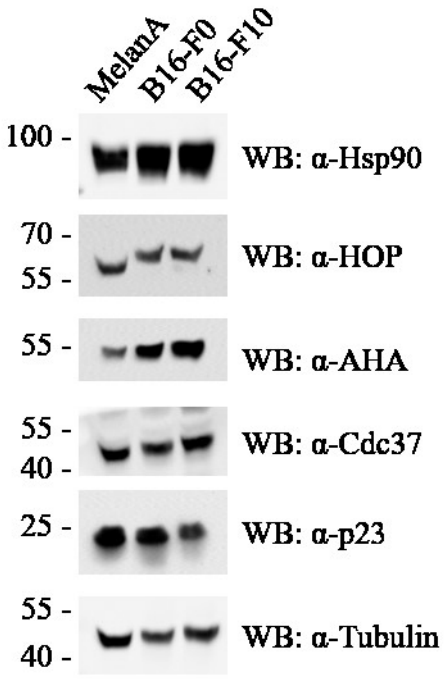

Figure 5.1 Components of the Hsp90 are altered in melanoma cell lines.

Western blot analysis of 20 μg of proteins from the indicated cell lines probed with anti-Hsp90, anti-HOP, anti-AHA, anti-Cdc37, anti-p23 and anti-Tubulin antibodies. Tubulin was used as a loading control. Images are representative of three replicative experiments.

5.2.2 Post-translational modifications of the Hsp90 system

Post-translational modifications of Hsp90 have been demonstrated to play a key role in co-chaperone recruitment, client activation, and sensitivity to Hsp90 inhibitors (Mollapour and Neckers, 2012; Zuehlke et al., 2015). Co-chaperone proteins are also known to be post-translationally modified although, the significance and mechanism of Hsp90 regulation is only beginning to be understood (Shao et al., 2003; Dunn et al., 2015; Bansal et al., 2004). We looked to assess the post-translational modification status of components of the Hsp90 system in melanoma by resolving different post-translationally modified species using 2-dimensional gel electrophoresis (2DGE). We were able to resolve species for Aha1 and HOP but did not resolve any Hsp90 species (Figure 5.2 A). Absence of Hsp90 species may have been due to the immobilized pH gradient (IPG) strips used for the isoelectric focusing step, which were pH 4-7. Non-modified Hsp90 has an approximate predicted isoelectric point (pI) of 4.8 (4.91 phosphosite or 4.69 ExPASy) with phosphorylation causing an acidic shift requiring resolution close to pH 4 (Hornbeck et al., 2015; Gasteiger et al., 2005). Although we were able to resolve species of Aha1 (predicted pI of 5.41) and HOP (predicted pI 6.4), we also see increased proteins levels in the transformed cells which limited the changes that could be attributed to modification status. To achieve increased resolution, we isolated endogenous Aha1 by immunoprecipitation (IP) using beads coupled to anti-AHA1 antibodies and show five species of Aha1 are present in MelanA cells (Figure 5.2 B). To determine if the five species of Aha1 identified were specific to melanoma cells, we also looked at the different species present in human breast adenocarcinoma MDA-MB-231 cells. We expressed both mouse and human Aha1 and see a similar distribution of species, suggesting that the five species identified are not specific to melanoma cells (Figure 5.2 C). Several sites along Aha1 are known to be subject to post-translational modification (Hornbeck et al., 2015). Treatment with lambda protein phosphatase resulted in a reduction in the identified spots seen by 2DGE (Figure 5.2 D). This preliminary investigation indicated that there are multiple species of phosphorylated Aha1 found within the cell.

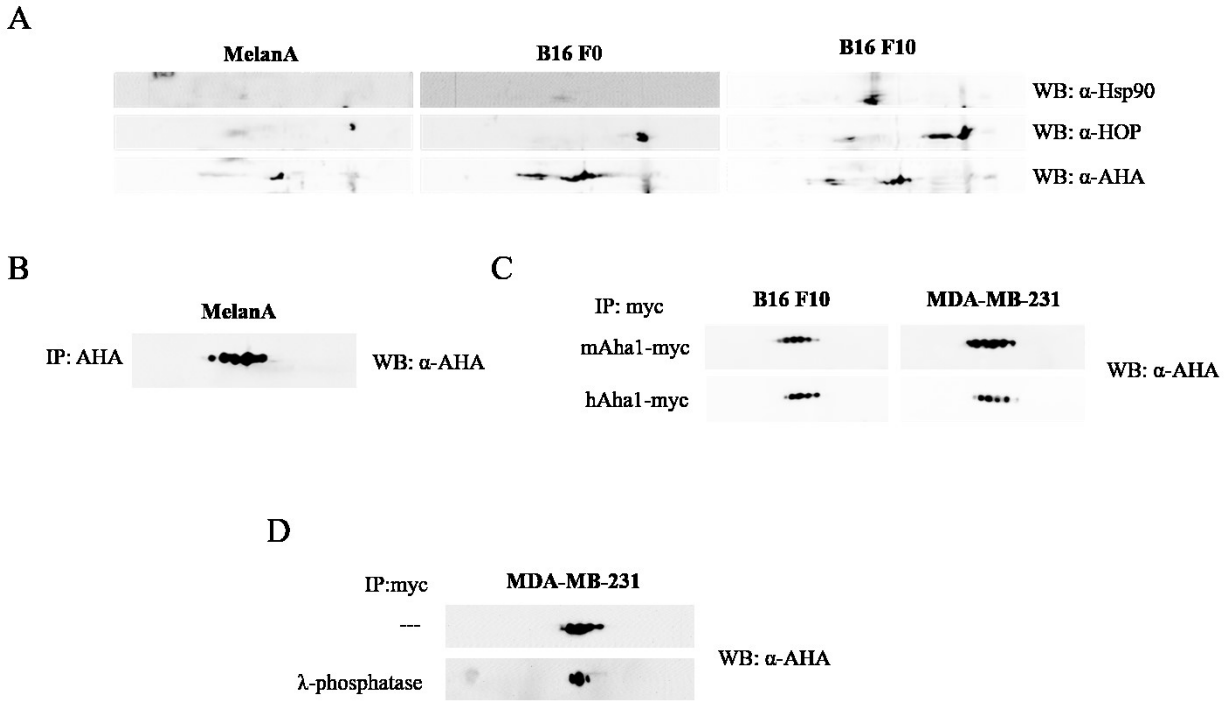

Figure 5.2 2DGE reveals different phosphorylated species of Aha1.

A. 2DGE and western blot of lysate from the indicated cell lines. **B.** 2DGE and western blot of Aha-IP from MelanA cells. **C.** 2DGE and western blot of myc-IP from indicated cell lines transfected with Aha1 from mouse (m) or human (h). **D.** 2DGE and western blot of myc-IP from cells transfected with human Aha1-myc. The IP sample was either left untreated or treated with lambda protein phosphatase as indicated.

Phosphorylation and other post-translational modifications are suggested as a method for co-chaperone recruitment to Hsp90, which is in vast excess of the co-chaperones (Sahasrabudhe et al., 2017; Li, J. et al., 2013). We wanted to determine if specific post-translational modifications, identified by 2DGE, may be responsible for Aha1 recruitment to Hsp90. Mimetic and non-modifiable Aha1 mutants, of residues known to be post-translationally modified, were made for expression in mammalian cell culture. We set out to investigate the interaction of the variants with Hsp90 by co-IP. Variants which showed changes to levels of Hsp90 would be further analyzed by 2DGE to determine if it represented a prominent species of Aha1 found in the cell. Upon expression of the Aha1 variants only the *N*-terminal mutant form of Aha1 (Δ27) showed a decrease in Hsp90 binding, while the post-translational modification mutants did not show changes in Hsp90 interaction (Figure 5.3 A). Interestingly, we were able to isolate the glucocorticoid receptor (GR) in complex with Hsp90 and the Aha1 phosphorylation mutants (Figure 5.3 A). As we did not see changes in interaction of the post-translational modification mutants with Hsp90 we did not proceed with further investigation by 2DGE. Future experiments should investigate different IP conditions as salt concentration plays a large role in the Aha1-Hsp90 interaction and therefore may reveal changes in interaction that we did not see (Panaretou et al., 2002). Interestingly, phosphorylation of Tyr 223, and the phospho-mimetic mutant (Y223E) were previously reported to promote the interaction of Aha1 with Hsp90 (Dunn et al., 2015). In our hands, Aha-Y223E showed very low expression levels making comparisons to other mutants difficult however, it did seem to show an increased interaction with Hsp90 (Figure 5.3 B). We did not see an abrogation of the interaction of the Y223F mutant with Hsp90 as was previously reported (Figure 5.3 B) (Dunn et al., 2015). There still remains much to be understood about the conditions in which co-chaperones and Hsp90 interact and the role of post-translational modifications.

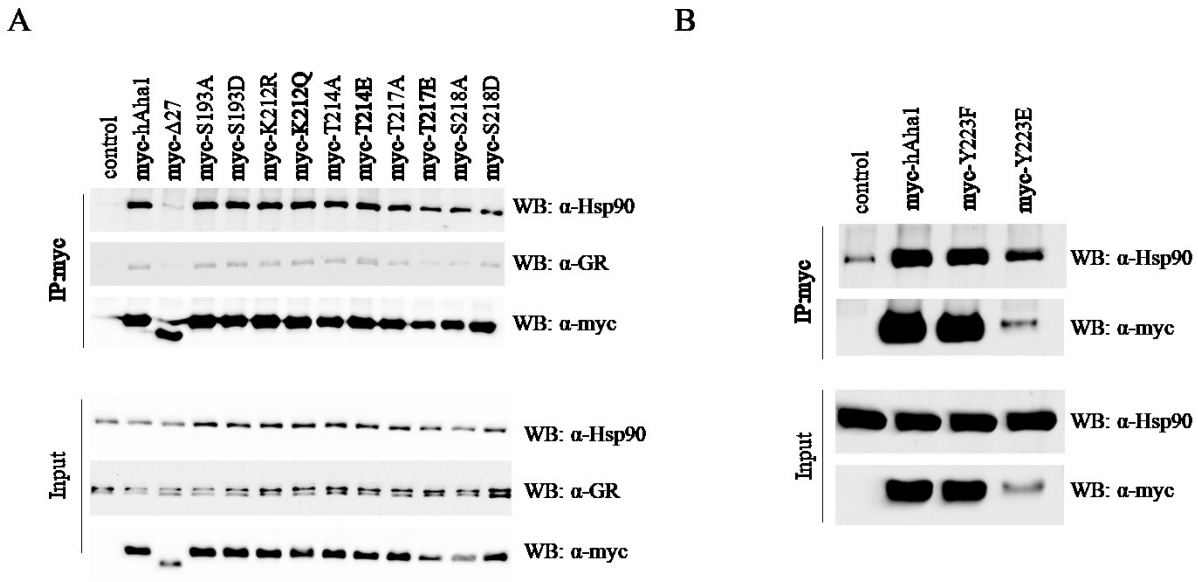

Figure 5.3 Hsp90 interaction with post-translational modification variants of Aha1.

A. and **B.** Aha1 myc-tagged mutants (as indicated) were transfected into MDA-MB-231 cells. After 48 hours cells were lysed and co-immunoprecipitations were performed. Western blot of IP and input were probed with anti-Hsp90, anti-GR, and anti-myc antibodies.

5.2.3 Aha1 regulation of Hsp90 inhibitor sensitivity

In mammalian cells the knockdown of AHA1 was shown to result in increased sensitivity to the Hsp90 inhibitor 17-AAG (Holmes et al., 2008). The deletion of Aha1 in mice results in no obvious developmental phenotype and the cells derived from these mice have only been shown to have minor defects in the activation of some Hsp90 clients (Echeverria et al., 2011). We wanted to determine if the deletion of Aha1 also results in increased sensitivity to Hsp90 inhibitors, specifically NVP-AUY922 which we have used in our yeast assays. Using mouse adult fibroblast (MAF) cells that have endogenous Ahsa1 gene deleted (Aha-/-) (received from Picard Lab, University of Geneva) we tested inhibitor sensitivity. Both wildtype and Aha1-/- cells were treated with varying concentrations of the Hsp90 inhibitor NVP-AUY922 for 48 hours before measuring cell viability using an MTT colourimetric assay. The Aha-/- MAFs show increased sensitivity to Hsp90 inhibitors, which is consistent with previous AHA1 silencing results (Figure 5.4) (Holmes et al 2008). Due to limited transfection efficiency of the MAFs, we were unable to determine if expression of Aha1 is able to provide a protective mechanism against Hsp90 inhibitors. Our results suggest that modulation of Aha1 might provide a therapeutic strategy for increased sensitivity to Hsp90 inhibitors.

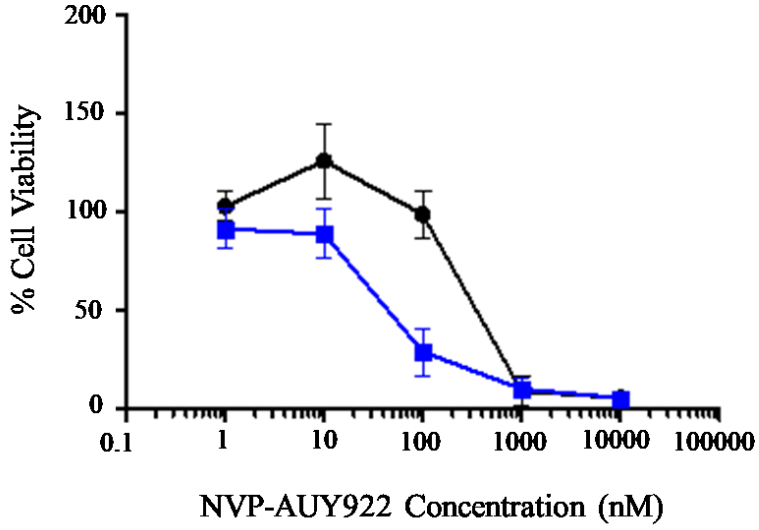

Figure 5.4 Aha1-/- cells have increased sensitivity to Hsp90 inhibitors.

Wildtype (black circles) and Aha1-/- (blue squares) MAF cells were treated with the indicated concentrations of NVP-AUY922 for 48 hours. Cell viability was measured using an MTT, colorimetric assay (n=3).

5.2.4 IRF3 phosphorylation is impaired in Aha-/- cells

Large scale interaction studies have been conducted to investigate the interaction between Hsp90, co-chaperones, and client proteins (Taipale et al., 2012; Zhao and Houry, 2013; Taipale et al., 2014; Rizzolo et al., 2017). Interestingly, one of these interactions studies revealed interferon regulatory factor 3 (IRF3) as a strong binding partner of Aha1 (Taipale et al., 2014). IRF3 is a transcription factor involved in an arm of the innate immune response (Newton and Dixit, 2012). When phosphorylated, IRF3 is translocated to the nucleus where it initiates the transcription of interferons (Lin, R. et al., 1999). This response is important for the detection of cell damage and chemical patterns associated with pathogens. Changes in Aha1 expression have been shown to result in alterations in the phosphorylation status of other Hsp90 clients (Holmes et al., 2008). We wanted to determine if Aha1 plays a role in the phosphorylation of IRF3 and therefore, its activation and initiation of the innate immune response. We used polyinosinic:polycytidylic acid (poly(I:C)), a dsRNA mimic, to examine the activation (phosphorylation status) of IRF3 when Aha1 is absent from cells. We transfected wildtype and Aha1-/- MAFs with poly(I:C) and examined IRF3 phosphorylation by western blot. IRF3 phosphorylation was reduced in Aha1-/- MAFs compared to wildtype controls (Figure 5.5). We expanded these findings showing that silencing of Aha1 in the human lung carcinoma cell line, A549, also results in a decrease in IRF3 phosphorylation when induced with poly(I:C) (Figure 5.6).

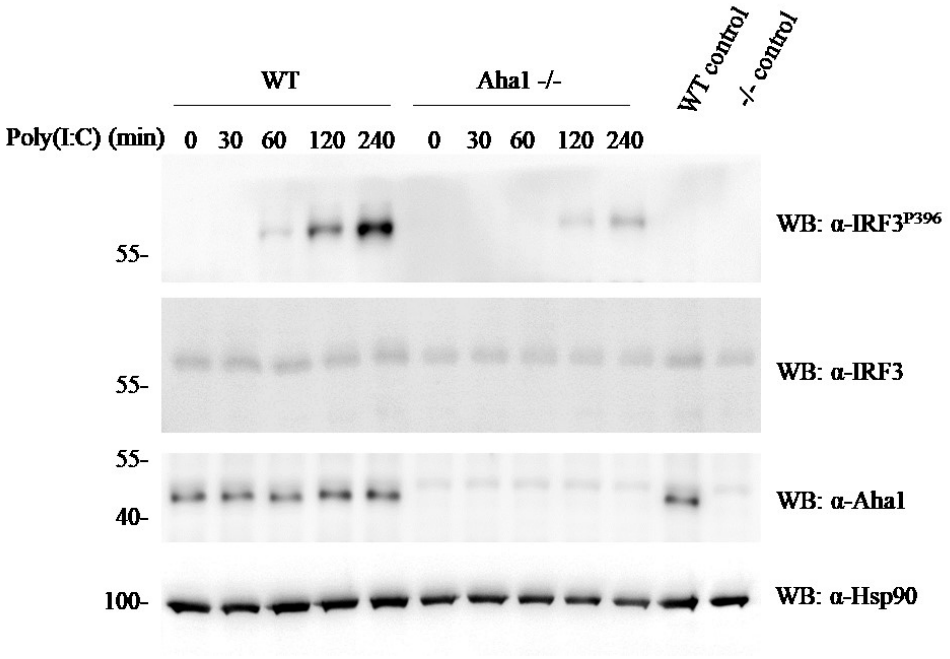

Figure 5.5 IRF3 phosphorylation is impaired in Aha1-/- cells stimulated with poly(I:C). Wildtype (WT) and Aha1-/- MAF cells were transfected with 1 µg of poly(I:C) for the indicated times. Changes in protein expression were analyzed by western blot with anti-IRF3^{P396}, anti-IRF3, anti-Aha1, and anti-Hsp90 antibodies. Images are representative of three replicative experiments.

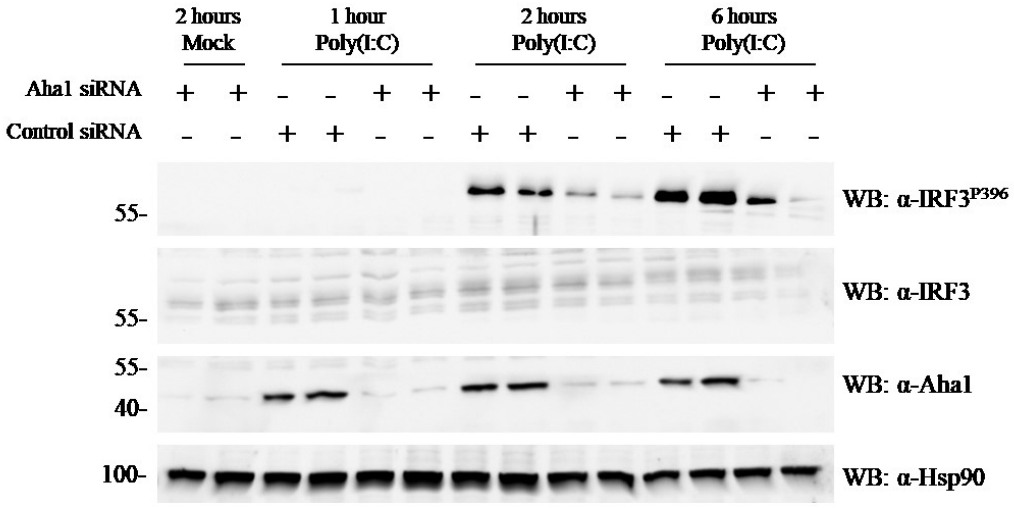

Figure 5.6 IRF3 phosphorylation is impaired when Aha1 is silenced in cells stimulated with poly(I:C).

A549 cells were transfected with siRNAs directed against directed against Ahsa1 or negative control siRNA for 48 hours before treatment with 1 μg of poly(I:C) for the indicated times. Changes in protein expression were analyzed by western blot with anti-IRF3^{P396}, anti-IRF3, anti-Aha1, and anti-Hsp90 antibodies. Images are representative of three replicative experiments.

5.2.5 Aha1 plays a role in anti-viral signalling

As Aha1 was originally identified as a protein that binds the cytoplasmic tail of VSVG, we wanted to further our investigation into the role of Aha1 in the immune response and look at changes upon viral infection (Sevier and Machamer, 2001). In collaboration with the Hobman Lab (University of Alberta) we compared the response of WT and Aha1-/- MAF cells to viral infection. We show that Aha1-/- cells infected with West Nile virus (WNV) show more robust viral genome replication compared to control cells at both 24 and 48 hours (Figure 5.7 A). We corroborated this result in A549 cells, showing that IRF3 phosphorylation is impaired when Aha1 is silenced, although to a lesser extent (Figure 5.7 B). These experiments need to be repeated, however, the same trend was seen when these experiments were conducted under slightly different conditions providing support for our conclusions.

Hsp90 is required for the activation of other components of the innate immune response including TBK1 (TANK-binding kinase) and IKKε (inhibitors of nuclear factor kappa-B), upstream kinases of IRF3 (Yang, K. et al., 2006; Broemer et al., 2004). To address if these upstream kinases are affected we probed for TBK1 and IKKε using antibodies that recognize total protein as well as specific phosphor-forms that indicate activation by western blot. Unfortunately, investigation into these upstream kinases was unsuccessful with our current antibodies and western blot protocol. Additional antibodies and/or methods will be required to continue investigation of upstream factors. We received reporter constructs to look at the downstream consequences of Aha1 knockout and induction of the innate immune response and will need to determine viable transfection methods to further this line of investigation. Overall, this is an exciting new finding for Aha1 and Hsp90 regulation in cells and provides an interesting starting point for continued investigation.

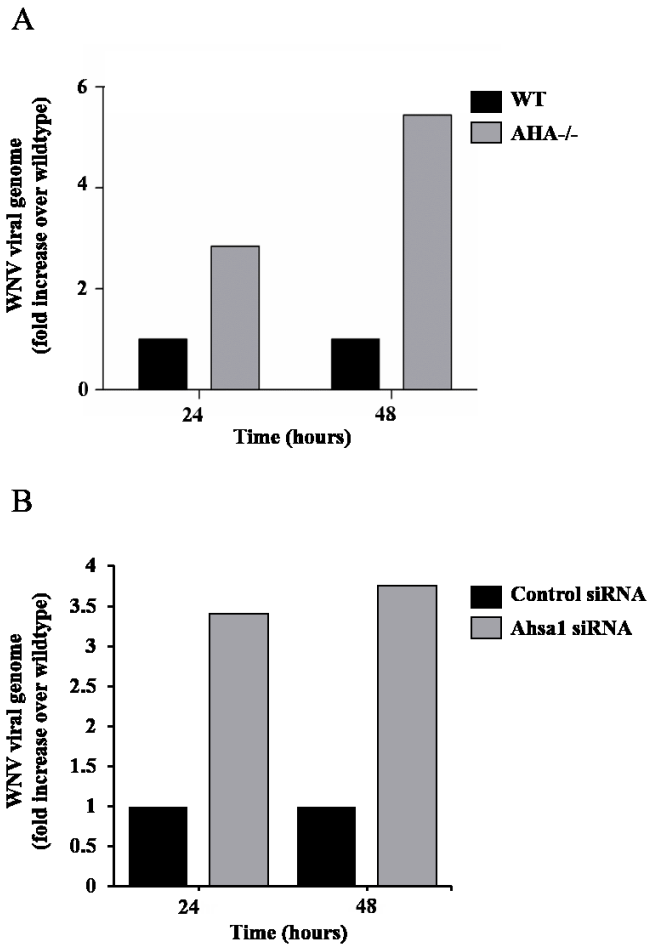

Figure 5.7 WNV replication is enhanced in the absence of Aha1.

A. WNV replication is enhanced in Aha1-/- cells. Wildtype and Aha1-/- MAF cells were infected with WNV for the indicated times. WNV genomic replication was measure using qrtPCR. WNV viral genome replication is shown as fold increase over wildtype (n=1). **B.** WNV replication is enhanced in Aha1 silenced cells. A549 cells were transfected with siRNA directed against Ahsa1 or negative control siRNA for 48 hours before being infected with WNV for the indicated times. WNV genomic replication was measured using qrtPCR. WNV viral genome replication is shown as fold increase over wildtype (n=1). qrtPCR experiments were conducted in collaboration with Dr. Anil Kumar and Eileen Reklow from Dr. Tom Hobman's Lab (University of Alberta).

5.3 Summary

The regulation of Hsp90 is complex. With Aha1 being the most potent stimulator of the Hsp90 ATPase activity identified to date, we wanted to better understand its biological relevance. In Chapter 5 we highlight a combination of approaches that we have used to investigate the role of Aha1 in Hsp90 function. Our initial experiments looked at the global expression of components of the Hsp90 system in melanoma cells (Figure 5.1). We found that in addition to increased levels of Hsp90, Aha1 levels were also increased in melanoma cells. This suggests that BRAF mutants, and other Hsp90 clients in the transformed cells, may require an increase in Hsp90 ATPase activity. Alternatively, we observed no change in Cdc37 expression levels in melanoma cells. It has been shown previously that the overexpression of Cdc37 supports increased cell proliferation and silencing Cdc37 destabilizes clients and sensitizes cancer cells to Hsp90 inhibitors (Stepanova et al., 2000; Schwarze et al., 2003; Smith, J. R. et al., 2009). The overall supportive role of Cdc37 in proliferation has championed its therapeutic potential and the targeting of the Hsp90-Cdc37 complex in cancer, although Cdc37 expression levels vary in cancer types (Uhlen et al., 2017; Gray et al., 2007; Li, T. et al., 2018). As Cdc37 is involved in the recruitment of kinases to Hsp90, maintaining steady state levels of Cdc37 may be beneficial to balance the activation of kinases involved in proliferation and those that are important for apoptosis. For some co-chaperones, including p23, assigning expression level changes to a role in specifically influencing Hsp90 function is more difficult as they also have Hsp90-independant roles in the cell (Echtenkamp et al., 2011; Forafonov et al., 2008). The co-chaperone HOP is overexpressed in a majority of cancers and is also substantially induced by stress conditions (Chao et al., 2013; Kubota et al., 2010; Uhlen et al., 2017). It was surprising, therefore, that we identified a shift in molecular weight of HOP and not a change in expression level. The shift in molecular weight suggests that HOP may be heavily post-translationally modified in the transformed cells or a specific splice variant is expressed. The function of splice variants and post-translationally modified proteins can differ significantly from those normally expressed with potential differences having implications in cancer development (Blair, C. A. and Zi, 2011; Shkreta et al., 2013).

Post-translational modifications play an important role in Hsp90 chaperone dynamics (Mollapour and Neckers, 2012; Soroka et al., 2012; Mollapour et al., 2014). We wanted to determine if specific post-translational modifications of Aha1 result in altered interaction with

Hsp90 or play a heightened role in cancer cells. Surprisingly, the introduction of mutations at sites known to be post-translationally modified did not alter the interaction of Aha1 with Hsp90 (Figure 5.3). This was unexpected especially since several sites have been previously shown to alter the Aha1-Hsp90 complex (Dunn et al., 2015). As we observed 5 distinct species of Aha1 using 2DGE (Figure 5.2) it will be interesting to see if the post-translational modifications that these species represent can be identified. This line of investigation may be aided by the ability to express Aha1 mutants as the sole source of Aha1 in the cell. We received mouse adult fibroblast (MAF) cells that have endogenous Ahsa1 deleted (Aha-/-) (received from Picard Lab, University of Geneva). While these cells have only been shown to have minor defects in the activation of some Hsp90 clients, we showed that similar to the knockdown of Aha1, the deletion of Aha1 results in increased sensitivity to Hsp90 inhibitors (Figure 5.4) (Echeverria et al., 2011; Holmes et al., 2008).

Our investigation into the role of Aha1 in IRF3 activation and the innate immune response is in the very early stages. While the loss of Aha1 results in a loss of IRF3 phosphorylation (Figure 5.5 and Figure 5.6), the mechanism through which this proceeds is far from being understood. Together with our results that show WNV replication is enhanced in the absence of Aha1 (Figure 5.7), it points to a role for Aha1 as a potential host restriction factor. The innate immune response has a dual role in the initiation and progression of cancer, and the role that IRF3 plays in this is poorly understood (Hagerling et al., 2015). IRF3 was recently suggested to be an important therapy against gastric cancer (Jiao et al., 2018). This fits with the idea that in addition to virulence factors, the aberrant innate immune response to gut microbial products also plays a role in the pathogenesis of colorectal cancer (Rakoff-Nahoum and Medzhitov, 2006; Yu et al., 2017). Future work in defining the mechanism behind Aha1 function and Aha1 regulation of Hsp90 in the innate immune response will be important for further therapeutic advancement.

Chapter 6 Discussion

6.1 Synopsis

Hsp90 is an essential molecular chaperone required for the folding, maturation, and activation of a diverse group of client proteins. Co-chaperone proteins guide the conformational transitions that accompany the ATPase cycle of Hsp90 and are responsible for client protein activation. Aha-type co-chaperones are the most potent stimulators of the Hsp90 ATPase activity, however, the mechanism of action is poorly understood. The focus of my doctoral work was on understanding the role that Aha-type co-chaperones play in Hsp90 regulation. My results provide new insight into the conserved motifs of the Aha-type co-chaperones and the mechanism of Hsp90 function.

6.2 The conserved NxNNWHW motif is important for Aha-type co-chaperone function

In Chapter 3, we show for the first time that the conserved *N*-terminal NxNNWHW motif is important for the function of Aha-type co-chaperones. Mutations of Hsp90, both previously and newly identified, show the importance of the NxNNWHW motif for the *in vivo* activity of the Aha-type co-chaperones and deletion of the NxNNWHW motif resulted in impaired co-chaperone-mediated ATPase stimulation of Hsp90 *in vitro*. Interestingly, the deletion of the NxNNWHW motif from both Aha1p and Hch1p results in an increase in the apparent affinity for ATP of Hsp90, but the lid dynamics leading to the closed catalytically active state of Hsp90 appear unimpaired by the NxNNWHW deletion. We show that while Sti1p displacement is equally efficient regardless of the presence of the NxNNWHW, there is a higher apparent Sba1p binding affinity when the NxNNWHW is deleted. We suggest that the NxNNWHW motif could be regulating Hsp90 in part by mediating nucleotide exchange and that nucleotide exchange during the Hsp90 functional cycle may be more important than the rate of catalysis.

6.2.1 Further understanding the NxNNWHW motif and purification tags

In our investigation of the NxNNWHW motif we reveal that the location of the 6xHis-tag, used for protein purification, impacts the function of Aha-type co-chaperones. Comparison of *N*- and *C*-terminally 6xHis-tagged Aha1p constructs revealed several important features about the Aha-type co-chaperones (Figure 3.6). The higher stimulation rate of *C*-terminally tagged Aha1p suggests that the *N*-terminal 6xHis-tag interferes with Hsp90 ATPase stimulation. This makes sense because the *N*-terminus of Aha1p is predicted to extend towards the ATP binding sites of the Hsp90. In addition, we show that the *N*- and *C*-terminally tagged NxNNWHW mutants of

Aha1p stimulate the ATPase activity to a similar level as *N*-terminally tagged Aha1p. If the *N*-terminal 6xHis-tag could replace the NxNNWHW motif, then we would have expected *N*-terminally tagged Aha1p$^{\Delta 11}$ to stimulate to the same degree as *C*-terminally tagged Aha1p. This suggests that the residues that make up the NxNNWHW motif are important for its function and not just the length.

The role of individual amino acids in the NxNNWHW motif can be examined by constructing single amino acid point mutations. Mutations in the NxNNWHW motif of Aha1p could be tested for their ability to rescue Hsc82p^{S25P}, as in Chapter 3. Point mutants in the NxNNWHW motif of Hch1p could be tested for their ability to rescue Hsp82p^{E381K} or to induce drug sensitivity to Hsp90 inhibitors (Armstrong et al., 2012; Horvat et al., 2014). All point mutants could also be tested in *in vitro* ATPase assays. This would determine if specific amino acids are responsible for the impairments seen by deleting the NxNNWHW motif. It is possible that multiple residues are responsible for the function of the NxNNWHW motif. As asparagine residues (N) are polar and generally found on the surface of proteins and tryptophan residues (W) are hydrophobic and normally within the hydrophobic core of a protein, the NxNN and WHW pieces of the NxNNWHW motif may play differing roles. We could construct mutations to multiple residues (*e.g.* NxNNWHW to AxAAWHW or NxNNAHA) and assess these mutants in a similar manner to the point mutants.

While our current strategy involves the movement of the 6xHis-tag from the *N*-terminus to the *C*-terminus of these proteins, there is still a possibility that the 6xHis-tag has an impact on the function of the protein. Future work should investigate feasible methods of purification tag cleavage. Current restraints include limited protein quantity and yield, incomplete or multiple cleavage sites and the remainder of a small portion of the protease cleavage site. The location of purification tags may have impacted previous conclusions made with the Aha-type co-chaperones. However, our finding that co-chaperone switching is not dependent on the NxNNWHW motif provides confidence in previous analyses. Nonetheless, co-chaperone switching takes place at the start of the Hsp90 cycle and we suggest that the NxNNWHW plays a role for re-setting the cycle. Therefore the presence of an *N*-terminal tag may interfere with specific functions and the location of purification tags should be evaluated in future work.

Sba1p is known to bind to the *N*-terminally dimerized state of Hsp90 and inhibit Hsp90 ATPase activity (Ali et al., 2006; Panaretou et al., 2002). We show that Sba1 binds with a higher apparent affinity in the Aha1p$^{\Delta 11}$-mediated ATPase stimulated reactions. This suggests that Hsp90 is stabilized in the *N*-terminally dimerized conformation by Aha1p$^{\Delta 11}$ and is more readily recognized by Sba1p. It was recently shown that the overexpression of Hch1p results in a decrease in Sba1p isolated with Hsp90 (Zuehlke et al., 2017). By isolating Hsp90 from yeast overexpressing Hch1p or Hch1p$^{\Delta 11}$ and assessing the level of Sba1p bound we may be able to show that loss of the NxNNWHW motif results in an increase in Hsp90 in an Sba1p-binding-competent state.

6.2.2 Understanding apparent K_m for ATP of Hsp90 in terms of Hsp90 inhibitors sensitivity

We report that stimulation by Aha1p results in no significant change in the apparent K_m for ATP of Hsp82p from Hsp82p alone. Interestingly, we revealed that stimulation by Hch1p results in a large increase in K_m for ATP. The overexpression of Hch1p, but not Aha1p, results in hyper-sensitivity to Hsp90 inhibitors (Armstrong et al., 2012). This suggests that Hch1p may alter sensitivity to Hsp90 inhibitors by influencing the K_m. A higher apparent K_m for ATP means a lower affinity for nucleotide. Therefore, in the presence of Hch1p, the nucleotide binding pocket of Hsp90 may be more available to bind to inhibitors. Interestingly, mutant forms of Hsp82p that are known to be rescued by the deletion of *HCH1*, including Hsp82p^{W585T} and Hsp82p^{A587T}, are hyper-sensitive to Hsp90 inhibition (Piper et al., 2003; Armstrong et al., 2012; Zuehlke et al., 2017). By determining the apparent K_m for ATP of these mutants we may be able to establish a link between inhibitor sensitivity and apparent K_m. If there is a connection, then we should see an increase in apparent K_m for ATP in these mutants. In addition, analysis of Hsp82p^{E381K} in regards to Hsp90 inhibitors and apparent K_m for ATP would provide information about mutants that require Hch1p for rescued temperature sensitive growth (Horvat et al., 2014).

Further analysis using the mutant Hsp82p^{A107N}, which is known to enforce lid closure and confer resistance to Hsp90 inhibition, could help understand this association (Prodromou et al., 2000; Millson et al., 2010). If the increase in apparent K_m for ATP by Hch1p stimulation is due to increase time in the open state, then we might expect Hsp82p^{A107N} would show no change in K_m for ATP in Hch1p-stimulated reactions. Double mutants Hsp82p$^{A107N/W585T}$ or Hsp82p$^{A107N/A587T}$ may show a restoration in K_m of these mutants to wildtype levels. It will be

interesting to determine the effect of the S25P mutation on both inhibitor sensitivity and apparent K_m. As the temperature sensitive phenotype of this mutant is rescued by the overexpression of both Aha1p and Hch1p, it may not be impaired in a similar manner to those mutants that are affected by the expression of Hch1p alone, such as Hsp82p^{A587T}, Hsp82p^{G313S}, Hsp82p^{W585T}, and Hsp82p^{E381K}. In addition, determining the apparent K_m for ATP of Hsp90 for Aha1p^{N} and its role in the rescue of Hsc82p^{S25P} may be useful. Overall, this line of investigation could prove valuable in understanding and employing Hsp90 inhibitors.

6.3 Residues of the conserved RKxK motif are differentially required for function of the Aha-type co-chaperones

In Chapter 4, we investigated the role of the conserved RKxK motif in Aha-type co-chaperone function. The RKxK motif of the Aha-type co-chaperones is thought to interact with the catalytic loop of Hsp90 for ATPase stimulation of Hsp90 (Meyer et al., 2003; Meyer et al., 2004; Horvat et al., 2014). Here we elucidate that ATPase stimulation by Aha1p requires only Lys 60 of the RKxK motif. In the same way, we found that only Lys 60 is required for rescue of temperature sensitive growth of Hsc82p^{S25P} by Aha1p. Our results replicate what has been previously described for the *in vivo* function of Hch1p (Horvat et al., 2014). However, in accordance with previous findings, Arg 59, Lys 60, and Lys 62 all play a role in ATPase stimulation of Hsp90 by Hch1p (Horvat et al., 2014). Together, these results point to a role for the RKxK motif in the initial stages of Aha-type co-chaperone interaction with Hsp90, which results in a small stimulatory effect. Interaction and full ATPase stimulation of Hsp90 by Aha1p requires a conformation change for which Lys 60 is necessary.

6.3.1 Addressing the RKxK motif in Aha1p^{N} function

The initial work which demonstrated the importance of the RKxK motif in Aha-type co-chaperones was done using mutants in the *N*-terminal domain of Aha1p alone (Aha1p^{N}) (Panaretou et al., 2002). While we have shown that both *N*- and *C*-terminally tagged versions of Hch1p RKxK mutants are impaired in ATPase stimulation, we also know that Hch1p and Aha1p^{N} are not functionally equivalent in cells (Horvat et al., 2014; Wolmarans et al., 2016). Therefore, the initial experiments that investigated the role of the RKxK mutants in Aha1p^{N} (Panaretou et al., 2002), should be repeated using *C*-terminally tagged protein. Similar to Aha1p, assays that address the *in vivo* role of Aha1p^{N} have been limited. As both Aha1p and Hch1p

rescue the temperature sensitive growth of Hsc82p^{S25P} it is possible that Aha1p^{N} would similarly rescue the poor growth phenotype of this mutation. If this is true then we could use this mutant to address the *in vivo* function of the RKxK mutants and would predict that similar to both Aha1p and Hch1p, Aha1p$^{N\text{-}K60A}$ will be impaired *in vivo*. Alternatively, the NxNNWHW motif is necessary for rescue of the S25P mutant by both Aha1p and Hch1p, suggesting that this mutation impairs later steps of the Hsp90 cycle. Deletion of the NxNNWHW motif does not alter the function of Aha1p^{N} and the *C*-terminal domain is necessary for full stimulation by Aha1p. In this way, Aha1p^{N} may not be able to rescue the S25P mutant and could not be used for further *in vivo* testing.

6.3.2 Further defining the RKxK motif

The binding of Hch1p and Aha1p^{N} to the middle domain of Hsp90 results in weak stimulation of Hsp90 ATPase activity. Early structural work revealed that the RKxK motif of Aha1p^{N} may be important for stabilizing the catalytic loop of Hsp90 in the active conformation (Meyer et al., 2004). Since that time we have come to recognize the many differences that exist between Aha1p^{N}, Hch1p and Aha1p (Armstrong et al., 2012; Horvat et al., 2014; Wolmarans et al., 2016). Of specific interest is that the binding of Hch1p to the isolated *N*-terminal and middle domain of Hsp90 shows a different interaction pattern when compared with Aha1p^{N} (Wolmarans et al., 2016). NMR chemical shift data reveals that 19 residues of the Hsp90 middle domain are shifted with Hch1p binding compared to only 10 residues of Aha1p^{N}, with only 2 residues of similarity (Wolmarans et al., 2016). Interestingly, Hch1p was also shown to result in a strong interaction between the *N*-terminal domain and middle domain of Hsp90 (Wolmarans et al., 2016). This highlights that the same structural model for interaction should not be applied for these co-chaperones. Structural models of full-length Hsp90 with co-chaperone are difficult due to the dynamic interaction and conformational rearrangements that take place. However, the NMR data suggests that resolving a structure between the isolated middle domain of Hsp90 and Hch1p may reveal important differences between the interactions of Hch1p and Aha1p. In addition, the PET fluorescence quenching method, briefly described for our use in understanding the lid dynamics with the NxNNWHW motif, could be used to analyze the effect of the co-chaperones on the conformational changes of Hsp90 associated with ATP hydrolysis (Schulze et al., 2016). As the N-M communication is shown to be increase in NMR studies, we predict that like Aha1p, Hch1p

would accelerate the N-M domain association (Schulze et al., 2016; Wolmarans et al., 2016). It is hard to predict the role of Aha1p^{N} in this function because NMR studies with Aha1p^{N} do not show N-M docking but, the addition of Aha1p^{N} does result in ATPase stimulation (Wolmarans et al., 2016). We could also analyze the RKxK mutants using the PET fluorescence quenching method to try and determine if there are changes to the kinetics of lid closure, N-M docking, and β-strand exchange. It would be interesting to see if the mutation to Lys 60 results in specific alterations. We may also be able perform single-turnover ATPase assays to assess changes in ATPase activity for each of the RKxK mutants in Hch1p and Aha1p^{N}. The rate of Aha1p-stimulated reactions limits the use of single turnover experiments. Interfering with the movement of the catalytic loop, as suggested with the RKxK mutants, should result in slower ATPase activity even in single turnover experiments.

6.3.3 Exploring the role of Ser 25 and other key residues

Temperature sensitive mutants are an important means to study essential proteins in yeast and have provided vital insight into the mechanistic and structural details of the Hsp90 system. Unlike classical temperature sensitive mutants, Hsp90 mutants do not lose their ability to fold at restrictive temperatures but rather, they have reduced function that is revealed by the increase substrate burden associated with increasing temperatures. This is important as alterations in co-chaperones are able to further influence temperature sensitive mutant function. The data shown here demonstrates that mutation of Ser 25 results in temperature sensitivity that is worsened by the deletion of *AHA1* and can be rescued by the overexpression of Aha1p. Temperature sensitive mutants of Hsp90 have most often been described to be exclusively effected by alterations in Hch1p but not Aha1p (Nathan et al., 1999; Armstrong et al., 2012; Horvat et al., 2014; Zuehlke et al., 2017). In the screen that identified the temperature sensitive mutant Hsc82p^{S25P} (Hsp82p^{S25P}), Hsc82p^{Q380K} (Hsp82p^{Q384K}) was also identified as a temperature sensitive mutant and both were shown to be rescue by the overexpression of Aha1p or Hch1p and displayed a further reduction in growth upon their deletion (Jill Johnson, University of Idaho). Together these temperature sensitive mutants provide a new way to understand the similarities between Aha-type co-chaperone regulation of Hsp90 and new mechanistic details of the Hsp90 co-chaperone cycle.

In the AMP-PNP-inhibited conformation of Hsp90 bound to Sba1p, Ser 25 is found at the interface between the *N*-terminal and middle domains of the Hsp90 dimer in close proximity to the catalytic loop and specifically to Gln 384 (Figure 6.1 A and B) (Ali et al., 2006). The close proximity of Ser 25 and Gln 384 taken together with the similar phenotypes of mutations of these residues suggests that the interplay between these residues is important. In a model aligning the closed Hsp90 dimer (2CG9 (Ali et al., 2006)) and the isolated middle domain (1HK7 (Meyer et al., 2003)), to demonstrate a conformation where Hsp90 is dimerized but the catalytic loop is closed, S25P is in close proximity to the catalytic loop and no longer within reach of Gln 384 (Figure 6.1 C) (Prodromou, 2012). The position of these residues is once again changed when the *N*-terminus of Aha1p is bound, although Ser 25 and Gln 384 remain apart (Meyer et al., 2004). To analyze the importance of this interaction we could determine if the expression of a double mutant construct Hsp82p$^{S25Q/Q384S}$ results in a restored growth phenotype at elevated temperatures. Normal growth by this mutant would suggest that the interaction between these two residues is important. Mutation of Glu 381 (Hsp82p^{E381K}) results in temperature sensitive growth that can be rescued by the overexpression of Hch1p, but not Aha1p (Nathan et al., 1997; Horvat et al., 2014). Due to the close proximity of Glu 381 with Ser 25 and Gln 384 it would be interesting to determine if their rescue by Hch1p is due to different or similar functions of Hch1p. Exacerbated growth phenotypes of double mutants (Hsp82p$^{S25P/E381K}$ or Hsp82p$^{E381K/Q384K}$) would suggest different functions of these residues and multiple modes of Hch1p action. Although the structure between the *N*-terminal domain of Aha1p and the middle domain of Hsp90 has been suggested to show that Aha1p is responsible for the release of Arg 380, it does not show Arg 380 in a position that would be in contact with ATP (Meyer et al., 2004). It is interesting that while the *N*-terminal motif is unresolved in the crystal structure, it may still be playing a role in the structure. Structural analysis in the absence of the NxNNWHW motif may help to understand the interaction between Aha1p and the catalytic loop.

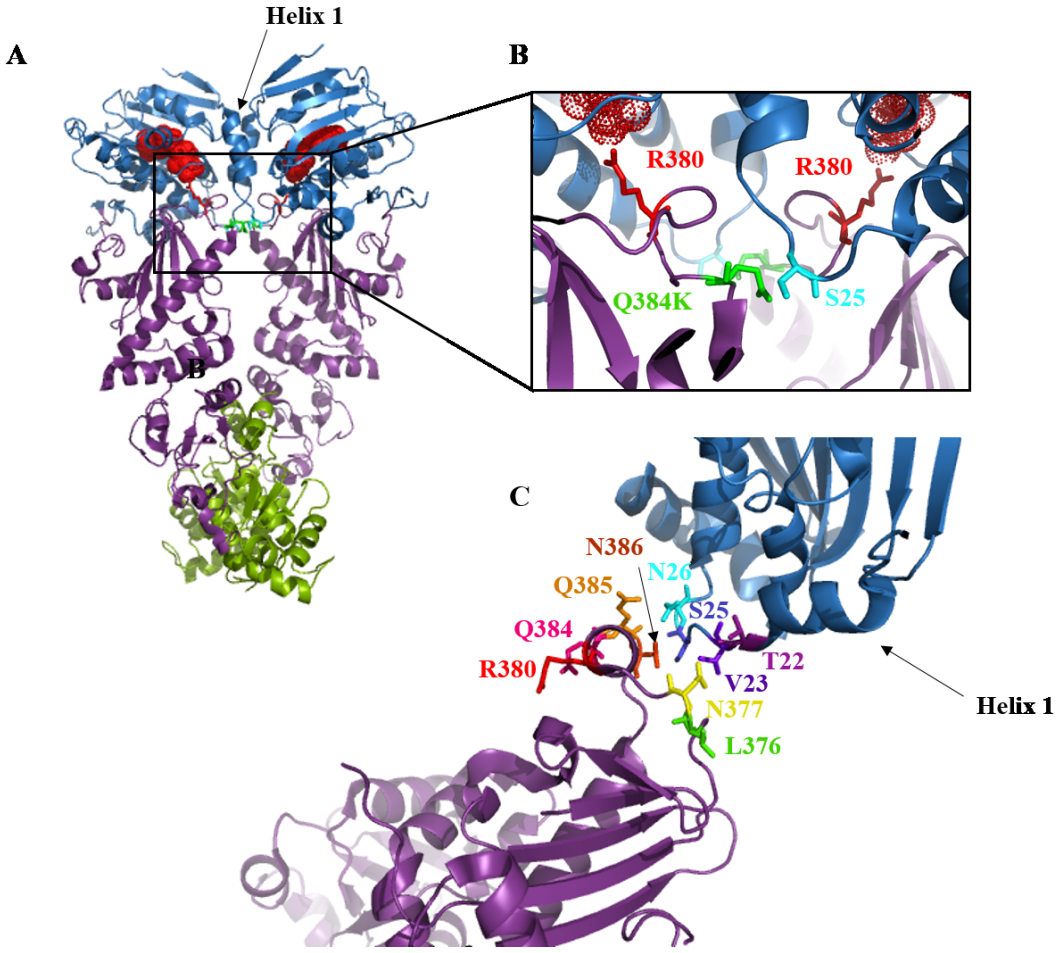

Figure 6.1 Crystal structure highlighting interaction of Hsp90.

A. Crystal structure of full length, closed Hsp90 dimer (*N*-terminal domains- blue, middle domains- purple, *C*-terminal domains- green, ATP- red) (2CG9 (Ali et al., 2006)). **B.** Highlighted complex between *N*-terminal domains of Hsp90 (blue) and middle domains (purple) shown in A with important residues highlighted and labeled in corresponding colours. **C.** Crystal structure of the middle domain (purple) (1HK7 (Meyer et al., 2003)) with the catalytic loop in the closed state with the *N*-terminal domain of Hsp90 (blue) (2CG9 (Ali et al., 2006)). Important residues are highlighted and labeled in corresponding colours.

Ser 25 resides just outside the *N*-terminal strap of the *N*-terminal domain. In the restructuring of Hsp90 for ATP hydrolysis, closure of the ATP lid allows α-helix 1 and β-strand 1 to remodel and exchange between the *N*-terminal domains, supporting *N*-terminal dimerization. Ser 25 is in close proximity to Thr 22 and Tyr 24, both part of the *N*-terminal domain that is remodelled for dimerization and formation of the catalytically active conformation of Hsp90 (Cunningham et al., 2008; Mollapour et al., 2010; Mollapour, Tsutsumi, Truman et al., 2011). In addition, mutation of Thr 22 and Tyr 24 have been shown to reduce interaction with Aha1p (Mollapour et al., 2010; Mollapour, Tsutsumi, Truman et al., 2011). Similar to Hsc82p^{S25P}, Hsp82p^{T22A} and Hsp82p^{T22E} both show defective chaperoning of v-Src that is rescued by the overexpression of Aha1p (Mollapour, Tsutsumi, Truman et al., 2011). The role of Hch1p with client has not been established. It would be interesting to determine if the deletion of *HCH1* in the Hsc82p^{S25P} mutant background results in a decrease in the chaperoning of v-Src and if this chaperoning can be restored by the re-expression of Hch1p or Aha1p. The *N*-terminal domains of Hsp90 are suggested to have the freedom to rotate as much as 180° (Daturpalli et al., 2017). This rotation, provided by the charged linker region that connects the *N*-terminal and middle domains of Hsp90, was suggested to expose regions of the *N*-terminal domain (residues 19-30) allowing the formation of an extensive client interaction site along the *N*-terminal, middle and *C*-terminal domains of Hsp90 (Daturpalli et al., 2017). If Ser 25 is important for stabilization of the closed conformation we would expect to see a decrease in *N*-terminal rotation if Ser 25 is mutated.

6.4 The conserved motifs in Aha-type co-chaperone Hsp90 ATPase stimulation

The Hsp90 catalytic cycle is coupled to conformation changes that are central to Hsp90 function. Conformational changes happen synergistically, involving a network of residues within all three domains and both monomers of Hsp90 (Hessling et al., 2009; Li, J. and Buchner, 2013; Richter et al., 2006; Schulze et al., 2016). How might the RKxK and NxNNWHW motif of Aha1p and Hch1p be involved in the Hsp90 catalytic cycle? In the open conformation, the ATP lids of Hsp90 are open leaving the nucleotide binding pocket available for nucleotide to bind and release (Weikl et al., 2000; Hessling et al., 2009). ATP binding and release happens rapidly and therefore, is not thought to be rate limiting to the catalytic cycle (Ratzke et al., 2012). In the apo conformation Arg 380 and the catalytic loop interact with the middle domain and help to stabilize Hsp90 in an open conformation (Meyer et al., 2003; Dollins et al., 2007; Cunningham et al., 2012; Huai et al., 2005). Release of Arg 380 is suggested to be a rate limiting step in ATP

hydrolysis along with rotation of the *N*-terminal domains (Cunningham et al., 2012; Southworth and Agard, 2011). The RKxK motif of Aha1p has been shown to remodel the catalytic loop of Hsp90 and our results show that the RKxK motif is important for Hch1p-mediated ATPase stimulation (Meyer et al., 2003; Meyer et al., 2004). This points to a role for the binding of Hch1p and the *N*-terminus of Aha1p to the middle domain of Hsp90 to potentially release Arg 380 and the catalytic loop (Figure 6.2). While this results in a small stimulatory effect, rearrangements of the *N*-terminal domains is also important. Hch1p but not Aha1p^{N} results in a docked state between the *N*-terminal and middle domains of Hsp90 (Wolmarans et al., 2016). In addition, the chimera between Hch1p and the *C*-terminus of Aha1p revealed that Hch1p does not recapitulate the activity of the *N*-terminus of Aha1p (Horvat et al., 2014). This suggests that while Hch1p brings the *N*-terminal and middle domains together, it is not in the same rearrangement that is required for the *C*-terminal domain of Aha1p to fully stimulate Hsp90. Therefore, while the *N*-terminus of Aha1p can prime Hsp90 for interaction with the *C*-terminal domain it does not provide further stimulation over and above that conferred by Hch1p. The *C*-terminal domain of Aha1p interacts with the *N*-terminal domains Hsp90 in the dimerized state for further ATPase stimulation (Figure 6.2) (Meyer et al., 2004; Hessling et al., 2009; Retzlaff et al., 2010). After ATP hydrolysis occurs, Hsp90 must also go through steps to release ADP and inorganic phosphate and allow for the initiation of a new cycle of ATP binding and hydrolysis. The order and kinetics of these reverse events are poorly understood. Our data points to a role for the NxNNWHW motif of Aha1p and Hch1p in ADP release after ATP hydrolysis (Figure 6.2).

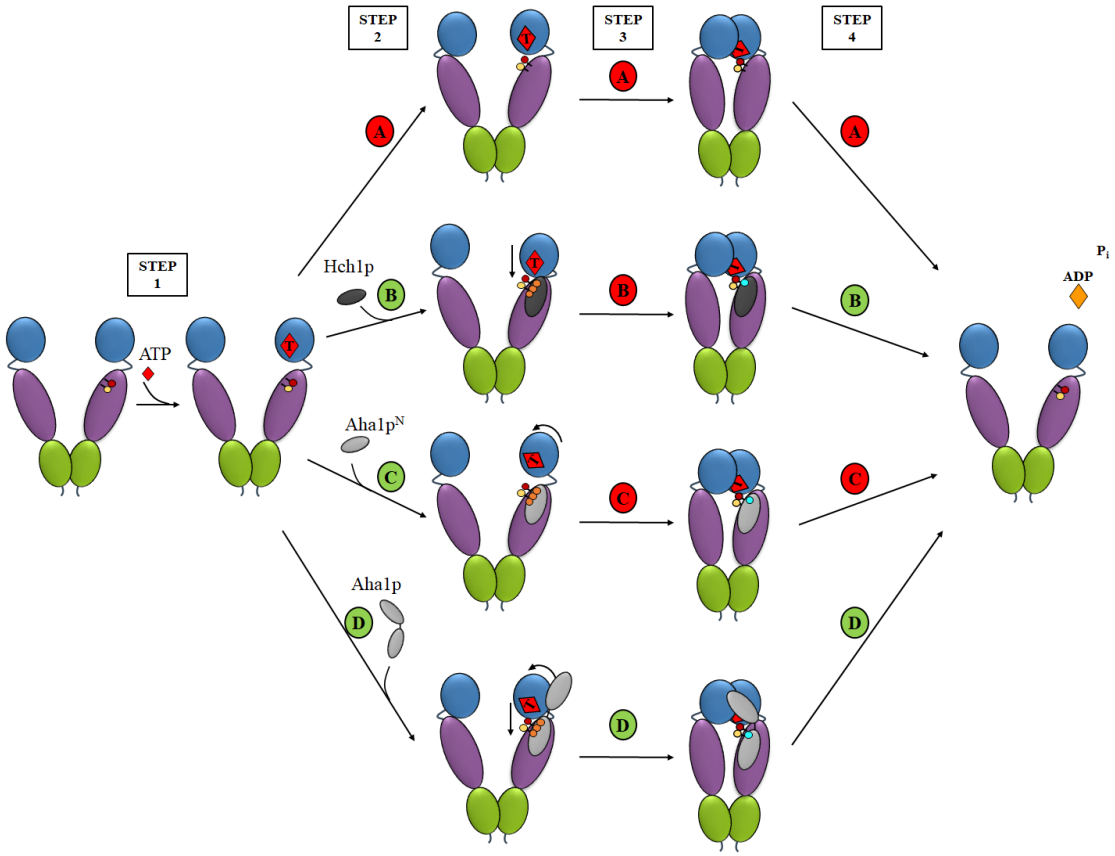

Figure 6.2 Model of the RKxK and NXNNWHW motif of Aha1p and Hch1p in stimulating Hsp90 ATP hydrolysis.

The ATP hydrolysis cycle of Hsp90 is shown without co-chaperone (A) or with Hch1p (B), Aha1p^N (C) or Aha1p (D). In the apo state Arg 380 (red circle) and the catalytic loop (yellow circle) of Hsp90 interact with the middle domain of Hsp90. ATP binds in the nucleotide binding pocket (Step 1). In the absence of co-chaperone, release of Arg 380 and rearrangement of the Hsp90 *N*-terminal domains is slow (Step 2 A). The addition of Hch1p, Aha1p^N, or Aha1p stimulates the release of Arg 380 and the catalytic loop through interaction with the RKxK motif (orange circles) (Step 2 B, C and D respectively). During Step 2 the binding of Hch1p also promotes the interaction of the *N*-terminal and middle domains of Hsp90 whereas, binding of the *N*-terminal domain of Aha1p promotes rearrangement in the *N*-terminal domain of Hsp90 that allows for faster Hsp90 *N*-terminal dimerization when the *C*-terminus of Aha1p is present (Step 3). The reopening of Hsp90 and release of ADP and inorganic phosphate (P_i) (Step 4) is enhanced by the presence of the NxNNWHW motif (blue circle) only with Hch1p or Aha1p.

6.5 Additional roles of the Aha-type co-chaperones

Chapter 5, outlines the ways that we have expanded our models and approaches to explore the biological relevance and regulation by the Aha-type co-chaperones. We show, using a melanoma progression model, that although the Hsp90 system is not universally regulated, both Hsp90 and Aha1 levels are increased in melanoma cells. We confirmed previous reports that deletion of Aha1 results in increased sensitivity to Hsp90 inhibitors. While examining the levels of the Hsp90 system we revealed that Aha1 is heavily post-translationally modified. The way in which we can isolate specific post-translationally modified co-chaperones will be work for future projects. Lastly, we have revealed a role for Aha1 in the activation of IRF3 and the innate immune response and show that Aha1 is important for immune response to viral infection. Together, these observations widen our view of Aha-type co-chaperones regulation and function.

6.5.1 The Hsp90 system and disease

The upregulation of Hsp90 has been shown to be an indicator of malignancy with elevated levels of heat shock proteins generally purported with poor prognosis (Wu et al., 2017; Wang, J. et al., 2013). With the recognition that the Hsp90 system is tightly integrated, targeting co-chaperones has been suggested as a way to more specifically alter Hsp90 activity (Blair, L. J. et al., 2014). We assessed the levels of co-chaperones in a melanoma progression model and found that there was no clear upregulation of all co-chaperones. Of interest to us, Aha1 was upregulated, supporting a need to increase our understanding of its role in Hsp90 function. Expanding this analysis to additional cancer models may reveal if co-chaperone changes can be linked to cancer type or are specific to lineage. While cellular levels of Hsp90 are important for understanding requirements of cancer cells, a role for extracellular Hsp90 (eHsp90) has slowly been gaining traction (Li, W. et al., 2007; Tsutsumi and Neckers, 2007; Wong and Jay, 2016; Rong et al., 2014). The mechanism of secretion is poorly understood, but it is known to be triggered by cell stress and linked to cancer metastasis (Li et al 2007, Wooley et al 2009, Yang et al 2014). Serum levels of eHsp90 have been shown to be elevated in cancer patients and eHsp90 has been shown to be a potential biomarker for hepatocellular carcinoma and leukemia (Wong and Jay, 2016; Sun et al., 2012). We have begun to investigate eHsp90 in melanoma and as a prognostic marker for inflammatory bowel disorders.

Hsp90 has a long standing role in immune response and immune modulation (Graner, 2016). One of best-defined roles of Hsp90 in the immunity is the stabilization and activation of the IκB kinase (Chen, G. et al., 2002; Broemer et al., 2004). Activation is known to be dependent on Cdc37 and Hsp90, with Hsp90 inhibition resulting in the loss of transcriptional response (Pittet, 2005; Broemer et al., 2004). Prior to our results, which reveal a defect in IRF3 phosphorylation when Aha1 is absent, a role for Hsp90 in the IRF3 arm of the innate immune system had not been identified. Defining the upstream and downstream factors that are also affected in this pathway will provide a better understanding for the role of Hsp90 in the immune system. It may also provide a more specific role for Aha1 in cells.

6.5.2 Re-assessing post-translational modifications

Hsp90 and many of its co-chaperones are known phospho-proteins (Walton-Diaz et al., 2013). The functional consequences of Hsp90 phosphorylation have been established showing altered co-chaperone interaction, client activation, and inhibitor sensitivity (Mollapour and Neckers, 2012; Walton-Diaz et al., 2013). While less is known about post-translational modifications of co-chaperone proteins, the functional consequences are similar to those of Hsp90 (Mollapour and Neckers, 2012). For the co-chaperone Cdc37, phosphorylation of Ser 13 by casein kinase 2 (CK2) is necessary for interaction with numerous kinases and for binding to Hsp90 for kinase activation (Miyata, 2009; Vaughan et al., 2008; Shao et al., 2003). Preventing the phosphorylation of Ser 13 on Cdc37 results in increased toxicity of Hsp90 inhibitors (Vaughan et al., 2008). In a similar way, phosphorylation of Sti1, p23, or FKBP2 results in altered Hsp90 interaction and client activation (Kobayashi et al., 2004; Longshaw et al., 2000; Miyata et al., 1997). It is difficult to assign consequences of post-translational modifications in the Hsp90 system. For example, CK2 phosphorylation of Hsp90 at Thr 22 affects ATPase activity, client activation, interaction with Aha1, and inhibitor sensitivity (Mollapour, Tsutsumi, Kim et al., 2011; Mollapour, Tsutsumi, Truman et al., 2011). Altered interaction of Hsp90 with Aha1 has been shown to influence all of these things as well. While the relative levels of co-chaperones proteins are able to influence the kinetics of Hsp90 cycle progression, the substoichiometric levels of co-chaperones compared to Hsp90 suggests that post-translational modifications may serve as a mechanism to control the interaction of co-chaperones with Hsp90 (Ghaemmaghami et al., 2003). This has been elegantly illustrated for phosphorylation events of Hsp90 where

phosphorylation on Tyr 197 results in dissociation of Cdc37, phosphorylation on Tyr 313 promotes Aha1 recruitment and therefore ATPase activity, and phosphorylation on Tyr 627 induces dissociation of client and co-chaperones (Xu, W. et al., 2012).

There is very little known about how post-translational modifications regulate Aha1. Tyr 223 of Aha1 has been shown to be phosphorylated by the tyrosine kinase c-Abl, which promotes the association of Aha1 and Hsp90 and alters the chaperoning of Hsp90 clients (Dunn et al., 2015). Using 2DGE we show that Aha1 undergoes multiple post-translational modification events *in vivo*. Although the expression of mimetic and non-modifiable mutants of Aha1 did not show alterations in Hsp90 interaction, we propose this is a consequence of the conditions used for these experiments and not lack of phenotype for all of the modification variants. More stringent conditions, a different cell line, or expression of the mutants as the sole source of Aha1 in cells may help to illustrate these differences. We can also purify these proteins to conduct *in vitro* analysis of interaction and stimulation ability of these mutants. Although we cannot predict the sites that will be important, we can suggest that they will affect client activation and inhibitor sensitivity.

6.6 Hsp90 clients

Interest in understanding Hsp90 stems from the fact that Hsp90 clients are involved in an extensive range of biological processes and a myriad of diseases. While the characteristics that define Hsp90 clients' remains poorly understood, a unifying feature is intrinsic instability (Taipale et al., 2012; Boczek et al., 2015). For instance, incorporation of specific residues of the Hsp90 client v-Src into the non-client c-Src showed a concomitant increase in instability and Hsp90 dependence (Boczek et al., 2015). Interestingly, *in vitro* reconstitution experiments show that while Hsp90 ATP hydrolysis is required for activation of v-Src by phosphorylated Cdc37 and Hsp90, only ATP binding to Hsp90 is necessary for stabilization (Boczek et al., 2015). A high-resolution cyro-electron microscopy structure of an Hsp90-Cdc37-Cdk4 was recently achieved, showing for the first time the interactions of full-length Hsp90 and Cdc37 with a client kinase (Verba et al., 2016). In this structure, Cdc37 binds the client Cdk4 in a partially unfolded state that is threaded through the closed middle domains of Hsp90 (Verba et al., 2016). The cycle that is proposed from this model suggests that the Cdc37-kinase complex can remain in contact with Hsp90 even after ATP hydrolysis and Hsp90 opening, allowing unfolded kinase to remain

in contact with Hsp90 and Cdc37 for additional Hsp90 cycles. Alternatively, when Hsp90 is open, Cdc37 can become dephosphorylated and Cdk4 would be accessible to degradation machinery (Verba et al., 2016). It was previously thought that Cdc37 prevents *N*-terminal dimerization and inhibits Hsp90 ATPase activity (Roe et al., 2004; Siligardi et al., 2002). Interestingly, while ATP hydrolysis was thought to be necessary for Hsp90 function (Pearl and Prodromou, 2000; Prodromou et al., 1997; Mishra and Bolon, 2014) it has now been shown that ATP binding may be sufficient (Zierer et al., 2016). Together, this builds on the dynamic nature of Hsp90 conformations and the idea that the time spent in certain conformation is the critical aspect of client activation (Mickler et al., 2009; Ratzke et al., 2012; Zierer et al., 2016).

What does this mean for the incorporation of the Aha-type co-chaperones into the Hsp90 client activation cycle? Our data supports a role for Aha-type co-chaperones in preparing Hsp90 for ATP hydrolysis (RKxK motif) and nucleotide release (NxNNWHW motif) which are required for resetting of the Hsp90 client activation cycle (Figure 6.3). This suggests that in the absence of Aha-type co-chaperones, clients may be bound to Hsp90 longer as ATP hydrolysis and cycle turnover is slower. This fits with the previous findings that the knockdown of Aha1 results in increased maturation of the difficult-to-fold Hsp90 client CFTR (Koulov et al., 2010; Wang, X. et al., 2006).

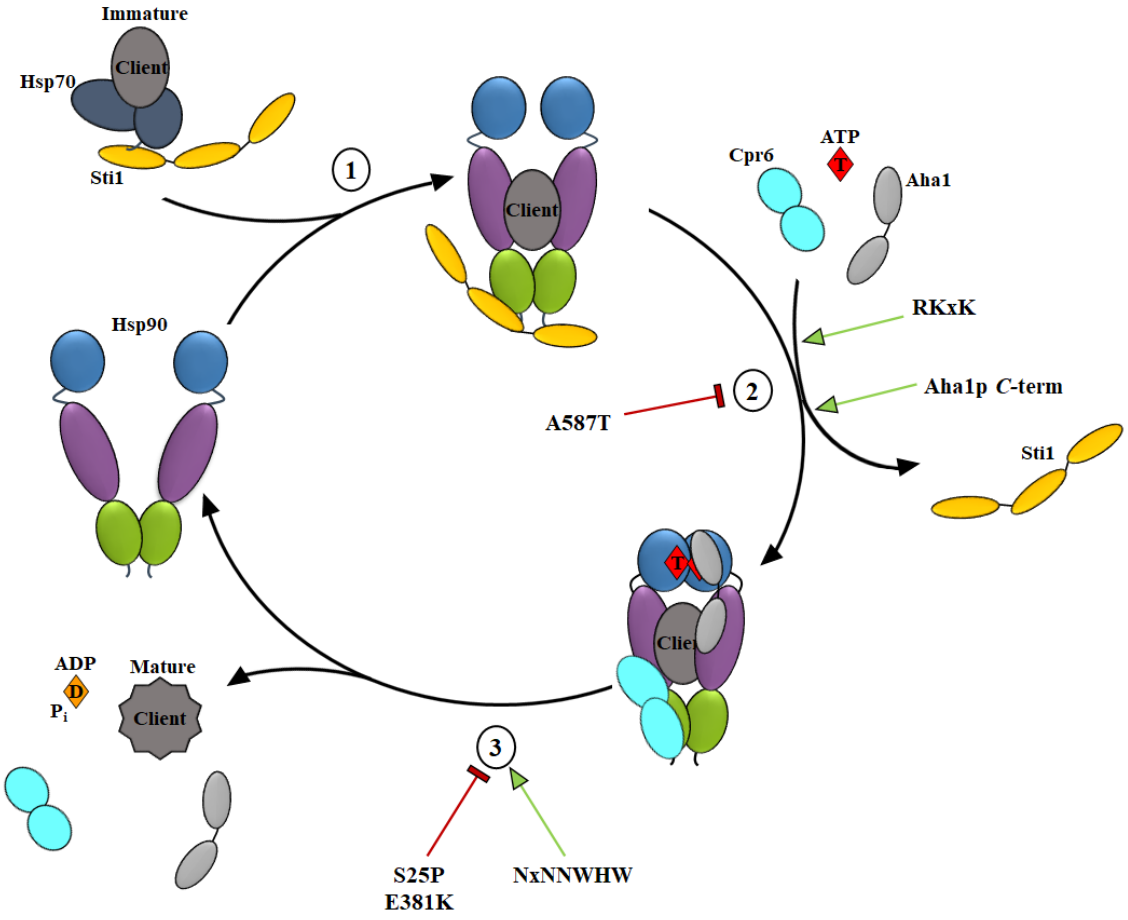

Figure 6.3 Model of the Aha-type co-chaperones in the Hsp90 client activation cycle. Immature client proteins associated with the Hsp70 chaperone system are recruited to Hsp90 by Sti1 (Step 1). Binding of Cpr6, ATP, and Aha1 are able displace Sti1 (Step 2). The RKxK motif of Aha-type co-chaperones stimulates rearrangements in Hsp90 important for Hsp90 closure. The *C*-terminal domain of Aha1 is needed for displacement of Sti1 (Wolmarans et al., 2016). Once the catalytically active, closed conformation of Hsp90 is achieved, ATP hydrolysis takes place and Hsp90 opening is needed for client release and re-setting of the Hsp90 cycle (Step 3). The NxNNWHW motif of the Aha-type co-chaperones stimulates the conformational changes needed for client release. Hsp82p mutants are shown at potential steps of inhibition.

Hsp90 mutants are an important means of defining the role of Aha-type co-chaperones in client activation. Our work with v-Src and Hsc82p^{S25P}, which is rescued by the overexpression of Aha1p but not Aha1p$^{\Delta 11}$, is an important step in this understanding. In this mutant, the levels of v-Src remains consistent however, v-Src activity is increased when Aha1p is overexpressed (Figure 3.11). This suggests that while Hsc82p^{S25P} can still bind to client, client activity is impaired because client release is impaired in the absence of Aha1p or when the NxNNWHW motif is deleted (Figure 6.3). By performing co-immunoprecipitation assays of Hsp90 and looking at client bound we may be able to more directly observe changes in client interaction. We could extend this analysis to include Hsp90 mutants that are restored by the deletion or overexpression of Hch1p, for example Hsp82p^{A587T} and Hsp82p^{E381K} respectively. Mutants that are rescued by the deletion of *HCH1* may have defects in client binding or achieving a closed catalytically active conformation that would be restored upon the deletion of *HCH1.* This idea is supported by our previous work which shows that the interaction of Hsp82p^{A587T} with Sba1p is impaired (Armstrong et al., 2012), suggesting that this mutation disfavours the *N*-terminally dimerized state (Figure 6.3). Alternatively, mutants that require Hch1p for restored function may have a defect in client turnover, shown by similar or increased amount of client binding, along with a decrease in client activity. In this case, client binding and activity would be restored to wildtype levels upon the addition of Hch1p, but not Hch1p$^{\Delta 11}$. Interestingly, the phenotypes seen by several mutants that are impaired by the deletion of *STI1*, are exacerbated by the presence of Aha-type co-chaperones (Reidy et al 2018). This suggests that defects in client loading can be made worse by quick turnover, highlighting the balance that is required in the Hsp90 system. In addition to looking at other clients such as v-Src, GR, and Ste11$^{\Delta N}$, we could extend our analysis to look at the effect of other co-chaperones on client binding and activation. This would highlight the importance of Aha-type co-chaperones in influencing client activation. Further biochemical and structural work would be required to reveal the mechanism.

6.7 Conclusion

The complex regulation mechanisms and highly dynamic nature of Hsp90 leave many questions to be explored. A central enigmatic element, is the role of ATP hydrolysis and the conformation consequences of hydrolysis on the activation of Hsp90 clients. The work described in this thesis focuses on understanding how the Aha-type co-chaperones regulate Hsp90 function. We highlight specific structural elements of the Aha-type co-chaperones are important for the

dynamics of Hsp90 nucleotide exchange. We reveal changes to co-chaperone-mediated ATPase stimulation and use yeast as a model organism to understand the *in vivo* effects of these co-chaperones on Hsp90. We suggest that focusing on elements of the Hsp90 cycle, such as exchange dynamics, may reveal new insight into the regulation of client activation. Future work towards placing the Aha-type co-chaperones within a structural context will be important to integrate their action into the conformational framework of the Hsp90 cycle.

References

Ali, M.M.U., Roe, S.M., Vaughan, C.K., Meyer, P., Panaretou, B., Piper, P.W., Prodromou, C., and Pearl, L.H. (2006). Crystal structure of an Hsp90-nucleotide-p23/Sba1 closed chaperone complex. Nature *440*(7087), 1013-1017. DOI:10.1038/nature04716

Ananthan, J., Goldberg, A.L., and Voellmy, R. (1986). Abnormal proteins serve as eukaryotic stress signals and trigger the activation of heat shock genes. Science *232*(4749), 522-524.

Anfinsen, C.B. (1973). Principles that govern the folding of protein chains. Science *181*(4096), 223-230.

Anfinsen, C.B., Haber, E., Sela, M., and White, F.H. (1961). The kinetics of formation of native ribonuclease during oxidation of the reduced polypeptide chain
. Proc Natl Acad Sci U S A *47*(9), 1309-1314.

Armstrong, H., Wolmarans, A., Mercier, R., Mai, B., and LaPointe, P. (2012). The co-chaperone Hch1 regulates Hsp90 function differently than its homologue Aha1 and confers sensitivity to yeast to the Hsp90 inhibitor NVP-AUY922. PLoS One *7*(11), e49322. DOI:10.1371/journal.pone.0049322

Ascierto, P.A., Kirkwood, J.M., Grob, J., Simeone, E., Grimaldi, A.M., Maio, M., Palmieri, G., Testori, A., Marincola, F.M., and Mozzillo, N. (2012). The role of BRAF V600 mutation in melanoma. J Transl Med *10*85. DOI:10.1186/1479-5876-10-85

Atkins, G.L., and Nimmo, I.A. (1980). Current trends in the estimation of Michaelis-Menten parameters. Anal. Biochem. *104*(1), 1-9.

Azevedo, C., Betsuyaku, S., Peart, J., Takahashi, A., Noël, L., Sadanandom, A., Casais, C., Parker, J., and Shirasu, K. (2006). Role of SGT1 in resistance protein accumulation in plant immunity. Embo J *25*(9), 2007-2016. DOI:10.1038/sj.emboj.7601084

Ballinger, C.A., Connell, P., Wu, Y., Hu, Z., Thompson, L.J., Yin, L.Y., and Patterson, C. (1999). Identification of CHIP, a novel tetratricopeptide repeat-containing protein that interacts with heat shock proteins and negatively regulates chaperone functions. Mol. Cell. Biol. *19*(6), 4535-4545.

Bansal, P.K., Abdulle, R., and Kitagawa, K. (2004). Sgt1 Associates with Hsp90: an Initial Step of Assembly of the Core Kinetochore Complex. Mol Cell Biol *24*(18), 8069-8079. DOI:10.1128/MCB.24.18.8069-8079.2004

Bardwell, J.C., and Craig, E.A. (1988). Ancient heat shock gene is dispensable. J Bacteriol *170*(7), 2977-2983.

Barrott, J.J., and Haystead, T.A.J. (2013). Hsp90, an unlikely ally in the war on cancer. Febs J. *280*(6), 1381-1396. DOI:10.1111/febs.12147

Basha, E., Jones, C., Blackwell, A.E., Cheng, G., Waters, E.R., Samsel, K.A., Siddique, M., Pett, V., Wysocki, V., and Vierling, E. (2013). An unusual dimeric small heat shock protein provides insight into the mechanism of this class of chaperones. J. Mol. Biol. *425*(10), 1683-1696. DOI:10.1016/j.jmb.2013.02.011

Beckmann, R.P., Mizzen, L.E., and Welch, W.J. (1990). Interaction of Hsp 70 with newly synthesized proteins: implications for protein folding and assembly. Science *248*(4957), 850-854.

Bertelsen, E.B., Chang, L., Gestwicki, J.E., and Zuiderweg, E.R.P. (2009). Solution conformation of wild-type E. coli Hsp70 (DnaK) chaperone complexed with ADP and substrate. Proc. Natl. Acad. Sci. U. S. A. *106*(21), 8471-8476. DOI:10.1073/pnas.0903503106

Blair, C.A., and Zi, X. (2011). Potential molecular targeting of splice variants for cancer treatment. Indian J Exp Biol *49*(11), 836-839.

Blair, L.J., Sabbagh, J.J., and Dickey, C.A. (2014). Targeting Hsp90 and its co-chaperones to treat Alzheimer's disease. Expert Opin. Ther. Targets *18*(10), 1219-1232. DOI:10.1517/14728222.2014.943185

Blatch, G.L., and Lässle, M. (1999). The tetratricopeptide repeat: a structural motif mediating protein-protein interactions. Bioessays *21*(11), 932-939. DOI:AID-BIES5>3.0.CO;2-N

Blond-Elguindi, S., Cwirla, S.E., Dower, W.J., Lipshutz, R.J., Sprang, S.R., Sambrook, J.F., and Gething, M.J. (1993). Affinity panning of a library of peptides displayed on bacteriophages reveals the binding specificity of BiP. Cell *75*(4), 717-728.

Boczek, E.E., Reefschläger, L.G., Dehling, M., Struller, T.J., Häusler, E., Seidl, A., Kaila, V.R.I., and Buchner, J. (2015). Conformational processing of oncogenic v-Src kinase by the molecular chaperone Hsp90. Pnas *112*(25), E3198.

Borkovich, K.A., Farrelly, F.W., Finkelstein, D.B., Taulien, J., and Lindquist, S. (1989). hsp82 is an essential protein that is required in higher concentrations for growth of cells at higher temperatures. Mol. Cell. Biol. *9*(9), 3919-3930.

Broemer, M., Krappmann, D., and Scheidereit, C. (2004). Requirement of Hsp90 activity for IkappaB kinase (IKK) biosynthesis and for constitutive and inducible IKK and NF-kappaB activation. Oncogene *23*(31), 5378-5386. DOI:10.1038/sj.onc.1207705

Brugge, J.S., Erikson, E., and Erikson, R.L. (1981). The specific interaction of the Rous sarcoma virus transforming protein, pp60src, with two cellular proteins. Cell *25*(2), 363-372.

Bryngelson, J.D., Onuchic, J.N., Socci, N.D., and Wolynes, P.G. (1995). Funnels, pathways, and the energy landscape of protein folding: a synthesis. Proteins *21*(3), 167-195. DOI:10.1002/prot.340210302

Bukau, B., Weissman, J., and Horwich, A. (2006). Molecular chaperones and protein quality control. Cell *125*(3), 443-451. DOI:10.1016/j.cell.2006.04.014

Burlison, J.A., Neckers, L., Smith, A.B., Maxwell, A., and Blagg, B.S.J. (2006). Novobiocin: redesigning a DNA gyrase inhibitor for selective inhibition of hsp90. J. Am. Chem. Soc. *128*(48), 15529-15536. DOI:10.1021/ja065793p

Calamini, B., and Morimoto, R.I. (2012). Protein homeostasis as a therapeutic target for diseases of protein conformation. Curr Top Med Chem *12*(22), 2623-2640.

Calderwood, S.K., and Gong, J. (2016). Heat Shock Proteins Promote Cancer: It's a Protection Racket. Trends Biochem Sci *41*(4), 311-323. DOI:10.1016/j.tibs.2016.01.003

Calderwood, S.K., Khaleque, M.A., Sawyer, D.B., and Ciocca, D.R. (2006). Heat shock proteins in cancer: chaperones of tumorigenesis. Trends Biochem. Sci. *31*(3), 164-172. DOI:10.1016/j.tibs.2006.01.006

Caplan, A.J. (2003). What is a co-chaperone? Cell Stress Chaperones *8*(2), 105-107.

Caplan, A.J., Mandal, A.K., and Theodoraki, M.A. (2007). Molecular chaperones and protein kinase quality control. Trends Cell Biol. *17*(2), 87-92. DOI:10.1016/j.tcb.2006.12.002

Cardinale, A., Chiesa, R., and Sierks, M. (2014). Protein Misfolding and Neurodegenerative Diseases. Int J Cell Biol *2014* DOI:10.1155/2014/217371

Carrigan, P.E., Nelson, G.M., Roberts, P.J., Stoffer, J., Riggs, D.L., and Smith, D.F. (2004). Multiple Domains of the Co-chaperone Hop Are Important for Hsp70 Binding. J. Biol. Chem. *279*(16), 16185-16193. DOI:10.1074/jbc.M314130200

Chadli, A., Bouhouche, I., Sullivan, W., Stensgard, B., McMahon, N., Catelli, M.G., and Toft, D.O. (2000). Dimerization and N-terminal domain proximity underlie the function of the molecular chaperone heat shock protein 90. Proc. Natl. Acad. Sci. U. S. A. *97*(23), 12524-12529. DOI:10.1073/pnas.220430297

Chang, H.C., and Lindquist, S. (1994). Conservation of Hsp90 macromolecular complexes in Saccharomyces cerevisiae. J. Biol. Chem. *269*(40), 24983-24988.

Chang, H.C., Nathan, D.F., and Lindquist, S. (1997). In vivo analysis of the Hsp90 cochaperone Sti1 (p60). Mol. Cell. Biol. *17*(1), 318-325.

Chant, I.D., Rose, P.E., and Morris, A.G. (1995). Analysis of heat-shock protein expression in myeloid leukaemia cells by flow cytometry. Br. J. Haematol. *90*(1), 163-168.

Chao, A., Lai, C., Tsai, C., Hsueh, S., Hsueh, C., Lin, C., Chou, H., Lin, Y., Chen, H., Chang, T., and Wang, T. (2013). Tumor Stress-Induced Phosphoprotein1 (STIP1) as a Prognostic Biomarker in Ovarian Cancer. PLoS One *8*(2), DOI:10.1371/journal.pone.0057084

Chatterjee, S., Huang, E.H.B., Christie, I., Kurland, B.F., and Burns, T.F. (2017). Acquired Resistance to the Hsp90 Inhibitor, Ganetespib, in KRAS-Mutant NSCLC Is Mediated via Reactivation of the ERK-p90RSK-mTOR Signaling Network. Mol. Cancer Ther. *16*(5), 793-804. DOI:10.1158/1535-7163.MCT-16-0677

Chen, B., Retzlaff, M., Roos, T., and Frydman, J. (2011). Cellular Strategies of Protein Quality Control. Cold Spring Harb Perspect Biol *3*(8), DOI:10.1101/cshperspect.a004374

Chen, B., Zhong, D., and Monteiro, A. (2006). Comparative genomics and evolution of the HSP90 family of genes across all kingdoms of organisms. BMC Genomics *7*156. DOI:10.1186/1471-2164-7-156

Chen, G., Cao, P., and Goeddel, D.V. (2002). TNF-induced recruitment and activation of the IKK complex require Cdc37 and Hsp90. Mol. Cell *9*(2), 401-410.

Chen, S., and Smith, D.F. (1998). Hop as an adaptor in the heat shock protein 70 (Hsp70) and hsp90 chaperone machinery. J. Biol. Chem. *273*(52), 35194-35200.

Chiosis, G., Huezo, H., Rosen, N., Mimnaugh, E., Whitesell, L., and Neckers, L. (2003). 17AAG: low target binding affinity and potent cell activity--finding an explanation. Mol. Cancer Ther. *2*(2), 123-129.

Chiosis, G., and Neckers, L. (2006). Tumor selectivity of Hsp90 inhibitors: the explanation remains elusive. ACS Chem. Biol. *1*(5), 279-284. DOI:10.1021/cb600224w

Chirico, W.J., Waters, M.G., and Blobel, G. (1988). 70K heat shock related proteins stimulate protein translocation into microsomes. Nature *332*(6167), 805-810. DOI:10.1038/332805a0

Connell, P., Ballinger, C.A., Jiang, J., Wu, Y., Thompson, L.J., Höhfeld, J., and Patterson, C. (2001). The co-chaperone CHIP regulates protein triage decisions mediated by heat-shock proteins. Nat. Cell Biol. *3*(1), 93-96. DOI:10.1038/35050618

Cox, M.B., and Johnson, J.L. (2018). Evidence for Hsp90 Co-chaperones in Regulating Hsp90 Function and Promoting Client Protein Folding. Methods Mol. Biol. *1709*397-422. DOI:10.1007/978-1-4939-7477-1_28

Cox, M.B., Riggs, D.L., Hessling, M., Schumacher, F., Buchner, J., and Smith, D.F. (2007). FK506-Binding Protein 52 Phosphorylation: A Potential Mechanism for Regulating Steroid Hormone Receptor Activity. Mol Endocrinol *21*(12), 2956-2967. DOI:10.1210/me.2006-0547

Csermely, P., Schnaider, T., Soti, C., Prohászka, Z., and Nardai, G. (1998). The 90-kDa molecular chaperone family: structure, function, and clinical applications. A comprehensive review. Pharmacol. Ther. *79*(2), 129-168.

Cunningham, C.N., Krukenberg, K.A., and Agard, D.A. (2008). Intra- and intermonomer interactions are required to synergistically facilitate ATP hydrolysis in Hsp90. J. Biol. Chem. *283*(30), 21170-21178. DOI:10.1074/jbc.M800046200

Cunningham, C.N., Southworth, D.R., Krukenberg, K.A., and Agard, D.A. (2012). The conserved arginine 380 of Hsp90 is not a catalytic residue, but stabilizes the closed conformation required for ATP hydrolysis. Protein Science *21*(8), 1162-1171. DOI:10.1002/pro.2103

da Rocha Dias, S., Friedlos, F., Light, Y., Springer, C., Workman, P., and Marais, R. (2005). Activated B-RAF is an Hsp90 client protein that is targeted by the anticancer drug 17-allylamino-17-demethoxygeldanamycin. Cancer Res. *65*(23), 10686-10691. DOI:10.1158/0008-5472.CAN-05-2632

Dalman, F.C., Scherrer, L.C., Taylor, L.P., Akil, H., and Pratt, W.B. (1991). Localization of the 90-kDa heat shock protein-binding site within the hormone-binding domain of the glucocorticoid receptor by peptide competition. J. Biol. Chem. *266*(6), 3482-3490.

D'Andrea, L.D., and Regan, L. (2003). TPR proteins: the versatile helix. Trends Biochem. Sci. *28*(12), 655-662. DOI:10.1016/j.tibs.2003.10.007

Daturpalli, S., Knieß, R.A., Lee, C., and Mayer, M.P. (2017). Large Rotation of the N-terminal Domain of Hsp90 Is Important for Interaction with Some but Not All Client Proteins. J. Mol. Biol. *429*(9), 1406-1423. DOI:10.1016/j.jmb.2017.03.025

DeBoer, C., Meulman, P.A., Wnuk, R.J., and Peterson, D.H. (1970). Geldanamycin, a new antibiotic. J. Antibiot. *23*(9), 442-447.

Deshaies, R.J., Koch, B.D., Werner-Washburne, M., Craig, E.A., and Schekman, R. (1988). A subfamily of stress proteins facilitates translocation of secretory and mitochondrial precursor polypeptides. Nature *332*(6167), 800-805. DOI:10.1038/332800a0

Dill, K.A. (1985). Theory for the folding and stability of globular proteins. Biochemistry *24*(6), 1501-1509. DOI:10.1021/bi00327a032

Dobson, C.M. (2003). Protein folding and misfolding. Nature *426*(6968), 884-890. DOI:10.1038/nature02261

Dollins, D.E., Warren, J.J., Immormino, R.M., and Gewirth, D.T. (2007). Structures of GRP94-nucleotide complexes reveal mechanistic differences between the hsp90 chaperones. Mol. Cell *28*(1), 41-56. DOI:10.1016/j.molcel.2007.08.024

Donnelly, A., and Blagg, B.S.J. (2008). Novobiocin and additional inhibitors of the Hsp90 C-terminal nucleotide-binding pocket. Curr. Med. Chem. *15*(26), 2702-2717.

Doyle, S.M., Genest, O., and Wickner, S. (2013). Protein rescue from aggregates by powerful molecular chaperone machines. Nat. Rev. Mol. Cell Biol. *14*(10), 617-629. DOI:10.1038/nrm3660

Dunn, D.M., Woodford, M.R., Truman, A.W., Jensen, S.M., Schulman, J., Caza, T., Remillard, T.C., Loiselle, D., Wolfgeher, D., Blagg, B.S.*, et al.* (2015). c-Abl Mediated Tyrosine Phosphorylation of Aha1 Activates Its Co-chaperone Function in Cancer Cells. Cell. Rep. *12*(6), 1006-1018. DOI:10.1016/j.celrep.2015.07.004

Dutta, R., and Inouye, M. (2000). GHKL, an emergent ATPase/kinase superfamily. Trends Biochem. Sci. *25*(1), 24-28.

Dyson, H.J., Wright, P.E., and Scheraga, H.A. (2006). The role of hydrophobic interactions in initiation and propagation of protein folding. Pnas *103*(35), 13057-13061.

Eccles, S.A., Massey, A., Raynaud, F.I., Sharp, S.Y., Box, G., Valenti, M., Patterson, L., de Haven Brandon, A., Gowan, S., Boxall, F.*, et al.* (2008). NVP-AUY922: a novel heat shock protein 90 inhibitor active against xenograft tumor growth, angiogenesis, and metastasis. Cancer Res. *68*(8), 2850-2860. DOI:10.1158/0008-5472.CAN-07-5256

Echeverria, P.C., Bernthaler, A., Dupuis, P., Mayer, B., and Picard, D. (2011). An interaction network predicted from public data as a discovery tool: application to the Hsp90 molecular chaperone machine. PLoS One *6*(10), e26044. DOI:10.1371/journal.pone.0026044

Echtenkamp, F.J., Zelin, E., Oxelmark, E., Woo, J.I., Andrews, B.J., Garabedian, M., and Freeman, B.C. (2011). Global functional map of the p23 molecular chaperone reveals an extensive cellular network. Mol. Cell *43*(2), 229-241. DOI:10.1016/j.molcel.2011.05.029

Eckert, K., Saliou, J., Monlezun, L., Vigouroux, A., Atmane, N., Caillat, C., Quevillon-Chéruel, S., Madiona, K., Nicaise, M., Lazereg, S.*, et al.* (2010). The Pih1-Tah1 cochaperone complex inhibits Hsp90 molecular chaperone ATPase activity. J. Biol. Chem. *285*(41), 31304-31312. DOI:10.1074/jbc.M110.138263

Ellis, J. (1996). Discovery of molecular chaperones. Cell Stress Chaperones *1*(3), 155-160.

Ellis, J. (1987). Proteins as molecular chaperones. Nature *328*(6129), 378-379. DOI:10.1038/328378a0

Eskew, J.D., Sadikot, T., Morales, P., Duren, A., Dunwiddie, I., Swink, M., Zhang, X., Hembruff, S., Donnelly, A., Rajewski, R.A.*, et al.* (2011). Development and characterization of a novel C-terminal inhibitor of Hsp90 in androgen dependent and independent prostate cancer cells. BMC Cancer *11*468. DOI:10.1186/1471-2407-11-468

Falsone, S.F., Leptihn, S., Osterauer, A., Haslbeck, M., and Buchner, J. (2004). Oncogenic mutations reduce the stability of SRC kinase. J. Mol. Biol. *344*(1), 281-291. DOI:10.1016/j.jmb.2004.08.091

Felts, S.J., and Toft, D.O. (2003). p23, a simple protein with complex activities. Cell Stress Chaperones *8*(2), 108-113.

Fidler, I.J., and Nicolson, G.L. (1976). Organ selectivity for implantation survival and growth of B16 melanoma variant tumor lines. J. Natl. Cancer Inst. *57*(5), 1199-1202.

Finley, D., Ciechanover, A., and Varshavsky, A. (1984). Thermolability of ubiquitin-activating enzyme from the mammalian cell cycle mutant ts85. Cell *37*(1), 43-55.

Flynn, G.C., Pohl, J., Flocco, M.T., and Rothman, J.E. (1991). Peptide-binding specificity of the molecular chaperone BiP. Nature *353*(6346), 726-730. DOI:10.1038/353726a0

Forafonov, F., Toogun, O.A., Grad, I., Suslova, E., Freeman, B.C., and Picard, D. (2008). p23/Sba1p Protects against Hsp90 Inhibitors Independently of Its Intrinsic Chaperone Activity. Mol Cell Biol *28*(10), 3446-3456. DOI:10.1128/MCB.02246-07

Freeman, B.C., Toft, D.O., and Morimoto, R.I. (1996). Molecular chaperone machines: chaperone activities of the cyclophilin Cyp-40 and the steroid aporeceptor-associated protein p23. Science *274*(5293), 1718-1720.

Galluzzi, L., Kepp, O., Chan, F.K., and Kroemer, G. (2017). Necroptosis: Mechanisms and Relevance to Disease. Annual Review of Pathology: Mechanisms of Disease *12*(1), 103-130. DOI:10.1146/annurev-pathol-052016-100247

Garcia-Ranea, J.A., Mirey, G., Camonis, J., and Valencia, A. (2002). p23 and HSP20/alpha-crystallin proteins define a conserved sequence domain present in other eukaryotic protein families. FEBS Lett. *529*(2-3), 162-167.

Garg, G., Khandelwal, A., and Blagg, B.S.J. (2016). Anticancer Inhibitors of Hsp90 Function: Beyond the Usual Suspects. Adv. Cancer Res. *129*51-88. DOI:10.1016/bs.acr.2015.12.001

Garraway, L.A., and Jänne, P.A. (2012). Circumventing cancer drug resistance in the era of personalized medicine. Cancer Discov *2*(3), 214-226. DOI:10.1158/2159-8290.CD-12-0012

Gaspar, N., Sharp, S.Y., Eccles, S.A., Gowan, S., Popov, S., Jones, C., Pearson, A., Vassal, G., and Workman, P. (2010). Mechanistic evaluation of the novel HSP90 inhibitor NVP-AUY922 in adult and pediatric glioblastoma. Mol. Cancer Ther. *9*(5), 1219-1233. DOI:10.1158/1535-7163.MCT-09-0683

Gasteiger, E., Hoogland, C., Gattiker, A., Duvaud, S., Wilkins, M.R., Appel, R.D., and Bairoch, A. (2005). Protein Identification and Analysis Tools on the ExPASy Server. In The Proteomics Protocols Handbook, Humana Press) pp. 571-607.

Ghaemmaghami, S., Huh, W., Bower, K., Howson, R.W., Belle, A., Dephoure, N., O'Shea, E.K., and Weissman, J.S. (2003). Global analysis of protein expression in yeast. Nature *425*(6959), 737-741. DOI:10.1038/nature02046

Giamas, G., Stebbing, J., Vorgias, C.E., and Knippschild, U. (2007). Protein kinases as targets for cancer treatment. Pharmacogenomics *8*(8), 1005-1016. DOI:10.2217/14622416.8.8.1005

Glynn, S.E., Martin, A., Nager, A.R., Baker, T.A., and Sauer, R.T. (2009). Structures of asymmetric ClpX hexamers reveal nucleotide-dependent motions in a AAA+ protein-unfolding machine. Cell *139*(4), 744-756. DOI:10.1016/j.cell.2009.09.034

Goldberger, R.F., Epstein, C.J., and Anfinsen, C.B. (1963). Acceleration of reactivation of reduced bovine pancreatic ribonuclease by a microsomal system from rat liver. J. Biol. Chem. *238*628-635.

Grad, I., and Picard, D. (2007). The glucocorticoid responses are shaped by molecular chaperones. Mol. Cell. Endocrinol. *275*(1-2), 2-12. DOI:10.1016/j.mce.2007.05.018

Graf, C., Kramer, G., Mayer, M.P., and Stankiewicz, M. (2009). Spatially and kinetically resolved changes in the conformational dynamics of the Hsp90 chaperone machine. The EMBO Journal *28*(5), 602-613. DOI:10.1038/emboj.2008.306

Graf, C., Lee, C., Eva Meier-Andrejszki, L., Nguyen, M.T.N., and Mayer, M.P. (2014). Differences in conformational dynamics within the Hsp90 chaperone family reveal mechanistic insights. Front Mol Biosci *1* DOI:10.3389/fmolb.2014.00004

Graner, M.W. (2016). Chapter Eight - HSP90 and Immune Modulation in Cancer. Adv. Cancer Res. *129*191-224. DOI://dx.doi.org/10.1016/bs.acr.2015.10.001

Gray, P.J., Stevenson, M.A., and Calderwood, S.K. (2007). Targeting Cdc37 inhibits multiple signaling pathways and induces growth arrest in prostate cancer cells. Cancer Res. *67*(24), 11942-11950. DOI:10.1158/0008-5472.CAN-07-3162

Grbovic, O.M., Basso, A.D., Sawai, A., Ye, Q., Friedlander, P., Solit, D., and Rosen, N. (2006). V600E B-Raf requires the Hsp90 chaperone for stability and is degraded in response to Hsp90 inhibitors. Proc. Natl. Acad. Sci. U. S. A. *103*(1), 57-62. DOI:10.1073/pnas.0609973103

Greene, M.K., Maskos, K., and Landry, S.J. (1998). Role of the J-domain in the cooperation of Hsp40 with Hsp70. Proc Natl Acad Sci U S A *95*(11), 6108-6113.

Gross, S., Rahal, R., Stransky, N., Lengauer, C., and Hoeflich, K.P. (2015). Targeting cancer with kinase inhibitors. J. Clin. Invest. *125*(5), 1780-1789. DOI:10.1172/JCI76094

Gupta, R.S. (1995). Phylogenetic analysis of the 90 kD heat shock family of protein sequences and an examination of the relationship among animals, plants, and fungi species. Mol. Biol. Evol. *12*(6), 1063-1073. DOI:10.1093/oxfordjournals.molbev.a040281

Haas, I.G., and Wabl, M. (1983). Immunoglobulin heavy chain binding protein. Nature *306*(5941), 387-389.

Hagerling, C., Casbon, A., and Werb, Z. (2015). Balancing the innate immune system in tumor development. Trends Cell Biol. *25*(4), 214-220. DOI:10.1016/j.tcb.2014.11.001

Hainzl, O., Lapina, M.C., Buchner, J., and Richter, K. (2009). The Charged Linker Region Is an Important Regulator of Hsp90 Function. J Biol Chem *284*(34), 22559-22567. DOI:10.1074/jbc.M109.031658

Hanahan, D., and Weinberg, R.A. (2011). Hallmarks of cancer: the next generation. Cell *144*(5), 646-674. DOI:10.1016/j.cell.2011.02.013

Harris, S.F., Shiau, A.K., and Agard, D.A. (2004). The crystal structure of the carboxy-terminal dimerization domain of htpG, the Escherichia coli Hsp90, reveals a potential substrate binding site. Structure *12*(6), 1087-1097. DOI:10.1016/j.str.2004.03.020

Harst, A., Lin, H., and Obermann, W.M. (2005). Aha1 competes with Hop, p50 and p23 for binding to the molecular chaperone Hsp90 and contributes to kinase and hormone receptor activation. Biochem. J. *387*(Pt 3), 789-796. DOI:10.1042/BJ20041283

Hartl, F.U., and Hayer-Hartl, M. (2009). Converging concepts of protein folding in vitro and in vivo. Nat. Struct. Mol. Biol. *16*(6), 574-581. DOI:10.1038/nsmb.1591

He, L., and Hiller, S. (2018). Common Patterns in Chaperone Interactions with a Native Client Protein. Angew. Chem. Int. Ed. Engl. *57*(20), 5921-5924. DOI:10.1002/anie.201713064

Hessling, M., Richter, K., and Buchner, J. (2009). Dissection of the ATP-induced conformational cycle of the molecular chaperone Hsp90. Nat. Struct. Mol. Biol. *16*(3), 287-293. DOI:10.1038/nsmb.1565

Hieronymus, H., Lamb, J., Ross, K.N., Peng, X.P., Clement, C., Rodina, A., Nieto, M., Du, J., Stegmaier, K., Raj, S.M.*, et al.* (2006). Gene expression signature-based chemical genomic prediction identifies a novel class of HSP90 pathway modulators. Cancer Cell *10*(4), 321-330. DOI:10.1016/j.ccr.2006.09.005

Hightower, L.E. (1980). Cultured animal cells exposed to amino acid analogues or puromycin rapidly synthesize several polypeptides. J. Cell. Physiol. *102*(3), 407-427. DOI:10.1002/jcp.1041020315

Höhfeld, J., and Hartl, F.U. (1994). Role of the chaperonin cofactor Hsp10 in protein folding and sorting in yeast mitochondria. J. Cell Biol. *126*(2), 305-315.

Holmes, J.L., Sharp, S.Y., Hobbs, S., and Workman, P. (2008). Silencing of HSP90 cochaperone AHA1 expression decreases client protein activation and increases cellular sensitivity to the HSP90 inhibitor 17-allylamino-17-demethoxygeldanamycin. Cancer Res. *68*(4), 1188-1197. DOI:10.1158/0008-5472.CAN-07-3268

Honoré, B., Leffers, H., Madsen, P., Rasmussen, H.H., Vandekerckhove, J., and Celis, J.E. (1992). Molecular cloning and expression of a transformation-sensitive human protein containing the TPR motif and sharing identity to the stress-inducible yeast protein STI1. J. Biol. Chem. *267*(12), 8485-8491.

Horibe, T., Kohno, M., Haramoto, M., Ohara, K., and Kawakami, K. (2011). Designed hybrid TPR peptide targeting Hsp90 as a novel anticancer agent. J Transl Med *9*8. DOI:10.1186/1479-5876-9-8

Hornbeck, P.V., Zhang, B., Murray, B., Kornhauser, J.M., Latham, V., and Skrzypek, E. (2015). PhosphoSitePlus, 2014: mutations, PTMs and recalibrations. Nucleic Acids Res. *43*(Database issue), 512. DOI:10.1093/nar/gku1267

Horvat, N.K., Armstrong, H., Lee, B.L., Mercier, R., Wolmarans, A., Knowles, J., Spyracopoulos, L., and LaPointe, P. (2014). A mutation in the catalytic loop of Hsp90 specifically impairs ATPase stimulation by Aha1p, but not Hch1p. J. Mol. Biol. *426*(12), 2379-2392. DOI:10.1016/j.jmb.2014.04.002

Huai, Q., Wang, H., Liu, Y., Kim, H., Toft, D., and Ke, H. (2005). Structures of the N-terminal and middle domains of E. coli Hsp90 and conformation changes upon ADP binding. Structure *13*(4), 579-590. DOI:10.1016/j.str.2004.12.018

Jackson, S.E. (2013). Hsp90: structure and function. Top Curr Chem *328*155-240. DOI:10.1007/128_2012_356

Jakob, U., Gaestel, M., Engel, K., and Buchner, J. (1993). Small heat shock proteins are molecular chaperones. J. Biol. Chem. *268*(3), 1517-1520.

Jakob, U., Lilie, H., Meyer, I., and Buchner, J. (1995). Transient Interaction of Hsp90 with Early Unfolding Intermediates of Citrate Synthase. Implications for heat shock in vivo. . J. Biol. Chem. *270*(13), 7288-7294. DOI:10.1074/jbc.270.13.7288

Jaya, N., Garcia, V., and Vierling, E. (2009). Substrate binding site flexibility of the small heat shock protein molecular chaperones. Proc Natl Acad Sci U S A *106*(37), 15604-15609. DOI:10.1073/pnas.0902177106

Jeng, W., Lee, S., Sung, N., Lee, J., and Tsai, F. (2015). Molecular chaperones: guardians of the proteome in normal and disease states version 1; referees: 2 approved]. F1000Research *4*(1448), DOI:10.12688/f1000research.7214.1

Jiang, J., Maes, E.G., Taylor, A.B., Wang, L., Hinck, A.P., Lafer, E.M., and Sousa, R. (2007). Structural Basis of J Cochaperone Binding and Regulation of Hsp70. Mol Cell *28*(3), 422-433. DOI:10.1016/j.molcel.2007.08.022

Jiao, S., Guan, J., Chen, M., Wang, W., Li, C., Wang, Y., Cheng, Y., and Zhou, Z. (2018). Targeting IRF3 as a YAP agonist therapy against gastric cancer. J. Exp. Med. *215*(2), 699-718. DOI:10.1084/jem.20171116

Jiménez, B., Ugwu, F., Zhao, R., Ortí, L., Makhnevych, T., Pineda-Lucena, A., and Houry, W.A. (2012). Structure of minimal tetratricopeptide repeat domain protein Tah1 reveals mechanism of its interaction with Pih1 and Hsp90. J. Biol. Chem. *287*(8), 5698-5709. DOI:10.1074/jbc.M111.287458

Joab, I., Radanyi, C., Renoir, M., Buchou, T., Catelli, M.G., Binart, N., Mester, J., and Baulieu, E.E. (1984). Common non-hormone binding component in non-transformed chick oviduct receptors of four steroid hormones. Nature *308*(5962), 850-853.

Johnson, B.D., Schumacher, R.J., Ross, E.D., and Toft, D.O. (1998). Hop modulates Hsp70/Hsp90 interactions in protein folding. J. Biol. Chem. *273*(6), 3679-3686.

Johnson, J.L., Beito, T.G., Krco, C.J., and Toft, D.O. (1994). Characterization of a novel 23-kilodalton protein of unactive progesterone receptor complexes. Mol Cell Biol *14*(3), 1956-1963.

Johnson, J.L., Zuehlke, A.D., Tenge, V.R., and Langworthy, J.C. (2014). Mutation of essential Hsp90 co-chaperones SGT1 or CNS1 renders yeast hypersensitive to overexpression of other co-chaperones. Curr. Genet. *60*(4), 265-276. DOI:10.1007/s00294-014-0432-3 [doi]

Johnson, J.L. (2012). Evolution and function of diverse Hsp90 homologs and cochaperone proteins. Biochim. Biophys. Acta *1823*(3), 607-613. DOI:10.1016/j.bbamcr.2011.09.020

Johnson, J.L., and Brown, C. (2009). Plasticity of the Hsp90 chaperone machine in divergent eukaryotic organisms. Cell Stress Chaperones *14*(1), 83-94. DOI:10.1007/s12192-008-0058-9

Johnson, J.L., and Toft, D.O. (1994). A novel chaperone complex for steroid receptors involving heat shock proteins, immunophilins, and p23. J. Biol. Chem. *269*(40), 24989-24993.

Jolly, C., and Morimoto, R.I. (2000). Role of the heat shock response and molecular chaperones in oncogenesis and cell death. J. Natl. Cancer Inst. *92*(19), 1564-1572.

Kamal, A., Thao, L., Sensintaffar, J., Zhang, L., Boehm, M.F., Fritz, L.C., and Burrows, F.J. (2003). A high-affinity conformation of Hsp90 confers tumour selectivity on Hsp90 inhibitors. Nature *425*(6956), 407-410. DOI:10.1038/nature01913

Kampinga, H.H., and Craig, E.A. (2010). The HSP70 chaperone machinery: J proteins as drivers of functional specificity. Nature Reviews Molecular Cell Biology *11*(8), 579-592. DOI:10.1038/nrm2941

Karagöz, G.E., Duarte, A.M.S., Akoury, E., Ippel, H., Biernat, J., Morán Luengo, T., Radli, M., Didenko, T., Nordhues, B.A., Veprintsev, D.B.*, et al.* (2014). Hsp90-Tau complex reveals

molecular basis for specificity in chaperone action. Cell *156*(5), 963-974. DOI:10.1016/j.cell.2014.01.037

Kaul, S., Murphy, P.J.M., Chen, J., Brown, L., Pratt, W.B., and Simons, S.S. (2002). Mutations at positions 547-553 of rat glucocorticoid receptors reveal that hsp90 binding requires the presence, but not defined composition, of a seven-amino acid sequence at the amino terminus of the ligand binding domain. J. Biol. Chem. *277*(39), 36223-36232. DOI:10.1074/jbc.M206748200

Kelley, P.M., and Schlesinger, M.J. (1978). The effect of amino acid analogues and heat shock on gene expression in chicken embryo fibroblasts. Cell *15*(4), 1277-1286.

Khandelwal, A., Crowley, V.M., and Blagg, B.S.J. (2016). Natural Product Inspired N-Terminal Hsp90 Inhibitors: From Bench to Bedside? Med Res Rev *36*(1), 92-118. DOI:10.1002/med.21351

Kim, Y.E., Hipp, M.S., Bracher, A., Hayer-Hartl, M., and Hartl, F.U. (2013). Molecular chaperone functions in protein folding and proteostasis. Annu. Rev. Biochem. *82*323-355. DOI:10.1146/annurev-biochem-060208-092442

Kim, Y.S., Alarcon, S.V., Lee, S., Lee, M.J., Giaccone, G., Neckers, L., and Trepel, J.B. (2009). Update on Hsp90 inhibitors in clinical trial. Curr Top Med Chem *9*(15), 1479-1492. DOI:10.2174/156802609789895728

Klettner, A. (2004). The induction of heat shock proteins as a potential strategy to treat neurodegenerative disorders. Drug News Perspect. *17*(5), 299-306.

Kobayashi, T., Nakatani, Y., Tanioka, T., Tsujimoto, M., Nakajo, S., Nakaya, K., Murakami, M., and Kudo, I. (2004). Regulation of cytosolic prostaglandin E synthase by phosphorylation. Biochem. J. *381*(Pt 1), 59-69. DOI:10.1042/BJ20040118

Koulov, A.V., LaPointe, P., Lu, B., Razvi, A., Coppinger, J., Dong, M.Q., Matteson, J., Laister, R., Arrowsmith, C., Yates, J.R., and Balch, W.E. (2010). Biological and structural basis for Aha1 regulation of Hsp90 ATPase activity in maintaining proteostasis in the human disease cystic fibrosis. Mol. Biol. Cell *21*(6), 871-884. DOI:10.1091/mbc.E09-12-1017

Kovacs, J.J., Cohen, T.J., and Yao, T. (2005). Chaperoning steroid hormone signaling via reversible acetylation. Nucl Recept Signal *3* DOI:10.1621/nrs.03004

Kravats, A.N., Hoskins, J.R., Reidy, M., Johnson, J.L., Doyle, S.M., Genest, O., Masison, D.C., and Wickner, S. (2018). Functional and physical interaction between yeast Hsp90 and Hsp70. Proc. Natl. Acad. Sci. U. S. A. *115*(10), E2219. DOI:10.1073/pnas.1719969115

Kriegenburg, F., Ellgaard, L., and Hartmann-Petersen, R. (2012). Molecular chaperones in targeting misfolded proteins for ubiquitin-dependent degradation. Febs J. *279*(4), 532-542. DOI:10.1111/j.1742-4658.2011.08456.x

Kriehuber, T., Rattei, T., Weinmaier, T., Bepperling, A., Haslbeck, M., and Buchner, J. (2010). Independent evolution of the core domain and its flanking sequences in small heat shock proteins. Faseb J. *24*(10), 3633-3642. DOI:10.1096/fj.10-156992

Kubota, H., Yamamoto, S., Itoh, E., Abe, Y., Nakamura, A., Izumi, Y., Okada, H., Iida, M., Nanjo, H., Itoh, H., and Yamamoto, Y. (2010). Increased expression of co-chaperone HOP with HSP90 and HSC70 and complex formation in human colonic carcinoma. Cell Stress Chaperones *15*(6), 1003-1011. DOI:10.1007/s12192-010-0211-0

Kundrat, L., and Regan, L. (2010). Balance between folding and degradation for Hsp90-dependent client proteins: a key role for CHIP. Biochemistry *49*(35), 7428-7438. DOI:10.1021/bi100386w

Kuznetsova, I., Turoverov, K., Uversky, V., Kuznetsova, I.M., Turoverov, K.K., and Uversky, V.N. (2014). What Macromolecular Crowding Can Do to a Protein. International Journal of Molecular Sciences *15*(12), 23090-23140. DOI:10.3390/ijms151223090

Lapidus, L.J. (2017). Protein unfolding mechanisms and their effects on folding experiments version 1; referees: 2 approved]. F1000Research *6*(1723), DOI:10.12688/f1000research.12070.1

LaPointe, P., Wei, X., and Gariépy, J. (2005). A role for the protease-sensitive loop region of Shiga-like toxin 1 in the retrotranslocation of its A1 domain from the endoplasmic reticulum lumen. J. Biol. Chem. *280*(24), 23310-23318. DOI:10.1074/jbc.M414193200

Laskey, R.A., Honda, B.M., Mills, A.D., and Finch, J.T. (1978). Nucleosomes are assembled by an acidic protein which binds histones and transfers them to DNA. Nature *275*(5679), 416-420. DOI:10.1038/275416a0

Laufen, T., Mayer, M.P., Beisel, C., Klostermeier, D., Mogk, A., Reinstein, J., and Bukau, B. (1999). Mechanism of regulation of hsp70 chaperones by DnaJ cochaperones. Proc. Natl. Acad. Sci. U. S. A. *96*(10), 5452-5457.

Lee, C., Hong, H., Chang, Y., and Chang, W. (2012). Inhibition of heat shock protein (Hsp) 27 potentiates the suppressive effect of Hsp90 inhibitors in targeting breast cancer stem-like cells. Biochimie *94*(6), 1382-1389. DOI:10.1016/j.biochi.2012.02.034

Lee, S., Sowa, M.E., Watanabe, Y., Sigler, P.B., Chiu, W., Yoshida, M., and Tsai, F. (2003). The structure of ClpB: a molecular chaperone that rescues proteins from an aggregated state. Cell *115*(2), 229-240.

Lemaux, P.G., Herendeen, S.L., Bloch, P.L., and Neidhardt, F.C. (1978). Transient rates of synthesis of individual polypeptides in E. coli following temperature shifts. Cell *13*(3), 427-434.

Levinthal, C. (1968). Are there pathways for protein folding? J. Chim. Phys. *65*44-45. DOI:10.1051/jcp/1968650044

Lewis, M.J., and Pelham, H.R. (1985). Involvement of ATP in the nuclear and nucleolar functions of the 70 kd heat shock protein. Embo J. *4*(12), 3137-3143.

Li, J., and Buchner, J. (2013). Structure, function and regulation of the hsp90 machinery. Biomed J *36*(3), 106-117. DOI:10.4103/2319-4170.113230

Li, J., Richter, K., and Buchner, J. (2011). Mixed Hsp90-cochaperone complexes are important for the progression of the reaction cycle. Nat. Struct. Mol. Biol. *18*(1), 61-66. DOI:10.1038/nsmb.1965; 10.1038/nsmb.1965

Li, J., Richter, K., Reinstein, J., and Buchner, J. (2013). Integration of the accelerator Aha1 in the Hsp90 co-chaperone cycle. Nat. Struct. Mol. Biol. *20*(3), 326-331. DOI:10.1038/nsmb.2502

Li, J., Soroka, J., and Buchner, J. (2012). The Hsp90 chaperone machinery: Conformational dynamics and regulation by co-chaperones. Biochimica Et Biophysica Acta (BBA) - Molecular Cell Research *1823*(3), 624-635. DOI:10.1016/j.bbamcr.2011.09.003

Li, T., Jiang, H., Tong, Y., and Lu, J. (2018). Targeting the Hsp90-Cdc37-client protein interaction to disrupt Hsp90 chaperone machinery. J Hematol Oncol *11* DOI:10.1186/s13045-018-0602-8

Li, W., Li, Y., Guan, S., Fan, J., Cheng, C., Bright, A.M., Chinn, C., Chen, M., and Woodley, D.T. (2007). Extracellular heat shock protein-90α: linking hypoxia to skin cell motility and wound healing. Embo J *26*(5), 1221-1233. DOI:10.1038/sj.emboj.7601579

Lin, R., Heylbroeck, C., Genin, P., Pitha, P.M., and Hiscott, J. (1999). Essential role of interferon regulatory factor 3 in direct activation of RANTES chemokine transcription. Mol. Cell. Biol. *19*(2), 959-966.

Lin, T., Bear, M., Du, Z., Foley, K.P., Ying, W., Barsoum, J., and London, C. (2008). The novel HSP90 inhibitor STA-9090 exhibits activity against Kit-dependent and -independent malignant mast cell tumors. Exp. Hematol. *36*(10), 1266-1277. DOI:10.1016/j.exphem.2008.05.001

Linderstrøm-Lang, K.U., and Schellmand, J.A. (1959). Protein structure and enzyme activity . The Enzymes *1*443-510.

Lindquist, S. (1986). The heat-shock response. Annu. Rev. Biochem. *55*1151-1191. DOI:10.1146/annurev.bi.55.070186.005443

Lindquist, S., and Craig, E.A. (1988). The heat-shock proteins. Annu. Rev. Genet. *22*631-677. DOI:10.1146/annurev.ge.22.120188.003215

Lipsich, L.A., Cutt, J.R., and Brugge, J.S. (1982). Association of the transforming proteins of Rous, Fujinami, and Y73 avian sarcoma viruses with the same two cellular proteins. Mol. Cell. Biol. *2*(7), 875-880.

Liu, Q., and Hendrickson, W.A. (2007). Insights into Hsp70 chaperone activity from a crystal structure of the yeast Hsp110 Sse1. Cell *131*(1), 106-120. DOI:10.1016/j.cell.2007.08.039

Liu, Y., Ye, J., Ogawa, L.S., Inoue, T., Huang, Q., Chu, J., Bates, R.C., Ying, W., Sonderfan, A.J., Rao, P.E., and Zhou, D. (2015). The HSP90 Inhibitor Ganetespib Alleviates Disease Progression and Augments Intermittent Cyclophosphamide Therapy in the MRL/lpr Mouse Model of Systemic Lupus Erythematosus. Plos One *10*(5), e0127361. DOI:10.1371/journal.pone.0127361

Livak, K.J., and Schmittgen, T.D. (2001). Analysis of relative gene expression data using real-time quantitative PCR and the 2(-Delta Delta C(T)) Method. Methods *25*(4), 402-408. DOI:10.1006/meth.2001.1262

Longshaw, V.M., Dirr, H.W., Blatch, G.L., and Lässle, M. (2000). The in vitro phosphorylation of the co-chaperone mSTI1 by cell cycle kinases substantiates a predicted casein kinase II-p34cdc2-NLS (CcN) motif. Biol. Chem. *381*(11), 1133-1138. DOI:10.1515/BC.2000.139

Loo, M.A., Jensen, T.J., Cui, L., Hou, Y., Chang, X.B., and Riordan, J.R. (1998). Perturbation of Hsp90 interaction with nascent CFTR prevents its maturation and accelerates its degradation by the proteasome. Embo J. *17*(23), 6879-6887. DOI:10.1093/emboj/17.23.6879

Lotz, G.P., Lin, H., Harst, A., and Obermann, W.M. (2003). Aha1 binds to the middle domain of Hsp90, contributes to client protein activation, and stimulates the ATPase activity of the molecular chaperone. J. Biol. Chem. *278*(19), 17228-17235. DOI:10.1074/jbc.M212761200

Luo, W., Dou, F., Rodina, A., Chip, S., Kim, J., Zhao, Q., Moulick, K., Aguirre, J., Wu, N., Greengard, P., and Chiosis, G. (2007). Roles of heat-shock protein 90 in maintaining and facilitating the neurodegenerative phenotype in tauopathies. Proc. Natl. Acad. Sci. U. S. A. *104*(22), 9511-9516. DOI:10.1073/pnas.0701055104

Luo, W., Sun, W., Taldone, T., Rodina, A., and Chiosis, G. (2010). Heat shock protein 90 in neurodegenerative diseases. Mol Neurodegener *5*24. DOI:10.1186/1750-1326-5-24

Maiti, P., Manna, J., Veleri, S., and Frautschy, S. (2014). Molecular Chaperone Dysfunction in Neurodegenerative Diseases and Effects of Curcumin. BioMed Research International *2014*e495091. DOI:10.1155/2014/495091

Marcu, M.G., Chadli, A., Bouhouche, I., Catelli, M., and Neckers, L.M. (2000). The heat shock protein 90 antagonist novobiocin interacts with a previously unrecognized ATP-binding domain in the carboxyl terminus of the chaperone. J. Biol. Chem. *275*(47), 37181-37186. DOI:10.1074/jbc.M003701200

Marozkina, N.V., Yemen, S., Borowitz, M., Liu, L., Plapp, M., Sun, F., Islam, R., Erdmann-Gilmore, P., Townsend, R.R., Lichti, C.F.*, et al.* (2010). Hsp 70/Hsp 90 organizing protein as a nitrosylation target in cystic fibrosis therapy. Proc. Natl. Acad. Sci. U. S. A. *107*(25), 11393-11398. DOI:10.1073/pnas.0909128107

Martin, A., Baker, T.A., and Sauer, R.T. (2008). Pore loops of the AAA+ ClpX machine grip substrates to drive translocation and unfolding. Nat. Struct. Mol. Biol. *15*(11), 1147-1151. DOI:10.1038/nsmb.1503

Martínez-Ruiz, A., Villanueva, L., González de Orduña, C., López-Ferrer, D., Higueras, M.A., Tarín, C., Rodríguez-Crespo, I., Vázquez, J., and Lamas, S. (2005). S-nitrosylation of Hsp90 promotes the inhibition of its ATPase and endothelial nitric oxide synthase regulatory activities. Proc. Natl. Acad. Sci. U. S. A. *102*(24), 8525-8530. DOI:10.1073/pnas.0407294102

Martinez-Yamout, M.A., Venkitakrishnan, R.P., Preece, N.E., Kroon, G., Wright, P.E., and Dyson, H.J. (2006). Localization of sites of interaction between p23 and Hsp90 in solution. J. Biol. Chem. *281*(20), 14457-14464. DOI:10.1074/jbc.M601759200

Mayer, M.P., and Bukau, B. (2005). Hsp70 chaperones: cellular functions and molecular mechanism. Cell. Mol. Life Sci. *62*(6), 670-684. DOI:10.1007/s00018-004-4464-6

Mayhew, M., da Silva, A.C., Martin, J., Erdjument-Bromage, H., Tempst, P., and Hartl, F.U. (1996). Protein folding in the central cavity of the GroEL-GroES chaperonin complex. Nature *379*(6564), 420-426. DOI:10.1038/379420a0

Mayor, A., Martinon, F., De Smedt, T., Pétrilli, V., and Tschopp, J. (2007). A crucial function of SGT1 and HSP90 in inflammasome activity links mammalian and plant innate immune responses. Nat. Immunol. *8*(5), 497-503. DOI:10.1038/ni1459

McCarthy, M.M., Pick, E., Kluger, Y., Gould-Rothberg, B., Lazova, R., Camp, R.L., Rimm, D.L., and Kluger, H.M. (2008). HSP90 as a marker of progression in melanoma. Ann. Oncol. *19*(3), 590-594. DOI:10.1093/annonc/mdm545

McClellan, A.J., Xia, Y., Deutschbauer, A.M., Davis, R.W., Gerstein, M., and Frydman, J. (2007). Diverse cellular functions of the Hsp90 molecular chaperone uncovered using systems approaches. Cell *131*(1), 121-135. DOI:10.1016/j.cell.2007.07.036

McLaughlin, S.H., Sobott, F., Yao, Z., Zhang, W., Nielsen, P.R., Grossmann, J.G., Laue, E.D., Robinson, C.V., and Jackson, S.E. (2006). The co-chaperone p23 arrests the Hsp90 ATPase cycle to trap client proteins. J. Mol. Biol. *356*(3), 746-758. DOI:10.1016/j.jmb.2005.11.085

McLaughlin, S.H., Ventouras, L., Lobbezoo, B., and Jackson, S.E. (2004). Independent ATPase activity of Hsp90 subunits creates a flexible assembly platform. J. Mol. Biol. *344*(3), 813-826. DOI:10.1016/j.jmb.2004.09.055

Mellatyar, H., Talaei, S., Pilehvar-Soltanahmadi, Y., Barzegar, A., Akbarzadeh, A., Shahabi, A., Barekati-Mowahed, M., and Zarghami, N. (2018). Targeted cancer therapy through 17-DMAG as an Hsp90 inhibitor: Overview and current state of the art. Biomed. Pharmacother. *102*608-617. DOI:10.1016/j.biopha.2018.03.102

Menezes, D.L., Taverna, P., Jensen, M.R., Abrams, T., Stuart, D., Yu, G.K., Duhl, D., Machajewski, T., Sellers, W.R., Pryer, N.K., and Gao, Z. (2012). The novel oral Hsp90 inhibitor NVP-HSP990 exhibits potent and broad-spectrum antitumor activities in vitro and in vivo. Mol. Cancer Ther. *11*(3), 730-739. DOI:10.1158/1535-7163.MCT-11-0667

Mercier, R., Wolmarans, A., Schubert, J., Neuweiler, H., Johnson, J.L., and LaPointe, P. (2019). The conserved NxNNWHW motif in Aha-type co-chaperones modulates the kinetics of Hsp90 ATPase stimulation. Nature Communications *10*(1), 1273. DOI:10.1038/s41467-019-09299-3

Meyer, P., Prodromou, C., Hu, B., Vaughan, C., Roe, S.M., Panaretou, B., Piper, P.W., and Pearl, L.H. (2003). Structural and functional analysis of the middle segment of hsp90: implications for ATP hydrolysis and client protein and cochaperone interactions. Mol. Cell *11*(3), 647-658. DOI:S1097276503000650

Meyer, P., Prodromou, C., Liao, C., Hu, B., Roe, S.M., Vaughan, C.K., Vlasic, I., Panaretou, B., Piper, P.W., and Pearl, L.H. (2004). Structural basis for recruitment of the ATPase activator Aha1 to the Hsp90 chaperone machinery. Embo J. *23*(3), 511-519. DOI:10.1038/sj.emboj.7600060

Mickler, M., Hessling, M., Ratzke, C., Buchner, J., and Hugel, T. (2009). The large conformational changes of Hsp90 are only weakly coupled to ATP hydrolysis. Nat. Struct. Mol. Biol. *16*(3), 281-286. DOI:10.1038/nsmb.1557

Millson, S.H., Prodromou, C., and Piper, P.W. (2010). A simple yeast-based system for analyzing inhibitor resistance in the human cancer drug targets Hsp90alpha/beta. Biochem. Pharmacol. *79*(11), 1581-1588. DOI:10.1016/j.bcp.2010.01.031

Mishra, P., and Bolon, D.N.A. (2014). Designed Hsp90 heterodimers reveal an asymmetric ATPase-driven mechanism in vivo. Mol. Cell *53*(2), 344-350. DOI:10.1016/j.molcel.2013.12.024

Misselwitz, B., Staeck, O., and Rapoport, T.A. (1998). J proteins catalytically activate Hsp70 molecules to trap a wide range of peptide sequences. Mol. Cell *2*(5), 593-603.

Miyata, Y. (2009). Protein kinase CK2 in health and disease: CK2: the kinase controlling the Hsp90 chaperone machinery. Cell. Mol. Life Sci. *66*(11-12), 1840-1849. DOI:10.1007/s00018-009-9152-0

Miyata, Y., Chambraud, B., Radanyi, C., Leclerc, J., Lebeau, M.C., Renoir, J.M., Shirai, R., Catelli, M.G., Yahara, I., and Baulieu, E.E. (1997). Phosphorylation of the immunosuppressant FK506-binding protein FKBP52 by casein kinase II: regulation of HSP90-binding activity of FKBP52. Proc. Natl. Acad. Sci. U. S. A. *94*(26), 14500-14505.

Miyata, Y., Nakamoto, H., and Neckers, L. (2013). The therapeutic target Hsp90 and cancer hallmarks. Curr. Pharm. Des. *19*(3), 347-365. DOI:10.2174/1381612811306030347

Mollapour, M., Bourboulia, D., Beebe, K., Woodford, M.R., Polier, S., Hoang, A., Chelluri, R., Li, Y., Guo, A., Lee, M.J.*, et al.* (2014). Asymmetric Hsp90 N domain SUMOylation recruits Aha1 and ATP-competitive inhibitors. Mol. Cell *53*(2), 317-329. DOI:10.1016/j.molcel.2013.12.007

Mollapour, M., and Neckers, L. (2012). Post-translational modifications of Hsp90 and their contributions to chaperone regulation. Biochim. Biophys. Acta *1823*(3), 648-655. DOI:10.1016/j.bbamcr.2011.07.018

Mollapour, M., Tsutsumi, S., Kim, Y.S., Trepel, J., and Neckers, L. (2011). Casein kinase 2 phosphorylation of Hsp90 threonine 22 modulates chaperone function and drug sensitivity. Oncotarget *2*(5), 407-417. DOI:10.18632/oncotarget.272

Mollapour, M., Tsutsumi, S., and Neckers, L. (2010). Hsp90 phosphorylation, Wee1 and the cell cycle. Cell. Cycle *9*(12), 2310-2316. DOI:10.4161/cc.9.12.12054

Mollapour, M., Tsutsumi, S., Truman, A.W., Xu, W., Vaughan, C.K., Beebe, K., Konstantinova, A., Vourganti, S., Panaretou, B., Piper, P.W.*, et al.* (2011). Threonine 22 phosphorylation attenuates Hsp90 interaction with cochaperones and affects its chaperone activity. Mol. Cell *41*(6), 672-681. DOI:10.1016/j.molcel.2011.02.011

Morimoto, R.I. (2011). The heat shock response: systems biology of proteotoxic stress in aging and disease. Cold Spring Harb. Symp. Quant. Biol. *76*91-99. DOI:10.1101/sqb.2012.76.010637

Morimoto, R.I. (1998). Regulation of the heat shock transcriptional response: cross talk between a family of heat shock factors, molecular chaperones, and negative regulators. Genes Dev. *12*(24), 3788-3796.

Morishima, Y., Kanelakis, K.C., Silverstein, A.M., Dittmar, K.D., Estrada, L., and Pratt, W.B. (2000). The Hsp organizer protein hop enhances the rate of but is not essential for glucocorticoid receptor folding by the multiprotein Hsp90-based chaperone system. J. Biol. Chem. *275*(10), 6894-6900.

Mumberg, D., Müller, R., and Funk, M. (1995). Yeast vectors for the controlled expression of heterologous proteins in different genetic backgrounds. Gene *156*(1), 119-122.

Murphy, S.M., Bergman, M., and Morgan, D.O. (1993). Suppression of c-Src activity by C-terminal Src kinase involves the c-Src SH2 and SH3 domains: analysis with Saccharomyces cerevisiae. Molecular and Cellular Biology *13*(9), 5290-5300. DOI:10.1128/MCB.13.9.5290

Nathan, D.F., and Lindquist, S. (1995). Mutational analysis of Hsp90 function: interactions with a steroid receptor and a protein kinase. Mol. Cell. Biol. *15*(7), 3917-3925.

Nathan, D.F., Vos, M.H., and Lindquist, S. (1999). Identification of SSF1, CNS1, and HCH1 as multicopy suppressors of a Saccharomyces cerevisiae Hsp90 loss-of-function mutation. Proc Natl Acad Sci U S A *96*(4), 1409-1414.

Nathan, D.F., Vos, M.H., and Lindquist, S. (1997). In vivo functions of the Saccharomyces cerevisiae Hsp90 chaperone. Proc. Natl. Acad. Sci. U. S. A. *94*(24), 12949-12956.

Neckers, L. (2002). Hsp90 inhibitors as novel cancer chemotherapeutic agents. Trends Mol Med *8*(4 Suppl), 55.

Neckers, L. (2006). Chaperoning oncogenes: Hsp90 as a target of geldanamycin. Handb Exp Pharmacol (172), 259-277.

Neckers, L., and Workman, P. (2012). Hsp90 molecular chaperone inhibitors: are we there yet? Clin. Cancer Res. *18*(1), 64-76. DOI:10.1158/1078-0432.CCR-11-1000

Nelson, G.M., Huffman, H., and Smith, D.F. (2003). Comparison of the carboxy-terminal DP-repeat region in the co-chaperones Hop and Hip. Cell Stress Chaperones *8*(2), 125-133.

Nelson, G.M., Prapapanich, V., Carrigan, P.E., Roberts, P.J., Riggs, D.L., and Smith, D.F. (2004). The heat shock protein 70 cochaperone hip enhances functional maturation of glucocorticoid receptor. Mol. Endocrinol. *18*(7), 1620-1630. DOI:10.1210/me.2004-0054

Newton, K., and Dixit, V.M. (2012). Signaling in Innate Immunity and Inflammation. Cold Spring Harb Perspect Biol *4*(3), DOI:10.1101/cshperspect.a006049

Nicolet, C.M., and Craig, E.A. (1989). Isolation and characterization of STI1, a stress-inducible gene from Saccharomyces cerevisiae. Mol. Cell. Biol. *9*(9), 3638-3646.

Nisemblat, S., Yaniv, O., Parnas, A., Frolow, F., and Azem, A. (2015). Crystal structure of the human mitochondrial chaperonin symmetrical football complex. Proc. Natl. Acad. Sci. U. S. A. *112*(19), 6044-6049. DOI:10.1073/pnas.1411718112

Obermann, W.M., Sondermann, H., Russo, A.A., Pavletich, N.P., and Hartl, F.U. (1998). In vivo function of Hsp90 is dependent on ATP binding and ATP hydrolysis. J. Cell Biol. *143*(4), 901-910.

Odunuga, O.O., Longshaw, V.M., and Blatch, G.L. (2004). Hop: more than an Hsp70/Hsp90 adaptor protein. Bioessays *26*(10), 1058-1068. DOI:10.1002/bies.20107

Ogura, T., and Wilkinson, A.J. (2001). AAA+ superfamily ATPases: common structure--diverse function. Genes Cells *6*(7), 575-597.

Onuchic, J.N., Luthey-Schulten, Z., and Wolynes, P.G. (1997). THEORY OF PROTEIN FOLDING: The Energy Landscape Perspective. Annual Review of Physical Chemistry *48*(1), 545-600. DOI:10.1146/annurev.physchem.48.1.545

Panaretou, B., Prodromou, C., Roe, S.M., O'Brien, R., Ladbury, J.E., Piper, P.W., and Pearl, L.H. (1998). ATP binding and hydrolysis are essential to the function of the Hsp90 molecular chaperone in vivo. Embo J. *17*(16), 4829-4836. DOI:10.1093/emboj/17.16.4829

Panaretou, B., Siligardi, G., Meyer, P., Maloney, A., Sullivan, J.K., Singh, S., Millson, S.H., Clarke, P.A., Naaby-Hansen, S., Stein, R.*, et al.* (2002). Activation of the ATPase activity of hsp90 by the stress-regulated cochaperone aha1. Mol. Cell *10*(6), 1307-1318. DOI:10.1016/S1097-2765(02)00785-2

Parsell, D.A., Kowal, A.S., Singer, M.A., and Lindquist, S. (1994). Protein disaggregation mediated by heat-shock protein Hsp104. Nature *372*(6505), 475-478. DOI:10.1038/372475a0

Patwardhan, C.A., Fauq, A., Peterson, L.B., Miller, C., Blagg, B.S.J., and Chadli, A. (2013). Gedunin inactivates the co-chaperone p23 protein causing cancer cell death by apoptosis. J. Biol. Chem. *288*(10), 7313-7325. DOI:10.1074/jbc.M112.427328

Pearl, L.H., and Prodromou, C. (2006). Structure and mechanism of the Hsp90 molecular chaperone machinery. Annu. Rev. Biochem. *75*271-294. DOI:10.1146/annurev.biochem.75.103004.142738

Pearl, L.H., and Prodromou, C. (2000). Structure and in vivo function of Hsp90. Curr. Opin. Struct. Biol. *10*(1), 46-51.

Pelham, H.R. (1986). Speculations on the functions of the major heat shock and glucose-regulated proteins. Cell *46*(7), 959-961.

Picard, D. (2006). Chaperoning steroid hormone action. Trends Endocrinol. Metab. *17*(6), 229-235. DOI:10.1016/j.tem.2006.06.003

Picard, D. (2002). Heat-shock protein 90, a chaperone for folding and regulation. Cell Mol. Life Sci. *59*(10), 1640-1648.

Picard, D., Khursheed, B., Garabedian, M.J., Fortin, M.G., Lindquist, S., and Yamamoto, K.R. (1990). Reduced levels of hsp90 compromise steroid receptor action in vivo. Nature *348*(6297), 166-168. DOI:10.1038/348166a0

Piper, P.W., Millson, S.H., Mollapour, M., Panaretou, B., Siligardi, G., Pearl, L.H., and Prodromou, C. (2003). Sensitivity to Hsp90-targeting drugs can arise with mutation to the Hsp90 chaperone, cochaperones and plasma membrane ATP binding cassette transporters of yeast. Eur. J. Biochem. *270*(23), 4689-4695.

Pirkl, F., and Buchner, J. (2001). Functional analysis of the Hsp90-associated human peptidyl prolyl cis/trans isomerases FKBP51, FKBP52 and Cyp40. J. Mol. Biol. *308*(4), 795-806. DOI:10.1006/jmbi.2001.4595

Pittet, D. (2005). Infection control and quality health care in the new millennium. Am J Infect Control *33*(5), 258-267. DOI:10.1016/j.ajic.2004.11.004

Polier, S., Samant, R.S., Clarke, P.A., Workman, P., Prodromou, C., and Pearl, L.H. (2013). ATP-competitive inhibitors block protein kinase recruitment to the Hsp90-Cdc37 system. Nat. Chem. Biol. *9*(5), 307-312. DOI:10.1038/nchembio.1212

Poulain, P., Gelly, J., and Flatters, D. (2010). Detection and Architecture of Small Heat Shock Protein Monomers. Plos One *5*(4), e9990. DOI:10.1371/journal.pone.0009990

Pratt, W.B., and Toft, D.O. (1997). Steroid receptor interactions with heat shock protein and immunophilin chaperones. Endocr. Rev. *18*(3), 306-360. DOI:10.1210/edrv.18.3.0303

Prodromou, C. (2012). The 'active life' of Hsp90 complexes. Biochim. Biophys. Acta *1823*(3), 614-623. DOI:10.1016/j.bbamcr.2011.07.020; 10.1016/j.bbamcr.2011.07.020

Prodromou, C., Roe, S.M., O'Brien, R., Ladbury, J.E., Piper, P.W., and Pearl, L.H. (1997). Identification and structural characterization of the ATP/ADP-binding site in the Hsp90 molecular chaperone. Cell *90*(1), 65-75.

Prodromou, C., Siligardi, G., O'Brien, R., Woolfson, D.N., Regan, L., Panaretou, B., Ladbury, J.E., Piper, P.W., and Pearl, L.H. (1999). Regulation of Hsp90 ATPase activity by tetratricopeptide repeat (TPR)-domain co-chaperones. Embo J. *18*(3), 754-762. DOI:10.1093/emboj/18.3.754

Prodromou, C., and Morgan, R.M.L. (2016). “Tuning” the ATPase Activity of Hsp90. Regulation of Ca2+-ATPases,V-ATPases and F-ATPases 469-490. DOI:10.1007/978-3-319-24780-9_23

Prodromou, C., Panaretou, B., Chohan, S., Siligardi, G., O’Brien, R., Ladbury, J.E., Roe, S.M., Piper, P.W., and Pearl, L.H. (2000). The ATPase cycle of Hsp90 drives a molecular ‘clamp’ via transient dimerization of the N-terminal domains. Embo J *19*(16), 4383-4392. DOI:10.1093/emboj/19.16.4383

Qian, Y.Q., Patel, D., Hartl, F.U., and McColl, D.J. (1996). Nuclear magnetic resonance solution structure of the human Hsp40 (HDJ-1) J-domain. J. Mol. Biol. *260*(2), 224-235. DOI:10.1006/jmbi.1996.0394

Queitsch, C., Sangster, T.A., and Lindquist, S. (2002). Hsp90 as a capacitor of phenotypic variation. Nature *417*(6889), 618-624. DOI:10.1038/nature749

Rajapandi, T., Greene, L.E., and Eisenberg, E. (2000). The molecular chaperones Hsp90 and Hsc70 are both necessary and sufficient to activate hormone binding by glucocorticoid receptor. J. Biol. Chem. *275*(29), 22597-22604. DOI:10.1074/jbc.M002035200

Rakoff-Nahoum, S., and Medzhitov, R. (2006). Role of the innate immune system and host-commensal mutualism. Curr. Top. Microbiol. Immunol. *308*1-18.

Ranson, N.A., Burston, S.G., and Clarke, A.R. (1997). Binding, encapsulation and ejection: substrate dynamics during a chaperonin-assisted folding reaction. J. Mol. Biol. *266*(4), 656-664. DOI:10.1006/jmbi.1996.0815

Ratzke, C., Berkemeier, F., and Hugel, T. (2012). Heat shock protein 90's mechanochemical cycle is dominated by thermal fluctuations. Proc. Natl. Acad. Sci. U. S. A. *109*(1), 161-166. DOI:10.1073/pnas.1107930108

Retzlaff, M., Hagn, F., Mitschke, L., Hessling, M., Gugel, F., Kessler, H., Richter, K., and Buchner, J. (2010). Asymmetric activation of the hsp90 dimer by its cochaperone aha1. Mol. Cell *37*(3), 344-354. DOI:10.1016/j.molcel.2010.01.006

Retzlaff, M., Stahl, M., Eberl, H.C., Lagleder, S., Beck, J., Kessler, H., and Buchner, J. (2009). Hsp90 is regulated by a switch point in the C-terminal domain. EMBO Rep *10*(10), 1147-1153. DOI:10.1038/embor.2009.153

Richter, K., and Buchner, J. (2011). Closing in on the Hsp90 chaperone-client relationship. Structure *19*(4), 445-446. DOI:10.1016/j.str.2011.03.007

Richter, K., Haslbeck, M., and Buchner, J. (2010). The heat shock response: life on the verge of death. Mol. Cell *40*(2), 253-266. DOI:10.1016/j.molcel.2010.10.006

Richter, K., Moser, S., Hagn, F., Friedrich, R., Hainzl, O., Heller, M., Schlee, S., Kessler, H., Reinstein, J., and Buchner, J. (2006). Intrinsic inhibition of the Hsp90 ATPase activity. J. Biol. Chem. *281*(16), 11301-11311. DOI:10.1074/jbc.M510142200

Richter, K., Muschler, P., Hainzl, O., and Buchner, J. (2001). Coordinated ATP hydrolysis by the Hsp90 dimer. J. Biol. Chem. *276*(36), 33689-33696. DOI:10.1074/jbc.M103832200

Richter, K., Muschler, P., Hainzl, O., Reinstein, J., and Buchner, J. (2003). Sti1 is a non-competitive inhibitor of the Hsp90 ATPase. Binding prevents the N-terminal dimerization reaction during the atpase cycle. J. Biol. Chem. *278*(12), 10328-10333. DOI:10.1074/jbc.M213094200

Richter, K., Reinstein, J., and Buchner, J. (2002). N-terminal residues regulate the catalytic efficiency of the Hsp90 ATPase cycle. J. Biol. Chem. *277*(47), 44905-44910. DOI:10.1074/jbc.M208457200

Richter, K., Walter, S., and Buchner, J. (2004). The Co-chaperone Sba1 connects the ATPase reaction of Hsp90 to the progression of the chaperone cycle. J. Mol. Biol. *342*(5), 1403-1413. DOI:10.1016/j.jmb.2004.07.064

Ritossa, F. (1962). A new puffing pattern induced by temperature shock and DNP in drosophila. Experientia *18*(12), 571-573. DOI:10.1007/BF02172188

Rizzolo, K., Huen, J., Kumar, A., Phanse, S., Vlasblom, J., Kakihara, Y., Zeineddine, H.A., Minic, Z., Snider, J., Wang, W.*, et al.* (2017). Features of the Chaperone Cellular Network Revealed through Systematic Interaction Mapping. Cell Rep *20*(11), 2735-2748. DOI:10.1016/j.celrep.2017.08.074

Roe, S.M., Ali, M.M.U., Meyer, P., Vaughan, C.K., Panaretou, B., Piper, P.W., Prodromou, C., and Pearl, L.H. (2004). The Mechanism of Hsp90 regulation by the protein kinase-specific cochaperone p50(cdc37). Cell *116*(1), 87-98.

Rong, B., Zhao, C., Liu, H., Ming, Z., Cai, X., Gao, W., and Yang, S. (2014). Identification and verification of Hsp90-beta as a potential serum biomarker for lung cancer. Am J Cancer Res *4*(6), 874-885.

Rospert, S., Glick, B.S., Jenö, P., Schatz, G., Todd, M.J., Lorimer, G.H., and Viitanen, P.V. (1993). Identification and functional analysis of chaperonin 10, the groES homolog from yeast mitochondria. Proc. Natl. Acad. Sci. U. S. A. *90*(23), 10967-10971.

Rüdiger, S., Germeroth, L., Schneider-Mergener, J., and Bukau, B. (1997). Substrate specificity of the DnaK chaperone determined by screening cellulose-bound peptide libraries. Embo J *16*(7), 1501-1507. DOI:10.1093/emboj/16.7.1501

Rutherford, S.L., and Lindquist, S. (1998). Hsp90 as a capacitor for morphological evolution. Nature *396*(6709), 336-342. DOI:10.1038/24550

Rye, H.S., Burston, S.G., Fenton, W.A., Beechem, J.M., Xu, Z., Sigler, P.B., and Horwich, A.L. (1997). Distinct actions of cis and trans ATP within the double ring of the chaperonin GroEL. Nature *388*(6644), 792-798. DOI:10.1038/42047

Sahasrabudhe, P., Rohrberg, J., Biebl, M.M., Rutz, D.A., and Buchner, J. (2017). The Plasticity of the Hsp90 Co-chaperone System. Mol. Cell *67*(6), 961.e5. DOI:10.1016/j.molcel.2017.08.004

Saibil, H. (2013). Chaperone machines for protein folding, unfolding and disaggregation. Nat. Rev. Mol. Cell Biol. *14*(10), 630-642. DOI:10.1038/nrm3658

Sanchez, E.R., Toft, D.O., Schlesinger, M.J., and Pratt, W.B. (1985). Evidence that the 90-kDa phosphoprotein associated with the untransformed L-cell glucocorticoid receptor is a murine heat shock protein. J. Biol. Chem. *260*(23), 12398-12401.

Sausville, E.A., Tomaszewski, J.E., and Ivy, P. (2003). Clinical development of 17-allylamino, 17-demethoxygeldanamycin. Curr Cancer Drug Targets *3*(5), 377-383.

Scheufler, C., Brinker, A., Bourenkov, G., Pegoraro, S., Moroder, L., Bartunik, H., Hartl, F.U., and Moarefi, I. (2000). Structure of TPR domain-peptide complexes: critical elements in the assembly of the Hsp70-Hsp90 multichaperone machine. Cell *101*(2), 199-210. DOI:10.1016/S0092-8674(00)80830-2

Schmid, A.B., Lagleder, S., Gräwert, M.A., Röhl, A., Hagn, F., Wandinger, S.K., Cox, M.B., Demmer, O., Richter, K., Groll, M., Kessler, H., and Buchner, J. (2012). The architecture of functional modules in the Hsp90 co-chaperone Sti1/Hop. Embo J. *31*(6), 1506-1517. DOI:10.1038/emboj.2011.472

Schmid, S., Götz, M., and Hugel, T. (2018). Effects of Inhibitors on Hsp90's Conformational Dynamics, Cochaperone and Client Interactions. Chemphyschem *19*(14), 1716-1721. DOI:10.1002/cphc.201800342

Schnell, S. (2014). Validity of the Michaelis-Menten equation--steady-state or reactant stationary assumption: that is the question. Febs J. *281*(2), 464-472. DOI:10.1111/febs.12564

Schopf, F.H., Biebl, M.M., and Buchner, J. (2017). The HSP90 chaperone machinery. Nature Reviews Molecular Cell Biology *18*(6), 345-360. DOI:10.1038/nrm.2017.20

Schuh, S., Yonemoto, W., Brugge, J., Bauer, V.J., Riehl, R.M., Sullivan, W.P., and Toft, D.O. (1985). A 90,000-dalton binding protein common to both steroid receptors and the Rous sarcoma virus transforming protein, pp60v-src. J. Biol. Chem. *260*(26), 14292-14296.

Schulze, A., Beliu, G., Helmerich, D.A., Schubert, J., Pearl, L.H., Prodromou, C., and Neuweiler, H. (2016). Cooperation of local motions in the Hsp90 molecular chaperone ATPase mechanism. Nat. Chem. Biol. *12*(8), 628-635. DOI:10.1038/nchembio.2111

Schwarze, S.R., Fu, V.X., and Jarrard, D.F. (2003). Cdc37 enhances proliferation and is necessary for normal human prostate epithelial cell survival. Cancer Res. *63*(15), 4614-4619.

Scroggins, B.T., and Neckers, L. (2007). Post-translational modification of heat-shock protein 90: impact on chaperone function. Expert Opin Drug Discov *2*(10), 1403-1414. DOI:10.1517/17460441.2.10.1403

Sevier, C.S., and Machamer, C.E. (2001). p38: A Novel Protein That Associates with the Vesicular Stomatitis Virus Glycoprotein. Biochem. Biophys. Res. Commun. *287*(2), 574-582. DOI:10.1006/bbrc.2001.5621

Shao, J., Prince, T., Hartson, S.D., and Matts, R.L. (2003). Phosphorylation of serine 13 is required for the proper function of the Hsp90 co-chaperone, Cdc37. J. Biol. Chem. *278*(40), 38117-38120. DOI:10.1074/jbc.C300330200

Sharma, S.K., De los Rios, P., Christen, P., Lustig, A., and Goloubinoff, P. (2010). The kinetic parameters and energy cost of the Hsp70 chaperone as a polypeptide unfoldase. Nat. Chem. Biol. *6*(12), 914-920. DOI:10.1038/nchembio.455

Shelton, L.B., Koren, J., and Blair, L.J. (2017). Imbalances in the Hsp90 Chaperone Machinery: Implications for Tauopathies. Front Neurosci *11*724. DOI:10.3389/fnins.2017.00724

Shimamura, T., Lowell, A.M., Engelman, J.A., and Shapiro, G.I. (2005). Epidermal growth factor receptors harboring kinase domain mutations associate with the heat shock protein 90 chaperone and are destabilized following exposure to geldanamycins. Cancer Res. *65*(14), 6401-6408. DOI:10.1158/0008-5472.CAN-05-0933

Shkreta, L., Bell, B., Revil, T., Venables, J.P., Prinos, P., Elela, S.A., and Chabot, B. (2013). Cancer-Associated Perturbations in Alternative Pre-messenger RNA Splicing. Cancer Treat. Res. *158*41-94. DOI:10.1007/978-3-642-31659-3_3

Sidera, K., and Patsavoudi, E. (2014). HSP90 inhibitors: current development and potential in cancer therapy. Recent Pat Anticancer Drug Discov *9*(1), 1-20.

Siligardi, G., Hu, B., Panaretou, B., Piper, P.W., Pearl, L.H., and Prodromou, C. (2004). Co-chaperone regulation of conformational switching in the Hsp90 ATPase cycle. J. Biol. Chem. *279*(50), 51989-51998. DOI:10.1074/jbc.M410562200

Siligardi, G., Panaretou, B., Meyer, P., Singh, S., Woolfson, D.N., Piper, P.W., Pearl, L.H., and Prodromou, C. (2002). Regulation of Hsp90 ATPase activity by the co-chaperone Cdc37p/p50cdc37. J. Biol. Chem. *277*(23), 20151-20159. DOI:10.1074/jbc.M201287200

Smith, D.F., and Toft, D.O. (1993). Steroid receptors and their associated proteins. Mol. Endocrinol. *7*(1), 4-11. DOI:10.1210/mend.7.1.8446107

Smith, J.R., and Workman, P. (2009). Targeting CDC37: an alternative, kinase-directed strategy for disruption of oncogenic chaperoning. Cell Cycle *8*(3), 362-372. DOI:10.4161/cc.8.3.7531

Smith, J.R., Clarke, P.A., de Billy, E., and Workman, P. (2009). Silencing the cochaperone CDC37 destabilizes kinase clients and sensitizes cancer cells to HSP90 inhibitors. Oncogene *28*(2), 157-169. DOI:10.1038/onc.2008.380

Solit, D.B., and Chiosis, G. (2008). Development and application of Hsp90 inhibitors. Drug Discov. Today *13*(1-2), 38-43. DOI:10.1016/j.drudis.2007.10.007

Soroka, J., Wandinger, S.K., Mäusbacher, N., Schreiber, T., Richter, K., Daub, H., and Buchner, J. (2012). Conformational switching of the molecular chaperone Hsp90 via regulated phosphorylation. Mol. Cell *45*(4), 517-528. DOI:10.1016/j.molcel.2011.12.031

Soti, C., Vermes, A., Haystead, T.A.J., and Csermely, P. (2003). Comparative analysis of the ATP-binding sites of Hsp90 by nucleotide affinity cleavage: a distinct nucleotide specificity of the C-terminal ATP-binding site. Eur. J. Biochem. *270*(11), 2421-2428.

Southworth, D.R., and Agard, D.A. (2011). Client-loading conformation of the Hsp90 molecular chaperone revealed in the cryo-EM structure of the human Hsp90:Hop complex. Mol. Cell *42*(6), 771-781. DOI:10.1016/j.molcel.2011.04.023

Stancato, L.F., Hutchison, K.A., Krishna, P., and Pratt, W.B. (1996). Animal and plant cell lysates share a conserved chaperone system that assembles the glucocorticoid receptor into a functional heterocomplex with hsp90. Biochemistry *35*(2), 554-561. DOI:10.1021/bi9511649

Stebbins, C.E., Russo, A.A., Schneider, C., Rosen, N., Hartl, F.U., and Pavletich, N.P. (1997). Crystal structure of an Hsp90-geldanamycin complex: targeting of a protein chaperone by an antitumor agent. Cell *89*(2), 239-250.

Stechmann, A., and Cavalier-Smith, T. (2004). Evolutionary origins of Hsp90 chaperones and a deep paralogy in their bacterial ancestors. J. Eukaryot. Microbiol. *51*(3), 364-373.

Stengel, F., Baldwin, A.J., Painter, A.J., Jaya, N., Basha, E., Kay, L.E., Vierling, E., Robinson, C.V., and Benesch, J.L.P. (2010). Quaternary dynamics and plasticity underlie small heat shock protein chaperone function. Proc. Natl. Acad. Sci. U. S. A. *107*(5), 2007-2012. DOI:10.1073/pnas.0910126107

Stepanova, L., Yang, G., DeMayo, F., Wheeler, T.M., Finegold, M., Thompson, T.C., and Harper, J.W. (2000). Induction of human Cdc37 in prostate cancer correlates with the ability of targeted Cdc37 expression to promote prostatic hyperplasia. Oncogene *19*(18), 2186-2193. DOI:10.1038/sj.onc.1203561

Street, T.O., Lavery, L.A., and Agard, D.A. (2011). Substrate binding drives large-scale conformational changes in the Hsp90 molecular chaperone. Mol Cell *42*(1), 96-105. DOI:10.1016/j.molcel.2011.01.029

Sullivan, W., Stensgard, B., Caucutt, G., Bartha, B., McMahon, N., Alnemri, E.S., Litwack, G., and Toft, D. (1997). Nucleotides and Two Functional States of hsp90. J. Biol. Chem. *272*(12), 8007-8012. DOI:10.1074/jbc.272.12.8007

Sun, L., Prince, T., Manjarrez, J.R., Scroggins, B.T., and Matts, R.L. (2012). Characterization of the interaction of Aha1 with components of the Hsp90 chaperone machine and client proteins. Biochim. Biophys. Acta *1823*(6), 1092-1101. DOI:10.1016/j.bbamcr.2012.03.014

Supko, J.G., Hickman, R.L., Grever, M.R., and Malspeis, L. (1995). Preclinical pharmacologic evaluation of geldanamycin as an antitumor agent. Cancer Chemother. Pharmacol. *36*(4), 305-315. DOI:10.1007/BF00689048

Szabo, A., Langer, T., Schröder, H., Flanagan, J., Bukau, B., and Hartl, F.U. (1994). The ATP hydrolysis-dependent reaction cycle of the Escherichia coli Hsp70 system DnaK, DnaJ, and GrpE. Proc. Natl. Acad. Sci. U. S. A. *91*(22), 10345-10349.

Taipale, M., Jarosz, D.F., and Lindquist, S. (2010). HSP90 at the hub of protein homeostasis: emerging mechanistic insights. Nat Rev Mol Cell Biol *11*(7), 515-528. DOI:10.1038/nrm2918

Taipale, M., Krykbaeva, I., Koeva, M., Kayatekin, C., Westover, K.D., Karras, G.I., and Lindquist, S. (2012). Quantitative analysis of HSP90-client interactions reveals principles of substrate recognition. Cell *150*(5), 987-1001. DOI:10.1016/j.cell.2012.06.047

Taipale, M., Tucker, G., Peng, J., Krykbaeva, I., Lin, Z., Larsen, B., Choi, H., Berger, B., Gingras, A., and Lindquist, S. (2014). A Quantitative Chaperone Interaction Network Reveals the Architecture of Cellular Protein Homeostasis Pathways. Cell *158*(2), 434-448. DOI:10.1016/j.cell.2014.05.039

Taxis, C., and Knop, M. (2006). System of centromeric, episomal, and integrative vectors based on drug resistance markers for Saccharomyces cerevisiae. BioTechniques *40*(1), 73-78. DOI:10.2144/000112040

Taylor, J.P., Hardy, J., and Fischbeck, K.H. (2002). Toxic proteins in neurodegenerative disease. Science *296*(5575), 1991-1995. DOI:10.1126/science.1067122

Teter, S.A., Houry, W.A., Ang, D., Tradler, T., Rockabrand, D., Fischer, G., Blum, P., Georgopoulos, C., and Hartl, F.U. (1999). Polypeptide flux through bacterial Hsp70: DnaK cooperates with trigger factor in chaperoning nascent chains. Cell *97*(6), 755-765.

Tissières, A., Mitchell, H.K., and Tracy, U.M. (1974). Protein synthesis in salivary glands of Drosophila melanogaster: relation to chromosome puffs. J. Mol. Biol. *84*(3), 389-398.

Todd, M.J., Viitanen, P.V., and Lorimer, G.H. (1994). Dynamics of the chaperonin ATPase cycle: implications for facilitated protein folding. Science *265*(5172), 659-666.

Tranguch, S., Cheung-Flynn, J., Daikoku, T., Prapapanich, V., Cox, M.B., Xie, H., Wang, H., Das, S.K., Smith, D.F., and Dey, S.K. (2005). Cochaperone immunophilin FKBP52 is critical to uterine receptivity for embryo implantation. Proc. Natl. Acad. Sci. U. S. A. *102*(40), 14326-14331. DOI:10.1073/pnas.0505775102

Tsutsumi, S., Mollapour, M., Prodromou, C., Lee, C., Panaretou, B., Yoshida, S., Mayer, M.P., and Neckers, L.M. (2012). Charged linker sequence modulates eukaryotic heat shock protein 90 (Hsp90) chaperone activity. Proc Natl Acad Sci U S A *109*(8), 2937-2942. DOI:10.1073/pnas.1114414109

Tsutsumi, S., and Neckers, L. (2007). Extracellular heat shock protein 90: A role for a molecular chaperone in cell motility and cancer metastasis. Cancer Science *98*(10), 1536-1539. DOI:10.1111/j.1349-7006.2007.00561.x

Tukaj, S., and Węgrzyn, G. (2016). Anti-Hsp90 therapy in autoimmune and inflammatory diseases: a review of preclinical studies. Cell Stress Chaperones *21*(2), 213-218. DOI:10.1007/s12192-016-0670-z

Uhlen, M., Zhang, C., Lee, S., Sjöstedt, E., Fagerberg, L., Bidkhori, G., Benfeitas, R., Arif, M., Liu, Z., Edfors, F.*, et al.* (2017). A pathology atlas of the human cancer transcriptome. Science *357*(6352), DOI:10.1126/science.aan2507

van den Berg, B., Ellis, R.J., and Dobson, C.M. (1999). Effects of macromolecular crowding on protein folding and aggregation. Embo J. *18*(24), 6927-6933. DOI:10.1093/emboj/18.24.6927

van Montfort, R.L., Basha, E., Friedrich, K.L., Slingsby, C., and Vierling, E. (2001). Crystal structure and assembly of a eukaryotic small heat shock protein. Nat. Struct. Biol. *8*(12), 1025-1030. DOI:10.1038/nsb722

Vartholomaiou, E., Echeverría, P.C., and Picard, D. (2016). Unusual Suspects in the Twilight Zone Between the Hsp90 Interactome and Carcinogenesis. Adv. Cancer Res. *129*1-30. DOI:10.1016/bs.acr.2015.08.001

Vaughan, C.K., Göhlke, U., Sobott, F., Good, V.M., Ali, M.M.U., Prodromou, C., Robinson, C.V., Saibil, H.R., and Pearl, L.H. (2006). Structure of an Hsp90 - Cdc37 - Cdk4 complex. Mol Cell *23*(5), 697-707. DOI:10.1016/j.molcel.2006.07.016

Vaughan, C.K., Mollapour, M., Smith, J.R., Truman, A., Hu, B., Good, V.M., Panaretou, B., Neckers, L., Clarke, P.A., Workman, P.*, et al.* (2008). Hsp90-dependent activation of protein kinases is regulated by chaperone-targeted dephosphorylation of Cdc37. Mol. Cell *31*(6), 886-895. DOI:10.1016/j.molcel.2008.07.021

Vaughan, C.K., Neckers, L., and Piper, P.W. (2010). Understanding of the Hsp90 molecular chaperone reaches new heights. Nat. Struct. Mol. Biol. *17*(12), 1400-1404. DOI:10.1038/nsmb1210-1400

Venton, D. (2016). Highlight—Chaperone Proteins Are Evolution's Helping Hand. Genome Biol Evol *8*(9), 2992-2993. DOI:10.1093/gbe/evw210

Verba, K.A., Wang, R.Y., Arakawa, A., Liu, Y., Shirouzu, M., Yokoyama, S., and Agard, D.A. (2016). Atomic structure of Hsp90-Cdc37-Cdk4 reveals that Hsp90 traps and stabilizes an unfolded kinase. Science *352*(6293), 1542-1547. DOI:10.1126/science.aaf5023

Walsh, N., Larkin, A., Swan, N., Conlon, K., Dowling, P., McDermott, R., and Clynes, M. (2011). RNAi knockdown of Hop (Hsp70/Hsp90 organising protein) decreases invasion via MMP-2 down regulation. Cancer Lett. *306*(2), 180-189. DOI:10.1016/j.canlet.2011.03.004

Walton-Diaz, A., Khan, S., Bourboulia, D., Trepel, J.B., Neckers, L., and Mollapour, M. (2013). Contributions of co-chaperones and post-translational modifications towards Hsp90 drug sensitivity. Future Med Chem *5*(9), 1059-1071. DOI:10.4155/fmc.13.88

Wan, P.T.C., Garnett, M.J., Roe, S.M., Lee, S., Niculescu-Duvaz, D., Good, V.M., Jones, C.M., Marshall, C.J., Springer, C.J., Barford, D., and Marais, R. (2004). Mechanism of activation of the RAF-ERK signaling pathway by oncogenic mutations of B-RAF. Cell *116*(6), 855-867.

Wang, J., Cui, S., Zhang, X., Wu, Y., and Tang, H. (2013). High Expression of Heat Shock Protein 90 Is Associated with Tumor Aggressiveness and Poor Prognosis in Patients with Advanced Gastric Cancer. PLoS One *8*(4), DOI:10.1371/journal.pone.0062876

Wang, L., Xie, C., Greggio, E., Parisiadou, L., Shim, H., Sun, L., Chandran, J., Lin, X., Lai, C., Yang, W.*, et al.* (2008). The chaperone activity of heat shock protein 90 is critical for maintaining the stability of leucine-rich repeat kinase 2. J. Neurosci. *28*(13), 3384-3391. DOI:10.1523/JNEUROSCI.0185-08.2008

Wang, X., Venable, J., LaPointe, P., Hutt, D.M., Koulov, A.V., Coppinger, J., Gurkan, C., Kellner, W., Matteson, J., Plutner, H.*, et al.* (2006). Hsp90 cochaperone Aha1 downregulation rescues misfolding of CFTR in cystic fibrosis. Cell *127*(4), 803-815. DOI:10.1016/j.cell.2006.09.043

Wang, Y., and McAlpine, S.R. (2015). N-terminal and C-terminal modulation of Hsp90 produce dissimilar phenotypes. Chem. Commun. (Camb.) *51*(8), 1410-1413. DOI:10.1039/c4cc07284g

Wang, Y., Mercier, R., Hobman, T.C., and LaPointe, P. (2013). Regulation of RNA interference by Hsp90 is an evolutionarily conserved process. Biochim. Biophys. Acta *1833*(12), 2673-2681. DOI:10.1016/j.bbamcr.2013.06.017

Wayne, N., Mishra, P., and Bolon, D.N. (2011). Hsp90 and client protein maturation. Methods Mol. Biol. *787*33-44. DOI:10.1007/978-1-61779-295-3_3

Weaver, A.J., Sullivan, W.P., Felts, S.J., Owen, B.A., and Toft, D.O. (2000). Crystal structure and activity of human p23, a heat shock protein 90 co-chaperone. J. Biol. Chem. *275*(30), 23045-23052. DOI:10.1074/jbc.M003410200

Wegele, H., Wandinger, S.K., Schmid, A.B., Reinstein, J., and Buchner, J. (2006). Substrate transfer from the chaperone Hsp70 to Hsp90. J. Mol. Biol. *356*(3), 802-811. DOI:10.1016/j.jmb.2005.12.008

Weikl, T., Abelmann, K., and Buchner, J. (1999). An unstructured C-terminal region of the Hsp90 co-chaperone p23 is important for its chaperone function. J. Mol. Biol. *293*(3), 685-691. DOI:10.1006/jmbi.1999.3172

Weikl, T., Muschler, P., Richter, K., Veit, T., Reinstein, J., and Buchner, J. (2000). C-terminal regions of Hsp90 are important for trapping the nucleotide during the ATPase cycle. J. Mol. Biol. *303*(4), 583-592. DOI:10.1006/jmbi.2000.4157

Weissman, J.S., Kashi, Y., Fenton, W.A., and Horwich, A.L. (1994). GroEL-mediated protein folding proceeds by multiple rounds of binding and release of nonnative forms. Cell *78*(4), 693-702.

Whitesell, L., Mimnaugh, E.G., De Costa, B., Myers, C.E., and Neckers, L.M. (1994). Inhibition of heat shock protein HSP90-pp60v-src heteroprotein complex formation by benzoquinone

ansamycins: essential role for stress proteins in oncogenic transformation. Proc. Natl. Acad. Sci. U. S. A. *91*(18), 8324-8328.

Whitesell, L., Shifrin, S.D., Schwab, G., and Neckers, L.M. (1992). Benzoquinonoid ansamycins possess selective tumoricidal activity unrelated to src kinase inhibition. Cancer Res. *52*(7), 1721-1728.

Whitesell, L., and Lindquist, S. (2005). HSP90 and the chaperoning of cancer. Nat. Rev. Cancer *5*(10), 761-772. DOI:10.1038/nrc1716

Whitesell, L., Santagata, S., Mendillo, M.L., Lin, N.U., Proia, D.A., and Lindquist, S. (2014). HSP90 empowers evolution of resistance to hormonal therapy in human breast cancer models. Proc Natl Acad Sci U S A *111*(51), 18297-18302. DOI:10.1073/pnas.1421323111

Wiech, H., Buchner, J., Zimmermann, R., and Jakob, U. (1992). Hsp90 chaperones protein folding in vitro. Nature *358*(6382), 169-170. DOI:10.1038/358169a0

Willhoft, O., Kerr, R., Patel, D., Zhang, W., Al-Jassar, C., Daviter, T., Millson, S.H., Thalassinos, K., and Vaughan, C.K. (2017). The crystal structure of the Sgt1-Skp1 complex: the link between Hsp90 and both SCF E3 ubiquitin ligases and kinetochores. Sci Rep *7* DOI:10.1038/srep41626

Williams, S.P., and Sigler, P.B. (1998). Atomic structure of progesterone complexed with its receptor. Nature *393*(6683), 392-396. DOI:10.1038/30775

Wolmarans, A., Lee, B., Spyracopoulos, L., and LaPointe, P. (2016). The Mechanism of Hsp90 ATPase Stimulation by Aha1. Scientific Reports *6*33179. DOI:10.1038/srep33179

Wong, D.S., and Jay, D.G. (2016). Chapter Six - Emerging Roles of Extracellular Hsp90 in Cancer. In Advances in Cancer Research, Whitesell, Jennifer Isaacs and Luke ed., Academic Press) pp. 141-163.

Wu, J., Liu, T., Rios, Z., Mei, Q., Lin, X., and Cao, S. (2017). Heat Shock Proteins and Cancer. Trends Pharmacol. Sci. *38*(3), 226-256. DOI:10.1016/j.tips.2016.11.009

Xu, W., Mollapour, M., Prodromou, C., Wang, S., Scroggins, B.T., Palchick, Z., Beebe, K., Siderius, M., Lee, M.J., Couvillon, A.*, et al.* (2012). Dynamic tyrosine phosphorylation modulates cycling of the HSP90-P50(CDC37)-AHA1 chaperone machine. Mol. Cell *47*(3), 434-443. DOI:10.1016/j.molcel.2012.05.015

Xu, Y., Singer, M.A., and Lindquist, S. (1999). Maturation of the tyrosine kinase c-src as a kinase and as a substrate depends on the molecular chaperone Hsp90. Proc. Natl. Acad. Sci. U. S. A. *96*(1), 109-114.

Xu, Y., and Lindquist, S. (1993). Heat-shock protein hsp90 governs the activity of pp60v-src kinase. Proc Natl Acad Sci U S A *90*(15), 7074-7078.

Xu, Z., Horwich, A.L., and Sigler, P.B. (1997). The crystal structure of the asymmetric GroEL-GroES-(ADP)7 chaperonin complex. Nature *388*(6644), 741-750. DOI:10.1038/41944

Xu, Z., Devlin, K.I., Ford, M.G., Nix, J.C., Qin, J., and Misra, S. (2006). Structure and interactions of the helical and U-box domains of CHIP, the C terminus of HSP70 interacting protein. Biochemistry *45*(15), 4749-4759. DOI:10.1021/bi0601508

Yamamori, T., Ito, K., Nakamura, Y., and Yura, T. (1978). Transient regulation of protein synthesis in Escherichia coli upon shift-up of growth temperature. J Bacteriol *134*(3), 1133-1140.

Yang, C.K., and He, S.D. (2016). Heat shock protein 90 regulates necroptosis by modulating multiple signaling effectors. Cell Death Dis *7*(3), e2126. DOI:10.1038/cddis.2016.25

Yang, K., Shi, H., Qi, R., Sun, S., Tang, Y., Zhang, B., and Wang, C. (2006). Hsp90 regulates activation of interferon regulatory factor 3 and TBK-1 stabilization in Sendai virus-infected cells. Mol. Biol. Cell *17*(3), 1461-1471. DOI:10.1091/mbc.e05-09-0853

Yifrach, O., and Horovitz, A. (1995). Nested cooperativity in the ATPase activity of the oligomeric chaperonin GroEL. Biochemistry *34*(16), 5303-5308. DOI:10.1021/bi00016a001

Yin, Z., Henry, E.C., and Gasiewicz, T.A. (2009). (-)-Epigallocatechin-3-gallate is a novel Hsp90 inhibitor. Biochemistry *48*(2), 336-345. DOI:10.1021/bi801637q

Young, J.C., Moarefi, I., and Hartl, F.U. (2001). Hsp90: a specialized but essential protein-folding tool. J. Cell Biol. *154*(2), 267-273.

Yu, P., Chen, X., and Li, P. (2017). Enhancing microbial production of biofuels by expanding microbial metabolic pathways. Biotechnol. Appl. Biochem. *64*(5), 606-619. DOI:10.1002/bab.1529

Zhang, M., Windheim, M., Roe, S.M., Peggie, M., Cohen, P., Prodromou, C., and Pearl, L.H. (2005). Chaperoned ubiquitylation--crystal structures of the CHIP U box E3 ubiquitin ligase and a CHIP-Ubc13-Uev1a complex. Mol. Cell *20*(4), 525-538. DOI:10.1016/j.molcel.2005.09.023

Zhang, T., Hamza, A., Cao, X., Wang, B., Yu, S., Zhan, C., and Sun, D. (2008). A novel Hsp90 inhibitor to disrupt Hsp90/Cdc37 complex against pancreatic cancer cells. Mol. Cancer Ther. *7*(1), 162-170. DOI:10.1158/1535-7163.MCT-07-0484

Zhao, R., and Houry, W.A. (2013). Molecular Interaction Network of the Hsp90 Chaperone System Landes Bioscience).

Zhao, R., Kakihara, Y., Gribun, A., Huen, J., Yang, G., Khanna, M., Costanzo, M., Brost, R.L., Boone, C., Hughes, T.R., Yip, C.M., and Houry, W.A. (2008). Molecular chaperone Hsp90 stabilizes Pih1/Nop17 to maintain R2TP complex activity that regulates snoRNA accumulation. J. Cell Biol. *180*(3), 563-578. DOI:10.1083/jcb.200709061

Zhou, W., and Yuan, J. (2014). Necroptosis in health and diseases. Semin. Cell Dev. Biol. *35*14-23. DOI:10.1016/j.semcdb.2014.07.013

Zhu, X., Zhao, X., Burkholder, W.F., Gragerov, A., Ogata, C.M., Gottesman, M.E., and Hendrickson, W.A. (1996). Structural analysis of substrate binding by the molecular chaperone DnaK. Science *272*(5268), 1606-1614.

Zierer, B.K., Rübbelke, M., Tippel, F., Madl, T., Schopf, F.H., Rutz, D.A., Richter, K., Sattler, M., and Buchner, J. (2016). Importance of cycle timing for the function of the molecular chaperone Hsp90. Nature Structural & Molecular Biology *23*(11), 1020-1028. DOI:10.1038/nsmb.3305

Zimmerman, S.B., and Trach, S.O. (1991). Estimation of macromolecule concentrations and excluded volume effects for the cytoplasm of Escherichia coli. J. Mol. Biol. *222*(3), 599-620.

Zimmermann, R., Sagstetter, M., J Lewis, M., and R. B. Pelham, H. (1988). Seventy-kilodalton heat shock proteins and an additional component from reticulocyte lysate stimulate import of M13 procoat protein into microsomes. The EMBO Journal *7*2875-80. DOI:10.1002/j.1460-2075.1988.tb03144.x

Zuehlke, A.D., Beebe, K., Neckers, L., and Prince, T. (2015). Regulation and function of the human HSP90AA1 gene. Gene *570*(1), 8-16. DOI:10.1016/j.gene.2015.06.018

Zuehlke, A.D., and Johnson, J.L. (2010). Hsp90 and co-chaperones twist the functions of diverse client proteins. Biopolymers *93*(3), 211-217. DOI:10.1002/bip.21292

Zuehlke, A.D., Moses, M.A., and Neckers, L. (2018). Heat shock protein 90: its inhibition and function. Philos. Trans. R. Soc. Lond. , B, Biol. Sci. *373*(1738), DOI:10.1098/rstb.2016.0527

Zuehlke, A.D., Reidy, M., Lin, C., LaPointe, P., Alsomairy, S., Lee, D.J., Rivera-Marquez, G.M., Beebe, K., Prince, T., Lee, S*., et al.* (2017). An Hsp90 co-chaperone protein in yeast is functionally replaced by site-specific posttranslational modification in humans. Nature Communications *8*15328. DOI:10.1038/ncomms15328